SIZE CLASSIFYING OF GRANULAR PARTICLES IN A VIBRATORY SCREENING SYSTEM

By

PAUL KENNETH TURNQUIST

Bachelor of Science
Kansas State University
Manhattan, Kansas
1957

Master of Science
Oklahoma State University
1961

Submitted to the faculty of the Graduate School of
the Oklahoma State University
in partial fulfillment of the requirements
for the degree of
DOCTOR OF PHILOSOPHY
May, 1965

SIZE CLASSIFYING OF GRANULAR PARTICLES IN A

VIBRATORY SCREENING SYSTEM

Thesis Approved:

Jay G. Porterfield
Thesis Advisor

R. I. Wilson

David L. Huebner

J. H. Boggs
Dean of the Graduate School

PREFACE

This investigation was made possible by the generous support of General Foods Corporation through the General Foods Fellowship administrated by the Institute of Food Technologists.

I considered it an honor and a privilege to work under Professor Jay G. Porterfield who served as major advisor. I express my appreciation to Professor Porterfield for advise, consultation, and inspiration through all phases of my study.

Appreciation is extended to Professor E. W. Schroeder, Head of the Agricultural Engineering Department for serving on the advisory committee and for his handling of the many administrative details.

I wish to thank Dr. Gordon L. Nelson of the Agricultural Engineering Department; Dr. David L. Weeks of the Statistics Department; and Professor E. J. Waller of the Civil Engineering Department for serving on the advisory committee. Their assistance and suggestions were appreciated.

Personnel of the research laboratory are to be commended for their work in building the special equipment. Jack Fryrear and Don McCracken contributed appreciable in preparing illustrative material.

I am particularly grateful to Peggy, my wife, for her endurance during this study and for the momentous task of typing this dissertation.

TABLE OF CONTENTS

LIST OF TABLES

LIST OF FIGURES

CHAPTER I

INTRODUCTION

Background

Sizing of particles is basic to many processing and manufacturing operations. The task is essentially one of separating a mass of particles into certain specified size groupings. To do this a person could make certain length measurements on the individual particles drawn from the mass. Another possibility is to use some inanimate device which eliminates the need for personal judgment. Most efforts have been directed at developing inanimate devices to perform specified sizing of particulate material. Many systems have been designed, constructed, and evaluated. One characteristic which seems to appear in all systems is that optimum capacity and optimum size differentiation cannot be obtained simultaneously. To achieve a high level of one requires that less stringent specifications be tolerated on the other.

A greater understanding of the physical, chemical, and electrical properties of the particle would be very helpful in developing better techniques for sizing. Knowledge of one of these properties has been used successfully in the gravity table which bases particle separation on differences in density. Electrical properties and shape considerations have been used to achieve acceptable sorting of particles.

The majority of sizing operations in the size range above 100

microns have been and are still being achieved with perforated surfaces. A great variety of screen configurations are available to meet the needs for the large number of particle characteristics encountered. Many mechanisms are used for imparting motion to the sieves, and an infinite number of combinations of displacement, velocity, and acceleration exists.

Few attempts have been made to analytically describe the screening process. One of the difficulties is to mathematically account for the interaction effects which exist between individual particles and the screening surface. A random occurence of events seems likely as particles compete for access to the apertures. This suggests that the passing of particulate material through apertures is of a statistical nature. One would expect these interaction effects to vary with changes in particle characteristics, screen configurations, and screen motion.

In view of the large amount of material that is sized by perforated surfaces, very little qualitative and quantitative information exists which would have general application concerning the passing of particles through apertures. Optimum sieving of a given material is usually determined experimentally under rather limited operation conditions, which does prove satisfactory in many cases.

Introduction of resonant vibrating screens in Germany in the 30's and later in the United States resulted in higher screening efficiency for many materials. Although better systems are being devised, the basic question regarding the nature of passing undersized particles through the aperture has not been answered. It is not difficult to rationalize that a particle one half the size of the aperture will pass more readily than one which is only slightly smaller than the aperture.

Some questions which arise are: What is a satisfactory means to describe the ease or difficulty that a particle has in passing through an opening? What are the effects of mixing varying proportions of different sizes of undersize and oversize particles? What effect does the length of screening surface have on the passing of particles? The statement has been made that 75% of the undersize particles will pass in less than 25% of the screen length (27). It recognizes that the undersize particles are of many different sizes, but gives no indication what effect the individual sizes have.

Answers to the above questions and others which pertain to the accurate sizing of particles becomes more important as demand for higher quality products continues to increase. In the manufacture of food products, knowledge and control of particle size is essential in basic ingredients and in the finished product (3). Factors affected are color, flavor, texture, consistency, and shelf life. Accurate sizing of agricultural seeds used for planting insure more uniformity in plant population and harvested product.

Statement of Problem

Introducing a mass of undersize particles to a screening system results in passage of some of the particles through the apertures. For a given set of conditions which define the system there should exist some average probability of passage. As the size of these particles decreases in relation to the aperture, other factors being equal, the average probability of passage should increase. There is evidence that particle size to aperture ratio is a basic characteristic of screening performance as is screen slope, feed rate, and motion parameters.

Gaudin (19) has developed an equation based on geometry for estimating the probability of passage for a sphere through a square aperture. No attempt was made to consider other important factors which would alter the estimate significantly.

Determination of these basic relationships between particle characteristics, screen parameters, and motion of screen would be of practical importance in analyzing and designing screening systems.

Objectives

Specific objectives of the study were to:

1. Establish basic relationships between particles and a single screen system by means of theoretical considerations and dimensional analysis.
2. Develop the necessary equations predicting the probability of particle passage using experimental data and the basic relationships established in No. 1.
3. Develop a method for selecting aperture dimensions, screen motion, and areas for a screening system having more than one screen to accomplish a given separation.

Limitations

One must necessarily introduce limitations in order to concentrate on specific factors. The following restrictions were imposed on the investigation:

1. One shape of undersize particles was used.
2. Two different sizes of particles were used in the experimental

work. One size class was used as undersize particles and the other was used as the oversize particles.

3. The majority of the experimental work was confined to working with the undersize particles.
4. Oversize particles were mixed with undersize particles to determine the effect on passage of the undersize particles for a limited number of test conditions.
5. Grain sorghum was selected as undersize particles and plastic balls as the oversize particles.
6. Square mesh steel wire cloth screens were used for all experimental work.
7. Approximated simple harmonic motion was imparted to a horizontal screen by an eccentrically driven four bar linkage.

Procedure

A large number of variables have measurable effect on the probability of particle passage. In view of this the factors were combined in dimensionless ratios to facilitate the experimental work. Existing information and theoretical calculations were used to form the ratios. Laboratory experiments were conducted using accepted statistical procedures.

CHAPTER II

REVIEW OF LITERATURE

A literature study was made and the subject matter was divided into four areas. These areas were: (1) Particle sizing systems; (2) Experimental work; (3) Particle size analysis; (4) Theoretical considerations.

Particle Sizing Systems

Harmond (20) stated that cleaning of agricultural seeds requires the removal of undesirable elements such as weed seeds, rocks, chaff, insect and animal droppings. Planting of contaminated seed may result in reduced yields and increased production costs. Some methods used for cleaning seed base separation on size, length, density, seed coat texture, terminal velocity, and color. As differences in properties increase between seed and contaminant, separation becomes easier. He also reported the development of an experimental machine at Oregon State College which cleans seed by electrostatic separation. Components of the unit were a feed hopper, conveyor belt, d.c. electrode, and divider to divert the separated fractions. Separation was dependent on seeds being good or poor conductors. Contaminated material was successfully removed from bentgrass, bluegrass, brome, clover, ground coffee, corn, mustard seed, rice, and vetch. It was found that high voltage (10,000-45,000 volts) treatment of chewings fescue, ryegrass, and subterranean clover did not statistically effect germination.

The Buell Engineering Company has designed a pneumatic classifier for the purpose of separating phosphate rock fines of less than 100 mesh (33). Primary air enters the unit from the top, drawing in the material to be separated. The entering airstream makes a sharp "U" turn into the upward inclined discharge duct which set up a counter clockwise eddy current. Fine material is carried out with the air stream but the coarse particles cannot make the sharp turn and proceed downward. A secondary air current crosses the coarse material near the outlet removing additional fines and reinforcing the eddy current. The "cut point" is varied by regulating the secondary air supply.

A compact rotary sieve has been designed by Chepil (6) for determining the size distribution and mechanical stability of dry soil aggregates. The drum of the unit is formed by five nested cylindrical shaped screens. The drum is sloped 4 deg. from the horizontal and rotates at 7 RPM. The largest screen is 12 1/2 in. in diameter and 22 in. long. Volume flow to the drum is about 60 cubic in. per min. Previously hand shaking of a flat sieve was used. Specific advantages of the rotary sieve over the flat sieve were: (1) More consistent results; (2) Variable personal factor is minimized; (3) Consistent results regardless of the size of soil sample used; (4) Less breakdown of clods; (5) Soil can be processed several times to determine its mechanical stability.

Moore (23) states that the proper use of gyratory screens offers an effective means of separating dry, free flowing granular material in mesh sizes ranging from 4 to 325. It is essential to select the proper screen size. This can be done with a 14 in. x 14 in. experimental sifter. Using the sifter, a scale, and stop watch, the penetration-

rate test can be conducted. "Flow through the sieve of a 500 gram test sample of stock is observed and timed by stop watch. Through-product is weighed and rate of penetration (lb./min./ft.^{2}) is conveniently calculated." After the test the screen should be visually inspected for blinding or plugging. He also advocates a taut screen. As a result of a free slapping cloth, "the efficient gyratory action is converted into a combination horizontal and vertical motion, adverse to efficient separation and normal screen-cloth life." It is recommended to ground the screen, discharge pan, and framework to minimize electrostatic charges. Mechanical plugging of the screen is usually due to undesirable particle size, thick layer of stock on screen, or inadequate ball-cleaner action.

Recently at the Quaker Oats' Mills, electrostatic separation has been installed and is being used to separate impurities such as rodent droppings from shelled corn (16). The method has also been applied to sesame seed. The product passes over several grounded conveyor rolls and then proceeds through a 30,000 volt electrostatic field. Different types of particles pick up different magnitudes of charge. As they leave the field they are deflected by varying amounts which are dependent upon the intensity of the charge.

The editors of Food Engineering discuss some of the machines which are currently used for sizing of dry solids (foods) and the grading of fruits and vegetables (15). Sifters, vibrating screens, classifiers, and rotary reels are discussed.

Sifters employ three types of motion: gyratory, reciprocating, or gyratory-reciprocating. Gyratory motion imparts a circular motion to the particles as they advance due to the screens' slope. "Circular

travel exposed particles to some 150% more openings than reciprocating motion; 44% more than combination motion." The reciprocating drive moves the particles in a straight line. Gyratory-reciprocating screens have spiral motion at the head end and approaches reciprocating motion at the discharge. The authors identify the following factors as affecting the rate at which particles pass through a screen opening: material density, shape, moisture, fat content, size of particles in relation to screen size, static electricity, and physical-chemical nature of particles.

Two major types of vibrating screens are used—inclined and horizontal. Inclined screens convey material by gravity forces and a circular or elliptical motion is imparted to the deck. Motion is imparted at 45 deg. to horizontal screens which creates forces that both convey material along and lift it above the deck. Vibrating screens are used in processing French fries, pickles, corn, shellfish, tomatoes, and other food products.

Classifiers are used to separate fine particles from air. The size range can vary from several microns up to 100 mesh. One advanced system has been designed which is a combination impact pulverizer and internal air classifier for lower micron range grinding.

Rotary reels are widely used in canneries. They have high capacities under continuous operation. Beans, mushrooms, beets, and oysters, to mention a few, are graded by this means. Many units are available for continuous sizing of fruits and vegetables. Two such units are the spool type grader and the roller sizer.

The National Starch Products Company employs a specially designed cyclonic unit which picks off light material from a vortex of swirling liquor (14). This produces a higher quality starch having a reduced

amount of unwanted protein. The housing of the separator is similar to a centrifugal pump housing. Two vertical plates divide the chamber into three cylindrical chambers. Mounted in the two plates are 480 horizontal separating venturi tubes. Starch liquor is pumped into the center section upon which the liquor enters the separating tubes tangentially. A vortex is formed in the cyclone chamber and the light (undesirable) liquor flows into the left chamber and the heavy (desired) liquor flows into the right chamber. Eight such separators are used in series. A high quality starch slurry is discharged from the eighth unit.

A great deal of particle sizing is performed in the mining of minerals. Attention will now be directed at reviewing some of these activities.

Faul and Davis (12) have developed several ways to facilitate recovery of minerals such as zircon, biotite, and muscovite. These minerals are used in geochemical studies to determine geologic age. The devices employ the principle of asymmetric vibration to separate gram amounts of pure minerals from rock.

One device of particular interest is used for separating mica from round grain materials. An aluminum plate 10 in. wide, 12 in. long, and 1/4 in. thick was mounted on the base of a commercial vibratory feeder. The plate was tilted 15 deg. to the side and was vibrated asymmetrically to its length. When adjusted to the proper amplitude, mica flakes advance lengthwise and fall off the far end. The rounder particles roll and bounce down the incline. The material is collected in a continuous spectrum ranging from flat to round particles.

Fink (13) discusses ways to reduce screen blinding in vibrating screens. Clogging of screens reduces the effective screen area and

necessitates reduction of the feed rate. Blinding of vibrating screens is usually due to one of three causes: improper motion, moisture present in finer particles, and irregular geometrical shape of the material.

Variables which effect screen motion are: frequency of vibration, amplitude, direction of rotation, and screen slope. An increase in amplitude is recommended as the mesh opening increases. Moisture in materials is usually most troublesome with openings up to 3/8 in. Occasionally this difficulty can be overcome by changing from a square aperture to a rectangular one. Often more drastic action is required, such as impacting the undersize of the screen with rubber balls or heating the screen so that wet clinging particles will dry and fall off. Heating is accomplished by passing low voltage current through the screen. In place of electric heating of large screens, flame heating has been used successfully. Gas burners are placed below the screen and direct a flame parallel to, or inclined at a slight angle, to the screen.

The author states that when exceptionally elongated materials are encountered more force is required to throw the particles out of the apertures than cubical material. This increased inertia force can be obtained by increasing speed and/or amplitude. Usually increasing amplitude is more effective.

The International Minerals and Chemical Corporation set up an electrostatic pilot plant for concentrating low grade coarse Florida pebble phosphate (25). This low grade ore contains undesirable quantities of silica. Removal of the silica increases the bone phosphate of lime (BPL) from about 60% to 73-77% by weight. The

resulting product has a ready market. The LeBaron-Lawver free fall process was employed. Ore enters the electrostatic separator in a uniform thin ribbon parallel to the electrodes. Potential across the electrodes is 40-70KV. The phosphate particles have positive charges and the quartz particles have negative charges. The particles are deflected in opposite directions due to the field. Ore particles not freed by crushing are too heavy to be deflected and essentially fall straight down to be collected in the center portion. Thus, three fractions are obtained: concentrates (high BPL), middlings, and tailings (containing silica). In this arrangement it is possible to grind the middlings and recycle them through the separator. On an average the BPL was increased by 6.2% and the silica content was reduced 7.5%.

A Jar-Bar Grissly Feeder is being built by a Johannesburg engineering firm (30). The unit is 48 in. wide and employs 8 rolls. Design is such that the unit acts as both a screen and feeder. The roll cross-section is elliptically shaped with the major axis of adjacent rolls at right angles. All rolls rotate in the same direction and the aperture between adjacent rolls remains constant throughout each revolution. Action of the unit alternately lifts and drops lumps of rock and at the same time imparts horizontal movement to the rock. The rocking motion results in rubbing and sifting. The fines drop through the apertures and clean rock discharges at the end of the unit.

A resonance screen called Resonex has been designed in Western Germany and has been manufactured by a British firm for use in South Africa (29). The entire unit is supported by rubber pillars which minimize the transmission of vibration to the base of the supporting

structure. An eccentric vibrates the screen at resonant frequency between 600-650 CPM. One feature of the drive is rubber buffers which control the length of stroke which can vary between 3/8 in. and 1 1/8 in. A unique feature is an "anti-gravity" rubber spring installed on each screening section which accelerates the normal screening force two to four times. Orientation of the components allows the screen to operate in the horizontal position. It is capable of dedusting tobacco which has a density of 2.8 lb./ft.^{3} and can handle materials having densities up to 150 lb./ft.^{3} A desirable feature is that the screen is unitised. Units can be combined to form a screen up to 120 ft. long. One prime mover is used for the combined units.

Utley (32) reports that one of the first Hewitt-Robins "Hi-G" screens in the sand and gravel industry was installed in Colorado. It was a 5 ft. x 10 ft. double deck unit which washed and classified about 170 tons per hr. Three size classifications between 1/7 in. and 1 1/2 in. were made. The two horizontal screens are interconnected by springs. A 5 HP motor drives a vibrator which moves the upper frame downward (and horizontally) and the lower frame upward (and horizontally) simultaneously during one half the cycle. This compresses the springs which stores energy for release during the second half cycle of motion. The mechanical vibrator is operated at the resonant frequency of the screen.

Sullivan (31) discusses the dynamic principles of the resonant vibrating screen. In Fig. 1 is shown the basic Schieferstein system. The external exciting force is applied to the oscillating body by an eccentric-elastic coupling. The force can also be applied as shown in Fig. 2. In this arrangement the vibrator RPM is far above the natural

frequency of the suspension system.

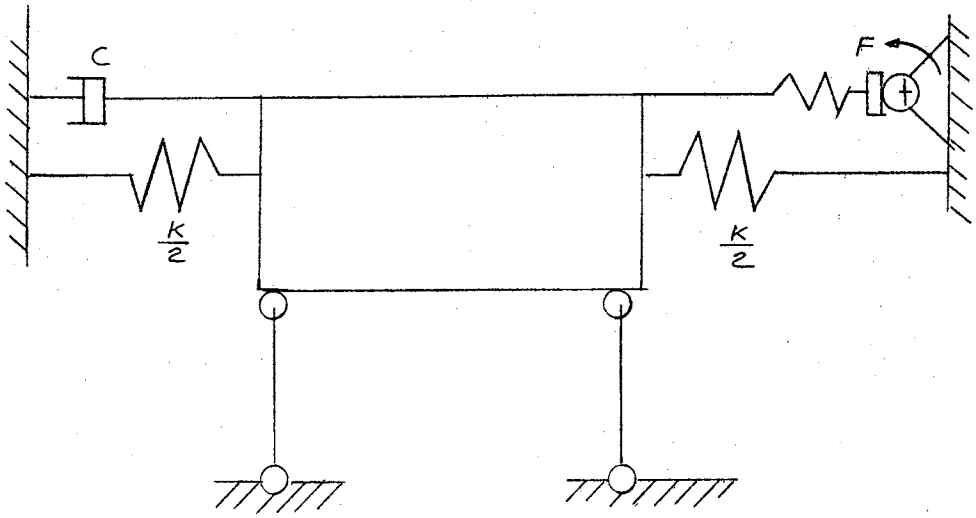

Fig. 1. Basic Schieferstein System Employing an Eccentric-Elastic Coupling.

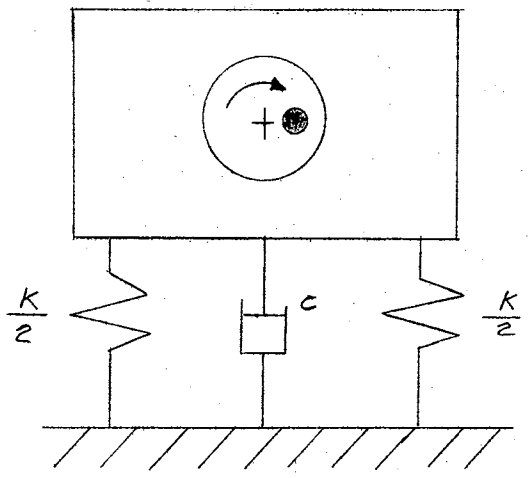

Fig. 2. Basic Schieferstein System Employing a Rotating Unbalance Carried in the Oscillating Body.

Fig. 3 shows the vector diagram for dynamic equilibrium when the frequency of the impressed force (F_o) is less than the natural frequency of the system. The impressed force leads the displacement by a phase angle ϕ which is less than 90 deg. The damping force lags the displacement by 90 deg. The impressed force needed to maintain motion must equal the vector sum of the spring force minus the inertia force plus damping force.

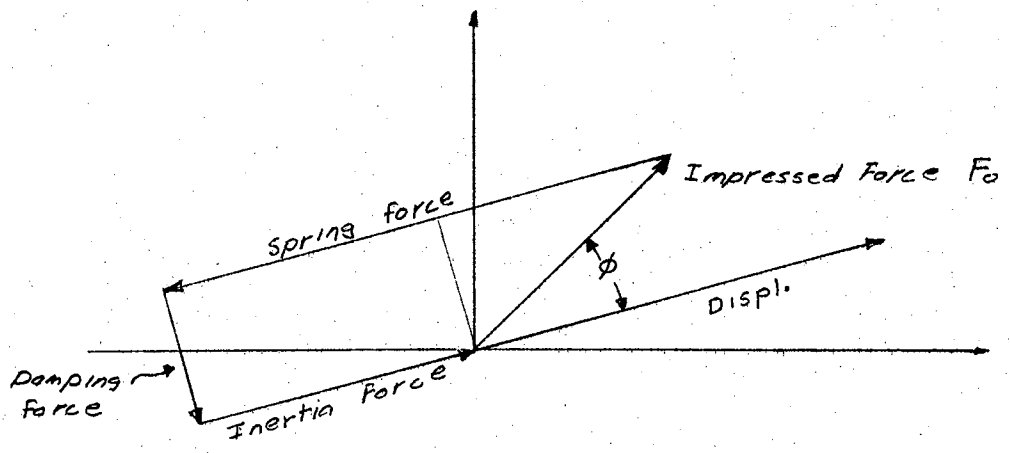

Fig. 3. Vector Diagram for Equilibrium Conditions in Forced Vibration, $W/W_n < 1$.

In Fig. 4 the RPM of the exciter has been increased and is equal to the natural frequency of the system. In this condition known as resonance, to maintain oscillation, (F_o) has only the damping force to overcome and the amplitude of the body will increase to whatever mechanical limits exist in the system.

Fig. 5 shows the vector diagram for equilibrium for frequency

ratios much greater than resonance. Spring force and damping is small and about 95% of the impressed force is used to overcome the inertia force.

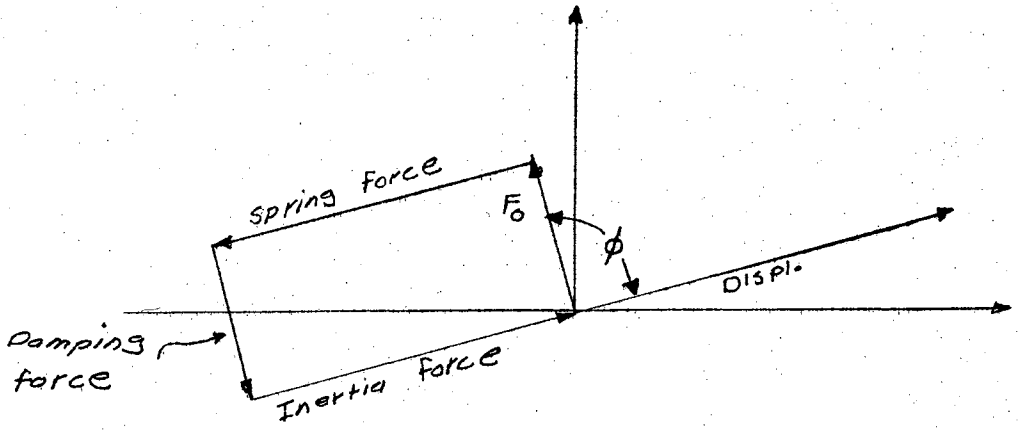

Fig. 4. Vector Diagram for Equilibrium Conditions at Resonance, $W/W_n = 1$.

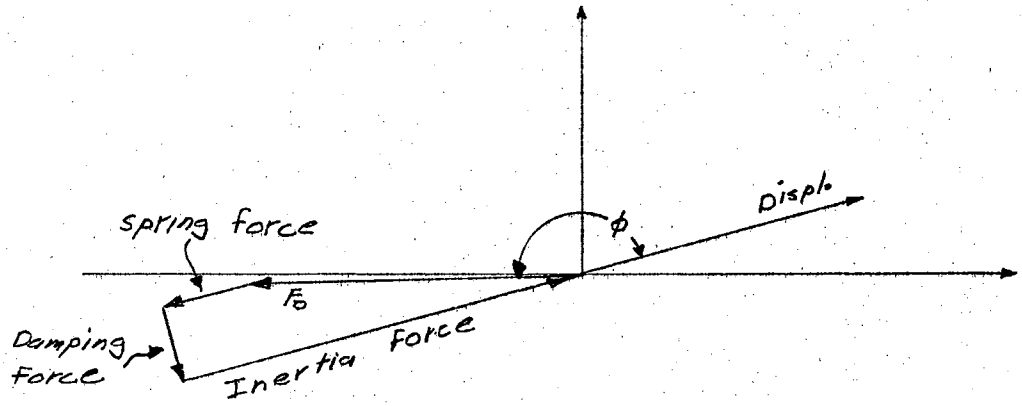

Fig. 5. Vector Diagram for Equilibrium Conditions at High Frequency Ratio, $W/W_n > 1$.

The stalling problem associated with this type of system can now be explained. Let the screen be tuned to resonance in the unloaded condition. As material enters the screen the weight of the structure increases. This additional weight reduces the natural frequency of the system and causes the frequency ratio to move above resonance. If the exciter cannot overcome the increased inertia force, the amplitude of the system decreases until dynamic equilibrium is again established. While this is occuring material is building up on the screen which further depresses the amplitude until the screen ceases to oscillate.

To overcome stalling, designers have modified the basic Schieferstein system as shown in Fig. 6. Buffers are added to apply

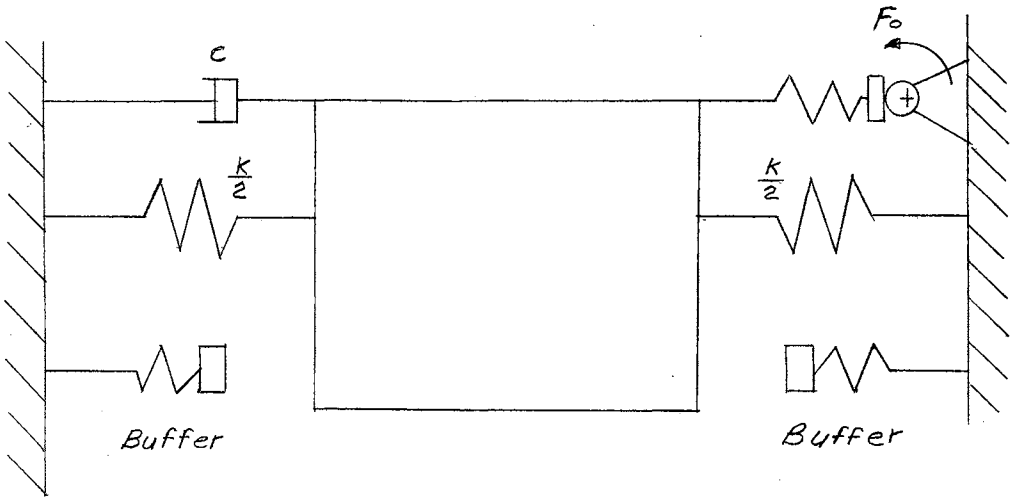

Fig. 6. Schieferstein System with Buffers Which Apply Solid Damping at the Stroke Limits.

"solid damping" to the system at the stroke limits which flattens the

peak of the resonance curve. The system is tuned under no-load operating conditions at a frequency ratio below resonance. When the load comes on the screen, the frequency ratio increases and moves into the flattened portion of the resonance region. With this arrangement material loads up to one-half the weight of the structure can be handled without loss of amplitude.

A sonic vibrating filter has been designed which is suitable for filtering solids or viscous materials (26). The unit has a screen suspended as a catenary with one edge clamped and the other edge driven by a 120-cycle electromagnetic vibrator. The vibrator is supported so that the higher order harmonies are superimposed on the fundamental mode of vibration. The vibration sets up a longitudinal wave front at the clamped edge which gradually changes to transverse waves at the bottom of the catenary. This motion induces a strong lateral feed displacement. Materials not passing through the filter move laterally with a circular motion to the end of the screen.

A new vibrating screen separator for continuous separation of wet and dry materials is now being marketed by a British firm (11). The unit can be fitted with four 48 in. diameter screens and it is claimed to have high capacity per unit area. The screen assembly is spring mounted to the base to isolate vibrations. A one HP vertically mounted electric motor with double-ended shafts drives the screens. An eccentric weight at the top end of the shaft drives the screen horizontally. On the lower end of the shaft an eccentric weight imparts vertical motion. Position of the lower weight is variable to give a phase shift between vertical and horizontal motion.

A very interesting device for sizing was noted in Chemical

Engineering Progress (10). It is a stationary screen of the sieve bend type. The screen was originally developed for use in coal mining but is now being used in the food processing industry. Particular applications have been in the corn starch industry, cane and beet sugar factories, potato processing plants, and pineapple juice plants.

Method of operation and geometry of the unit is shown in Fig. 7.

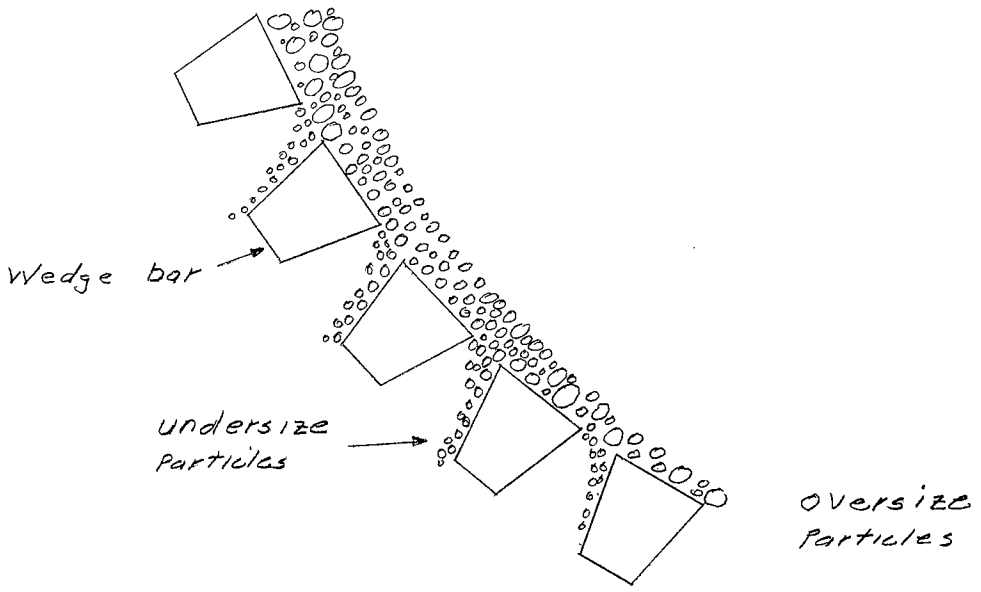

Fig. 7. Curved Stationary Screen.

The concave sieve bend is stationary and is composed of parallel metalic wedge bars having equal openings for the entire curvature. The feed slurry is directed vertically and tangentially over the full width of the screen. The slurry flows down the concave surface at right angles to the openings. A boundary layer drag is formed which causes a thin

layer on the underside to peel off and deflect through the openings of the wedge bars. The size of separation is determined by the thickness of the layer peeled off and the opening between the wedge bars. The size of separation is always smaller than the bar openings. Coarse screens will produce separations which are approximately one-half the slot openings. Since the particles passing are appreciably smaller than the slot size, the unit has high capacity and good non-clogging properties.

To characterize the unit, the following parameters were identified: slot width, velocity of slurry, density of medium, screen length, radius of curvature, undersize volume flow, and total volume flow. A Reynolds number was formulated:

$$Re = \frac{V\ s\ \rho}{\mu}$$

V = Velocity at feet spout (cm/sec.)

ρ = Density (gm/cc)

S = Screen slot width (cm)

μ = Kinematic viscosity of medium (Stokes)

Experiments have shown that above a critical Reynolds number (300) there is little change in the ratio of volume passing through the bars (undersize) to total volume (feed). For a feed spout velocity of 10 ft./sec., most material will have a Reynolds number greater than 300 for all screens down to 0.35 mm slot width. For slot width of .05 mm orifice-type feed nozzles are used to produce the needed higher velocities.

Cirlyptic screens are being used mainly in screening flour and dry milk solids (5). The head end of the screen is driven with a circular

motion in a horizontal plane. The discharge end moves in an elliptical path which results in a back and forth rocking. The sifter's success is attributed to irregular movement which provides many angles of approach for the particles with respect to the sieve openings. Due to the vigorous motion secondary vibrations are not needed to keep the screen open. Up to four fractions can be obtained without the nesting of sieves. Successively larger mesh screens receive the overs of the previous screen. Adjustable barriers control time that material is in each section. Time can be varied from three seconds to several minutes and maximum capacity is 1000 lbm./min.

In many cases the screening of solid particles becomes difficult due to build up of static electricity charges on the particles. A method was developed to eliminate static charges in the laboratory screening of polystyrene plastic spheres (2). Pieces of dry ice were placed on each screen. Humidified nitrogen gas was passed upward through the screening unit. The dry ice cooled the particles below room temperature and a thin film of water condensed on the particles when exposed to the gas stream. The liquid film prevented static charge buildup. After screening, the particles were spread out and allowed to dry. The water film did not appear to hamper the separation in any way.

Eck and Walter (9) identify the following main factors which influence the capacity of a sifter:

1. The input capacity in pounds per hr.
2. Bulk density of the materials.
3. Shape and nature of particles.
4. The range of particle size permissible in the finished product.

5. The percentage of in-range yield required.
6. Temperature of the material as it enters the sifter.
7. Electrostatic or other unusual characteristics of the material.

A rule of thumb is that the more exacting the requirements, the more difficult and expensive the sifting operation will be. The authors identify the following parameters as necessary in specifying industrial sifters:

1. Screen area needed.
2. Type and style of sieve.
3. Anti-clogging devices for screens (rubber ball-type, leather and nylon figure-eights, jack chains, etc.)
4. Mesh size and wire diameter.

Allen (1) considers the following material properties as relevant in separation of dry particles: size, density, shape, surface, hardness, porosity, friability, interparticle friction, surface moisture, angle of repose, tendency to agglomerate, hygroscopicity, electrostatic charge, abrasiveness, and bulk density. He suggests that particle size can be specified in several ways. Spherical particles or nearly so can be characterized by diameter. Long narrow particles require some combination of two dimensions. Extremely small particles are often designated in terms of the aperture through which the particle will pass. Sifting is defined as any separation performed on a screen or sieve. If undersize particles are substantially smaller than the aperture and oversize particles are much larger, a large amount of material can be sifted on a small area.

Particle shape is very important. It affects interparticle

friction which determines the ease with which fine particles settle to the screen surface. Screen motion should distribute material over the entire screening area, cause fines to settle to the screen surface, and discharge oversize particles. Motion applied to the screen can be in a horizontal plane, vertical plane, or a combination of the two. Motion which introduces a vertical component causes material to leave the screen part of the time thus reducing the time for the undersize particles to pass through the aperture. However, vertical motion assists in breaking down clusters of particles and is best for coarse sifting or where the undersize particles are considerably smaller than the mesh openings. Horizontal rotary motion causes the material to move in overlapping circles from inlet to outlet which maximizes the number of openings to which the particles are exposed.

Experimental Work

Considerable descriptive material exists in the literatures as evidenced by the previous section. However, one finds a limited amount of experimental work published.

Fowler and Lim (17) report the results from an experiment using a single deck Denver-Dillon screen vibrated by an off-balance flywheel. Amplitude of vibration for all tests was fixed at 7/64 in. Screen size, 10 in. wide x 24 in. long, remained constant for all tests. Clean dry river sand was the experimental material. Screen analysis of the sand showed a reasonable proportion of oversize and undersize particles for the screen sizes selected in the experiment. "A statistically planned experiment of 4 x 4 x 4 x 4 = 256 runs was designed in which the four levels of each of the four factors were split arbitrarily into pseudo-

factors giving a 2^8 full factorial design. This design was split into 4 blocks of 64 runs with the block differences confounded with the third order interaction." The four main factors in the experiment were: A - feed rate, B - speed of vibration, C - screen slope, and D - aperture size. Levels of the factors are shown in TABLE I. In conducting a given test, sand was metered onto the screen and allowed to flow until steady state conditions were reached. Then two samples of both undersize and oversize particles were collected in 10 sec. Amount of undersize particles in the oversize sample was determined. The quantities were expressed in a per cent effectiveness term, 100% occuring when all undersize particles pass through the aperture.

TABLE I

LEVELS OF FACTORS USED IN THE EXPERIMENTAL WORK BY FOWLER AND LIM.

Level	Feed Rate lb./min.	Frequency Rev./min.	Inclination Deg.	Screen Aperture Microns
00	5.50	952	6	276
01	7.25	1130	11	318
10	10.00	1326	15	447
11	15.45	1489	19	596

Analysis of variance indicated that feed rate and aperture have the greatest effect on separation effectiveness with aperture effect being considerably more significant than feed rate. Statistically

significant first order interactions were obtained between feed rate and aperture, and frequency with screen slope. Qualitative nature of the results were:

1. Effectiveness increases as feed rate decreases.
2. Effectiveness increases as screen aperture increases.
3. Effectiveness increases as screen slope increases up to 15 deg., but then descreases as slope increases.
4. Effectiveness increases as frequency increases to 1130 RPM and then decreases slightly as frequency increases.

The authors also identify the following variables which can influence the effectiveness of separation.

1. Variables due to the material being screened.
   a. Bulk specific gravity of feed.
   b. Particle shape.
   c. Percentage of near size, 0.7 to 1.5 times the screen aperture, material in the feed.
   d. Moisture content of the feed.
   e. Static charge generation.
   f. Stickiness of the material.
   g. Abrasion resistance to attrition.
2. Mechanical variables due to the type of screen used.
   a. Length and width of screen.
   b. Amplitude of vibration.
   c. Frequency of vibration.
   d. Slope of screen.
   e. Direction of vibration.
   f. Capacity of the screen.

3. Variables due to the screen cloth.

   a. Size of aperture.

   b. Per cent of open area.

   c. Shape of opening, square, circular, etc.

   d. Feed rate necessary to prevent blinding.

   e. Resistance of screen material to distortion.

   f. Variance in apertures over the screen.

Limited information is given in some experimental work as reported by Sinden (27). Tests were conducted using a 3 x 5 ft. screen with 1/4 in. openings. Slope was 17 deg. No mention was made of the material nature or the type of motion imparted to the screen. Graphical results are presented in Fig. 8 and 9. He makes some rather interesting comments concerning the general subject of sizing particles with vibratory screens. Screening action is best when the screen is covered with a layer one lump deep. Increasing feed rate above this will decrease efficiency unless the additional load consists of lumps much larger than the screen openings. "Capacity is directly proportional to the width of screening surface. The length of screen has but little effect on capacity." All particles less than about 1/2 the opening size will fall through quickly. Particles 1/2 - 3/4 of the opening will pass by the time they have advanced over a few openings. For a given screen over 75% of the undersize particles will pass in less than 25% of the length. Efficiency and capacity of a screen decrease as the wire diameter increases for a given size of opening. This reduction is approximately proportional to the per cent change in open area.

Additional experimental work is reported by Fowler and Lim (18). Based on experimental work with three materials, a non-homogenous

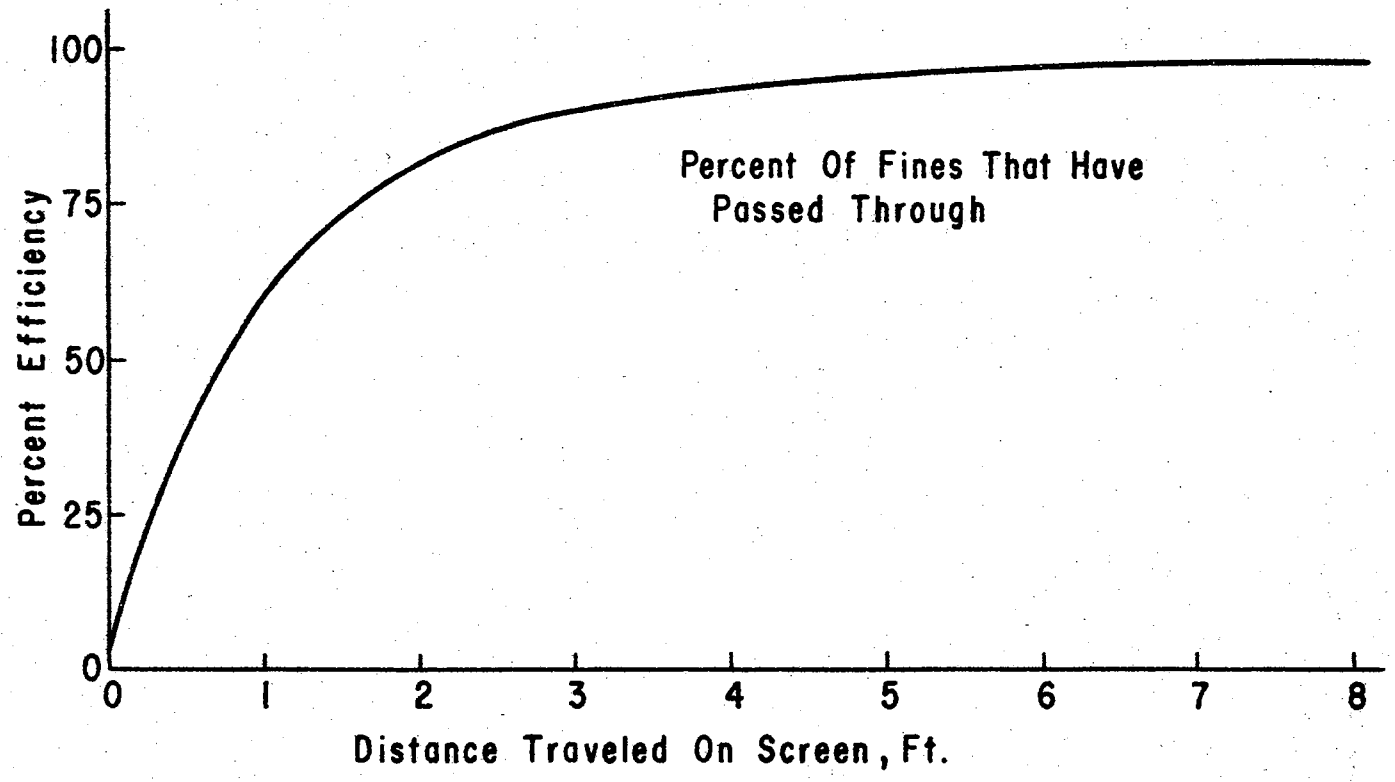

Fig. 8. Per Cent Efficiency Versus Distance Traveled on Screen.

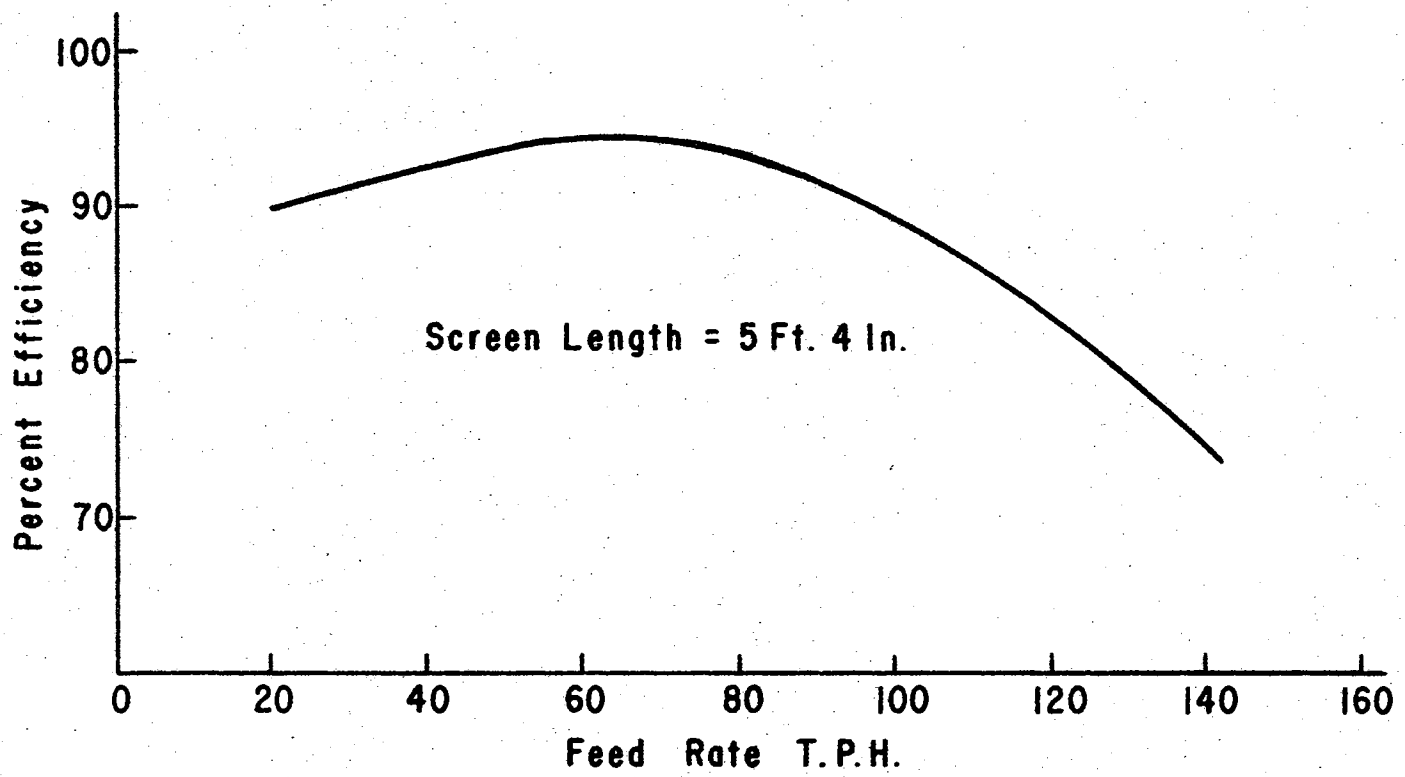

Fig. 9. Per Cent Efficiency Versus Feed Rate.

polynomial equation predicting effectiveness was developed. Form of the equation was:

$$e = A + Bs + Cs^2 + Da + Na^2 + Fw + G\cos\theta + Has$$

where: e = the percentage effectiveness

A, B, C, D, N, F, G, and H are constants

s = specific gravity

a = amplitude

w = frequency of vibration

θ = screen slope

Materials used in the tests were coal, limestone, and barites which were in the crushed state. The median size of the material was approximately 5.5 mm. The equation developed allowed prediction of effectiveness of separation at the 95% confidence level.

Particle Size Analysis

In order to describe any sizing operation the size and distribution of particles must be known. Considerable effort has been expended in developing techniques to more accurately describe sample makeup. Berg and Kovac (3) state that control and knowledge of particle size is of primary importance in food manufacturing. Spice makers have found for example that size reduction to the 100-400 mesh size will provide a desirable surface area to volume ratio which permits maximum release of natural flavor. Conventional methods used to determine particle size and size distribution are microscopic examination, sieving, and

gravitational sedimentation methods. These methods have been criticized as, "tedious, time consuming, inaccurate, unreliable, and limited either as to size range or to products." The authors discuss the principle of the Coulter Counter which eliminates some of the undesirable features of other methods. It can determine the number and size of particles suspended in an electrically conductive liquid. A dilute suspension of particles in an electrolyte flow through a small aperture one at a time with immersed electrodes on either side. Particle passage changes resistance between the electrodes and a voltage pulse proportional to particle volume is produced. The pulse is amplified, sized, and counted. Pulses are fed to a threshold circuit with an adjustable screenout voltage level. Thus only pulses exceeding a set level are counted. Data is obtained for plotting (log - log) particle volume versus relative count above threshold level. The pulses can be used as feed back information to adjust controls on size reducing machines, sifters, and other processing machinery.

It has been estimated that one cup of all-purpose flour contains more than one-hundred billion individual particles (7). The U.S.D.A. has established that endosperm particles must be smaller than 0.006 in. in diameter to be called flour. Fineness of flour is considered as an important property influencing the quality of cakes, cookies, and bread. Much effort has been devoted to measuring the size distribution of flour. Direct observation through a microscope was first used. This was tedious and left much to be desired. Various sedimentation methods have also been divided. Techniques utilizing the difference in behavior of different size particles in electrical, thermal, and optical fields have been developed to determine the size distribution of subsieve particles.

Because the various techniques differ in principle, the size distributions are not always comparable, thus the researcher is confronted with the task of presenting his information in such a way that others will understand it and will be able to use it to improve the quality of flour.

Testing of electroformed micro-mesh sieves has shown that they are precise in the 20-100 micron range (21). Three screens were calibrated and then checked for precision. Samples of monocalcium phosphate were sized on the three screens. The separated fractions were analyzed by accurate sedimentation and electronic sizing and counting. These calibrated values were than compared with the nominal openings as determined by microscopic measurement. The precision was checked by taking two samples in two size ranges and running them five times by two different operators. Statistically there was no significant difference between operators at the 99.9% level.

An instrument for measurement of particle size in the 0.1 to 5.0 micron range is reported in the Journal of Scientific Instruments (28). The device speeds up the settling process by replacing gravitational forces with centrifugal forces. For the design speed of 500 RPM, the centrifugal force on a particle varies from 90 g's at the center to 330 g's at the point of extraction. The centrifuge has to run about one min. for extraction of a 5 micron particle and about 8 hrs. for a 0.1 micron particle.

Theoretical Considerations

Dallavalle (8) presents a theoretical analysis which was originally developed by Fagerholt.

Parameters in the Analysis

$F_w(d)$	Particle weight-size distribution function, lbm.
d	Particle size, in.
d_o	Lower limit of particle size on screen, in.
d_{max}	Maximum particle size that can pass screen, in.
$W_{d,t}$	Mass of particles of size d at time t on the screen lbm.
α	Probability of passing through the screen $1/in.^2 sec.$
t	Sieving time, sec.
b	Constant value of $F_w(d)$ between d_o and d_{max}.
R_t	Fraction of material retained on the screen.

A general particle weight-size distribution curve is assumed as shown in Fig. 10.

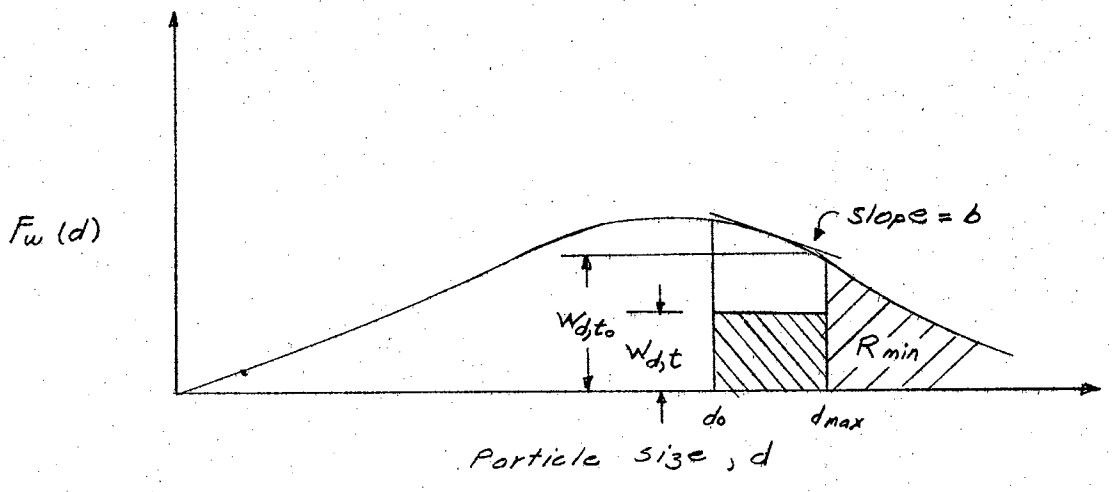

Fig. 10. Particle Weight-Size Distribution Curve.

Assumptions made in the analysis were:

1. Batch type sifter.
2. Particles in the size range 0 to d_o fall through the aperture instantaneously. Time is considered to be zero at d_o.
3. The distribution function is assumed to be a straight line between d_o and d_{max}.
4. Particles slightly less than d_{max} pass just as readily as ones slightly larger than d_o.

The particle screening rate is proportional to the number of particles on the screen.

$$\frac{d\,(W_{d,t})}{dt} = -\alpha\,(d_{max} - d)^2\; W_{d,t}$$

Integrating

$$\frac{W_{d,t}}{W_{d,t_o}} = \text{EXP}\left[-\alpha\,(d_{max} - d)^2\, t\right] \qquad \text{for } d \leq d_{max}$$

Then the expression for the material retained on the screen at any instant in time is:

$$R_t = \int_o^{\infty} F_W(d) \times \frac{W_{d,t}}{W_{d,t_o}} \times d(d)$$

or

$$R_t = F_W(d) \int_{d_o}^{d_{max}} e^{-\alpha (d_{max} - d)^2 t}\; d(d) + R_{min}$$

R_{min} is the material larger than d_{max}.

Integrating R_t by use of the probability function yields:

$$R_t = \frac{b}{2}\sqrt{\frac{\Pi}{\alpha t}} + R_{min} \qquad \text{for } t > 0$$

Fig. 11 is the graphical representation of the above equation. This relation indicates that the sieving operation would require an infinite time to pass all the particles between d_o and d_{max}.

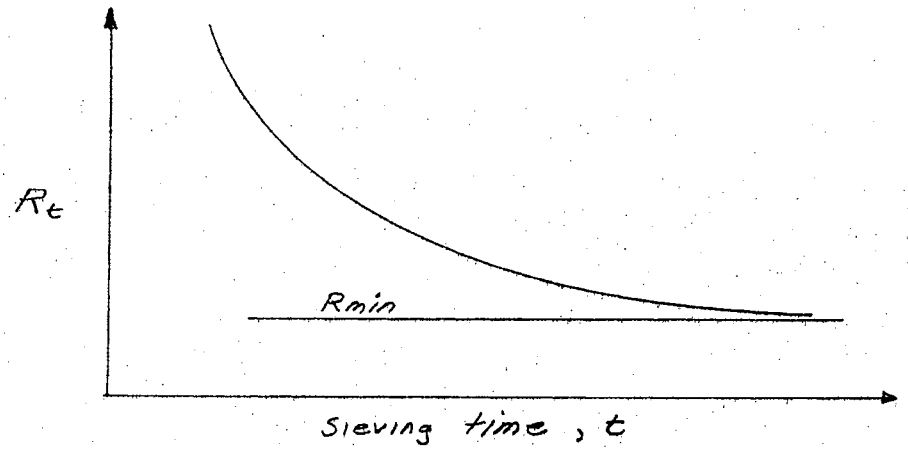

Fig. 11. Weight of Material Retained on Screen Versus Sieving Time.

Bodziony (4) has developed an integro-differential equation to describe the screening process. The general solution is:

$$\int_{D_{min}}^{D_{max}} c(D,t)\,dD \times \frac{dc(D,t)}{dt} = -\lambda\,(D, D_s) \times C(D, t)$$

where

$C(D, t) = \frac{dV(D,t)}{dD}$ = Rate of change of total volume with respect to diameter

$\frac{dc(D,t)}{dt}$ = Time rate of change of C (D,t)

$\lambda(D,D_s)$ is a proportionality factor which is a function of the screen, motion, and grain size. He then describes two cases. Case A considers a narrow range of particle sizes less than the aperture size which results in a finite period of sifting time. Case B considers two ranges of particle size, one larger than the aperture and one smaller. To achieve perfect separation in Case B requires an infinite time. Some experimental results using sea sand indicate that test values and theoretical values were compatible.

CHAPTER III

THEORY

An analysis of passing particles through the apertures of wire cloth screen should consider analytical and statistical concepts. Using the analytical approach to describe the motion of the screen and its effect on a single particle under idealized conditions should give general behavior of a mass of particles. Numerous particles in a system will introduce interaction effects not present when only a single particle is considered. In most cases these interactions are evaluated most efficiently by experimental procedures.

The path of an idealized particle on a non-perforated vibrating surface can be predicted analytically with reasonable accuracy. If the surface is replaced with a wire cloth screen, a certain amount of randomness in the path occurs. This can be described with the aid of Fig. 12. Assume that the average net movement of the particle per oscillation of the screen is to the right. Let (ℓ) be some characteristic length of the particle and let (ℓ) be less than (a), which implies an undersize particle. If the particle impacts the wire at point A, back scattering occurs. Considering the wire and particle as rigid bodies, the angle of scatter will equal the angle of impact at the instant before and after impact. Since the screen must be placed in a gravity field (G) to function as a sizing device, the particle will be deflected down as indicated by the dotted line. The particle may or

may not pass through the aperture (a), depending on the magnitude of (ℓ), (a), particle velocity after impact, location of the impact point, and motion of the screen. The particle could also impact at point B. In this case, forward scatter occurs, and the likelehood of passage is dependent on the same factors as in backscattering. For net movement of a particle to the right, the direction and magnitude of screen velocity must be such that the particle velocity is augmented when forward scattering occurs and suppressed when backscattering happens. Net movement to the right will occur when the resultant screen velocity (V) is in first quadrant. Consideration of numerous particles in the system will induce greater randomness of individual particle motion. Deflection concepts which apply for a single particle will also apply for a mass of particles. However individual particles can collide with each other. These collisions will cause secondary, tertiary, quartic, etc. scattering effects. If (ℓ) is greater than (a) and the screen is infinite in length, the scattering would continue ad infinitum.

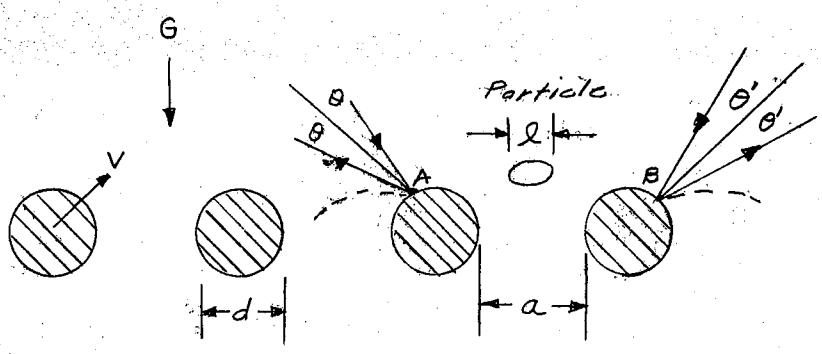

Fig. 12. Particle Scattering.

Dimensional Analysis

Consideration of the many parameters required to define a screening system favors the use of dimensional analysis. Parameters which have measurable effects on the system can be combined into dimensionless ratios which reduce the number of variables. These ratios can then be treated as variables. Failure to consider an important parameter will result in an uncontrolled random variable which will render the analysis ineffective. Achieving correct formulation of the ratios depends on proper application of known theoretical relations and general knowledge of the system. Quantitative relationships must be obtained by experimental procedures.

Murphy (24) states that dimensional analysis is based on two axioms: 1. absolute numerical equality of quantities may exist only when the quantities are similar qualitatively, and 2. the ratio of the magnitudes of two like quantities is independent of the units used in their measurement, provided that the same units are used for evaluating each.

The utilization of dimensional analysis requires that variables which have a measurable influence on the system be identified, and then grouped into dimensionless ratios called pi terms. Langhaar (22) has developed a rigorous theorem which states that the number of dimensionless products in a complete set is equal to the total number of variables minus the rank of their dimensional matrix. There is no unique set of pi terms. Other terms can be formed by multiplication or division of terms within the set.

A prediction equation relating the pi terms can be formulated by

analysis of laboratory observations. Murphy (24) suggests the following procedure for evaluating the function. Arrange the observations so that all the pi terms except one are held constant, then vary it to establish a relationship with the quantity being observed. The relationship established is called a component equation. Repeat this procedure for each of the pi terms. The resulting relationship between the observed quantity and all the individual pi terms can be combined to give the general relationship in equation 3 - 1. Obtaining this combination is not always simple. If the component equations are of the form $\Pi_1 = A\Pi_s^{\,h}$, the pi terms will combine by multiplication and the general prediction equation will have the form of equation 3 - 2.

$$\Pi_1 = F(\Pi_2, \Pi_3, \Pi_4, \ldots \Pi_s) \qquad 3 - 1$$

$$\Pi_1 = K_1 \Pi_2^{K2} \Pi_3^{K3} \Pi_4^{K4} \ldots \Pi_s^{Ks} \qquad 3 - 2$$

If the component equation plot as straight line on arithmetic paper, then it can be shown that the pi terms will combine to be a sum and will have the form of equation 3 - 3 (24).

$$\Pi_1 = K_1 F(\Pi_2) + K_2 F(\Pi_3) + .. K_s F(\Pi_s) + K \qquad 3 - 3$$

Selection of Basic Quantities

The system selected for investigating the passage of particles through apertures consists of:

1. A square aperture plain steel wire cloth screen with double

crimp weave.

2. Approximated simple harmonic motion imparted to the horizontally positioned screen in a gravity field.
3. One size class of grain sorghum representing the undersize particles.
4. One size class of plastic balls representing the oversize particles.

A schematic drawing of the system is shown in Fig. 13.

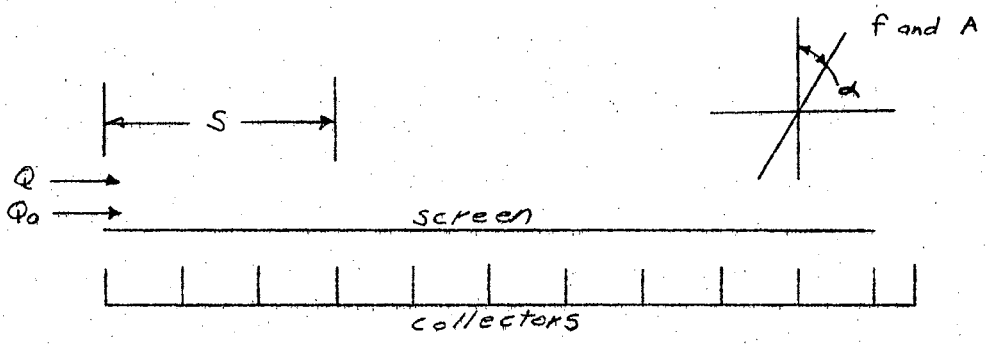

Fig. 13. Schematic Diagram of the Screening System Selected for Investigation.

The dimensional analysis for the screening system is presented in TABLE II.

The first area of investigation was to study the behavior of passing undersize particles through the screen without introducing any oversize particles. For this part of the study Π_1 was the dependent variable. Π_2, Π_6, Π_7, Π_8, Π_9, Π_{10}, and Π_{11} were the independent

variables. Π_3, Π_4, and Π_5 were held constant. Π_{14} was zero, and Π_{12}, Π_{13}, Π_{15}, and Π_{16} were not relevant since no oversize particles were present.

The second area of investigation was to study the effects on undersize particle passage when oversize particles were introduced in varying proportions. For this part of the study, Π_1 was observed as Π_{14} varied. All other ratios were held constant.

TABLE II

BASIC PARAMETERS IN THE PHYSICAL SYSTEM

No.	Symbol	Parameter	Dimensions
1.	P	Ratio of "throughs" to total quantity of particles measured at S.	0
2.	α	Angle with respect to the vertical at which motion is imparted to the horizontal screen. deg.	0
3.	S	A length measured from the head end of the screen. in.	L
4.	a	Aperture opening of the square mesh screen. in.	L
5.	d	Wire diameter of screen. in.	L
6.	A	Amplitude of Vibration. in.	L
7.	l_{1u}	Length of undersize particles, in.	L
8.	l_{2u}	Maximum width of undersize particles. in.	L
9.	l_{3u}	Minimum width of undersize particles. in.	L
10.	l_{10}	Length of oversize particles, in.	L

TABLE II (Continued)

No.	Symbol	Parameter	Dimensions
11.	l_{20}	Length of oversize particles, in.	L
12.	f	Frequency of Vibration. cps	T^{-1}
13.	ρ_u	Density of undersize particles. lbm./in.^{3}	ML^{-3}
14.	ρ_o	Density of oversize particles. lbm./in.^{3}	ML^{-3}
15.	ρ	Air density. lbm./in.^{3}	ML^{-3}
16.	Q	Mass flow rate of undersize particles per unit width of screen. lbm./in.-sec.	$ML^{-1}T^{-1}$
17.	Q_o	Mass flow rate of oversize particles per unit width of screen. lbm./in.-sec.	$ML^{-1}T^{-1}$
18.	G	Earths gravitational field lbf./lbm.	FM^{-1}
19.	μ	Air absolute viscosity. lbf.-sec./in.^{2}	FTL^{-2}
20.	Ne	Newton's Second Law Coefficient lbf./lbm.-in./sec.^{2}	$FM^{-1}L^{-1}T^2$

Dimensions: F = Force M = Mass
L = Length T = Time

Number of pi terms = 20-4 = 16

One possible set of pi terms:

$\Pi_1 = P$

$\Pi_2 = \alpha$

$\Pi_3 = \rho_u / \rho$

$\Pi_4 = l_{2u}/l_{3u}$

$\Pi_5 = l_{2u}/l_{1u}$

$\Pi_6 = d/a$

$\Pi_7 = Ne\rho f A l_{2u}/\mu$

$\Pi_8 = Q/\rho_u f a^2$

$\Pi_9 = Nef^2A/G$

$\Pi_{10} = S/l_{2u}$

$\Pi_{11} = l_{3u}/a$

$\Pi_{12} = l_{10}/l_{3u}$

$\Pi_{13} = l_{20}/l_{10}$

$\Pi_{14} = Q_o/Q$

$\Pi_{15} = P_o/P_u$

$\Pi_{16} = l_{20}/a$

Discussion of the Dimensionless Ratios

Since the study was limited to two size classes of particles Π_3, Π_4, Π_5, Π_{12}, Π_{13}, Π_{15}, and Π_{16} remained constant throughout the entire investigation. Thus Π_1 was considered as the dependent variable and Π_2, Π_6, Π_7, Π_8, Π_9, Π_{10}, Π_{11}, and Π_{14} as the independent variables.

P was defined as the ratio of throughs to totals, measured at S. This ratio measures the response of the system due to changes in the other variables. The numerical value was obtained by dividing the weight of particles which pass through the screen between zero and S by the total weight of undersize material which was metered onto the screen. Therefore it is possible to make S sufficiently large so that P approaches unity. Likewise if S is sufficiently small, P will approach zero. In repeated sampling, P serves as an index of the probability of particle passage.

α is the angle with respect to the vertical at which motion is imparted to the horizontal screen. If for a small α, the frequency and amplitude are sufficient to induce the particles to hop, the net advance (Fig. 12) to the right will be relatively small and the number of opportunities per unit of travel, for passage through the apertures would be relatively high. As α increases, the hopping effect will diminish and the net advance will increase. It is possible to reach a point where the particles do not appear to leave the surface but merely slide along. The question arises: Is it more desirable to have the hopping effect, or the sliding effect? This would depend on the nature of the material being sized. It is true that when particles are not in contact with the screen, the opportunity for passing is lost. However, a more vigorous action is present which discourages clustering of the

material and encourages continual reorientation of the particles.

d/a is the ratio of the wire diameter in the screen to the square aperture opening. As this ratio increases, all other factors remaining constant, the number of apertures per unit screen width and length decreases. This ratio also serves as an index of roughness for the screen.

$N\rho fAl_{2u}/\mu$ is a form of Reynolds number. It is known from theory and experimental work that drag effects on particles are related to Reynolds number. This ratio seems appropriate since the particles are accelerating and decelerating in the presence of air. The average velocity in the screen is characterized by the product of frequency and amplitude. This velocity serves to describe the particle velocity in the fluid medium.

$Q/\rho_u fa^2$ is the ratio of volume flow of undersize particles per unit time to the volume swept out by the apertures per unit time. This ratio is tenable on the grounds that an increase in the volume flow rate of undersize particles would necessitate an increase in the volume swept out by the apertures, other factors being equal.

Nef^2A/G is a form of the Froude number which is an index of inertia forces to gravity forces. This type of screening system would not function without gravity forces. The magnitude of the inertia forces of the particles will be dependent on the motion in the screen. The product, Nef^2A was selected as the most appropriate means to represent the particle inertia forces.

S/l_{2u} was considered as the screen length index required to achieve a specified level of separation. If all other pi terms are held constant, variations in this ratio will cause variations in P up to

some value of s/l_{2u}. For small values of the ratio, the response P would be small. As the ratio increases, it seems likely that P would approach unity. Beyond some point large increases in S/l_{2u} would be needed to obtain relatively small increases in response.

l_{3u}/a is the ratio of the minimum dimension of the particle to the square aperture opening. For particles to be classified as undersize, $l_{3u} < a$, and $l_{2u} < a^2$. Gaudin (19) recognized the importance of this ratio in his analysis which considered only particle and screen geometry. When this ratio is small, the particles would fall through readily. As the ratio approaches unity, orientation of the particles becomes more critical, thus the total number passing would diminish per unit length of screen.

Q_o/Q is the mixing ratio of oversize particles to undersize particles. As this ratio increases, the oversize particles are more successful in reducing the number of apertures available for undersize passage.

Theoretical Analysis Under Idealized Conditions

It is extremely difficult to mathematically appraise interaction effects between particles and screen and among individual particles. However, to provide a rational basis for selecting screen motion parameters, an idealized condition was analyzed. The following assumptions were made in the analysis.

1. Simple harmonic motion was imparted to a horizontal non-perforated surface.
2. The motion was applied in a straight line path which was at an angle α with respect to the vertical.

3. Sufficient motion was imparted to the screen to insure that the particle executed small hops.
4. Minimum peak acceleration permitted in the screen was 385.728 in./sec.^{2}
5. The particle was assumed to have no relative movement with respect to the surface when in contact with the surface.
6. The particle was assumed to remain in contact with the surface until conditions were such that the particle would execute another hop.
7. The system was placed in a vacuum.

The physical system is shown in Fig. 14.

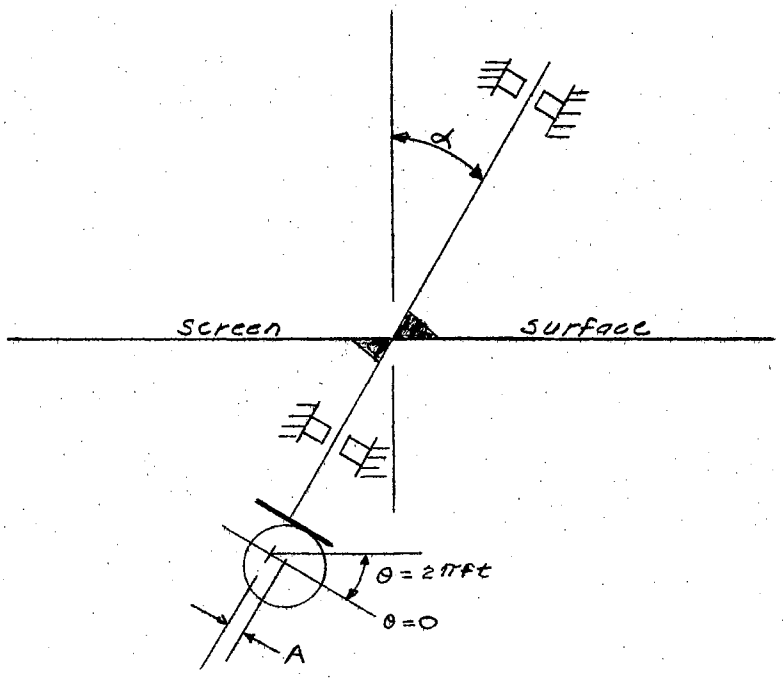

Fig. 14. Schematic of Theoretical Screening System.

Equations of motion are:

$$D = A \sin 2\Pi ft \qquad 3 - 4$$

$$\dot{D} = 2\Pi fA\cos 2\Pi ft \qquad 3 - 5$$

$$\ddot{D} = -4\Pi^2 f^2 A \sin 2\Pi ft \qquad 3 - 6$$

D = Displacement of a point on the screen (in.)

A = Maximum amplitude (in.)

f = Frequency (cps)

t = Elapsed time for rotation from reference position (sec.)

$\dot{D}$ = Velocity of a point on the screen (in./sec.)

$\ddot{D}$ = Acceleration of a point on the screen (in./sec.^{2})

The following references were used:

1. Displacement is zero when θ is zero. This occurs at the mid-point of surface travel.
2. Positive sign indicates up and negative sign down.

In TABLE III the proper signs for the angular positions are given.

TABLE III

SIGN CONVENTION FOR THE THEORETICAL SCREENING SYSTEM

θ Deg.	D in.	$\dot{D}$ in./sec.	$\ddot{D}$ in./sec.^{2}
0 - 90	+	+	-
90 - 180	+	-	-
180 - 270	-	-	+
270 - 0	-	+	+

Oscillation Effects of the Particle

The particle will execute a small hop if: (a) surface acceleration downward is equal to or greater than the acceleration effects due to the earth's gravity field and, (b) the velocity of the surface is up. In referring to TABLE III it is observed that particle hopping can be initiated only when $0 < \theta < 90$. Mathematically the following equations would apply for (a).

$$\ddot{y} \leq \ddot{D} \cos \alpha \qquad 3 - 7$$

$\ddot{y}$ = Acceleration due to earths gravitational field and is 385.728 in./sec.^{2} at Stillwater, Oklahoma.

Since $2\Pi ft = \theta$, then:

$385.728 = (4\Pi^2 f^2 A \sin\theta) \cos \alpha$

$$\theta = \sin^{-1}\left(\frac{385.728}{4\Pi^2 f^2 A \cos \alpha}\right) \qquad 3 - 8$$

θ = Angular position at which the particle commences hopping action.

Assuming zero relative velocity between particle and surface, the absolute particle velocity at the instant it leaves the surface is:

$$V = 2\Pi fA \cos\left[\sin^{-1}\left(\frac{385.728}{4\Pi^2 f^2 A \cos \alpha}\right)\right] \qquad 3 - 9$$

As the particle executes a hop, the surface may proceed through several complete cycles of motion. The particle will then impact the surface upon which another hop will occur when the condition in equation 3 - 8 is met. From this idealized concept the distance traversed in the horizontal direction can be calculated for one hop. The time between successive hops can also be calculated. An average horizontal velocity of the particle gives an indication of the conveying rate and the number of tries for particle passage. As the average velocity decreases, the probability of passing would increase, if the surface were a screen. This is obtained at the expense of the conveying rate. Another theoretical index related to passage is the angle at which the particle intercepts the surface. If the particle approaches perpendicular to the surface magnitude of forward or back scatter would tend to be diminished, thereby enhancing the possibility of passage.

A Fortran program was written for the IBM 1620 computer to solve the analytical equations. Equations 3 - 4, 3 - 5, 3 - 6, 3 - 8, 3 - 9, and Newton's 2nd Law were utilized. Conditions were selected such that Reynold's number was varied as the Froude number was held constant and vice versa.

Input to the program was:

1. Frequency (f) cps Initial - Final - Increment
2. Amplitude (A) in. One value
3. Alpha (α) deg. One value
4. Increment (AINC) deg. An increment
5. Increment (Bit) decimal A second increment

The increments control accuracy of the solution.

Output was:

1. Alpha (α) deg.
2. Frequency (f) cps
3. Amplitude (A) in.
4. Maximum acceleration in the mechanism (G) "g's"
5. Average horizontal velocity of particle (VEL) in./sec.
6. Angle with respect to the vertical at which particle impacts surface. (I) deg.
7. REY = $\Pi_7 \times \mu/Ne \times \rho \times l_{2u}$
8. FROUD = $\Pi_9 \times G/Ne$

The system was evaluated for the following range of conditions:

1. Frequency, 20 - 50 cps
2. Alpha, 35 - 65 deg.
3. REY, 20 - 62
4. FROUD, 22 - 70

Evaluation of Theoretical Calculation

The theoretical calculations are presented in Appendix A-I. Graphical analysis for some of the calculations is presented in Fig. 15, 16, 17, and 18.

Fig. 15 shows the relationship between the average horizontal velocity of a particle and screen velocity. Two unique features are revealed in this plot: (1) Horizontal particle velocity is a linear function of REY (screen velocity) when FROUD is constant and, (2) the intercept angle (I) is a function of (α) and FROUD. Thus for a constant value of (α) and FROUD, the intercept angle does not change with changes in REY. Equation 3 - 8 provides an insight to these findings. The

product f^2A remains constant while fA increases, therefore the initial velocity of the particle increases linearly. This increases the horizontal velocity and the maximum particle height which results in a greater horizontal displacement and time for impact to occur. Drag effects will tend to dimish the theoretical velocities. Introducing a mass of particles will also tend to diminish the theoretical velocities. It is unlikely that a particle could follow the idealized trajectory without encountering other particles.

Qualitative response of the system due to an increase in Π_7 is hypothesized as follows. Increasing Π_7 while holding all other pi terms constant requires that the feed rate Q be decreased in order to hold Π_8 constant. This means that fewer particles must travel with greater horizontal velocity on the screen. The layering effect of particles would be decreased which should increase the response. The increased horizontal particle velocity would tend to distribute the undersize particles further down the screen, thus lowering the response for the level of Π_{11} selected. It appears that experimental observations are needed to determine the net response due to increasing Π_7.

The horizontal velocity versus FROUD is shown in Fig. 16. REY was held constant at 53.28. A feature not depicted on the graph is that the intercept angle varies for each point calculated. The general trend is an increasing (I) with an increase in (α). Since REY remained constant, the drag effect on the particle should remain constant. The plots appear to be a family of curves. Taking larger values of the FROUD should cause the 65 deg. plot to break and assume some minimum value as do the other curves. In Fig. 17, REY was held constant at 61.27.

Qualitative response of the system due to an increase in Π_9 is

hypothesized as follows. Increasing Π_9 while holding all other pi terms constant requires that the feed rate Q be increased in order to hold Π_8 constant. This means that a greater quantity of particles must travel at a horizontal velocity dependent on the values selected for Π_2 and Π_7. For example let REY = 53.28 and α = 65 deg., Fig. 16. As Π_9 increases the horizontal particle velocity increases. The layering effect would be greater which would tend to lower the response. The increased velocity would distribute the particles further down the screen thus lowering the response for the level of Π_{11} selected. The net effect would be a decrease in system response for an increase in Π_9. Now consider α = 45 deg. and REY = 61.27, Fig. 17. Here the horizontal velocity decreases initially with an increase in Π_9. This would tend to increase response, however the depth of material would increase and lower the response. The net effect would have to be determined experimentally. At FROUD = 50, the horizontal velocity commences to increase and the response would be as described for α = 65 deg. and REY = 53.28.

For two levels of FROUD 24.00 and 41.40, the intercept angle (I) versus the angle (α) at which motion is imparted to the horizontal screen is shown in Fig. 18. As might be expected, (I) increases with (α). Changes in the intercept angle will alter the scattering effects previously described.

Maximum acceleration in the mechanism was used in design of the apparatus.

This theoretical analysis provides a general concept of system response to those parameters which can be treated mathematically.

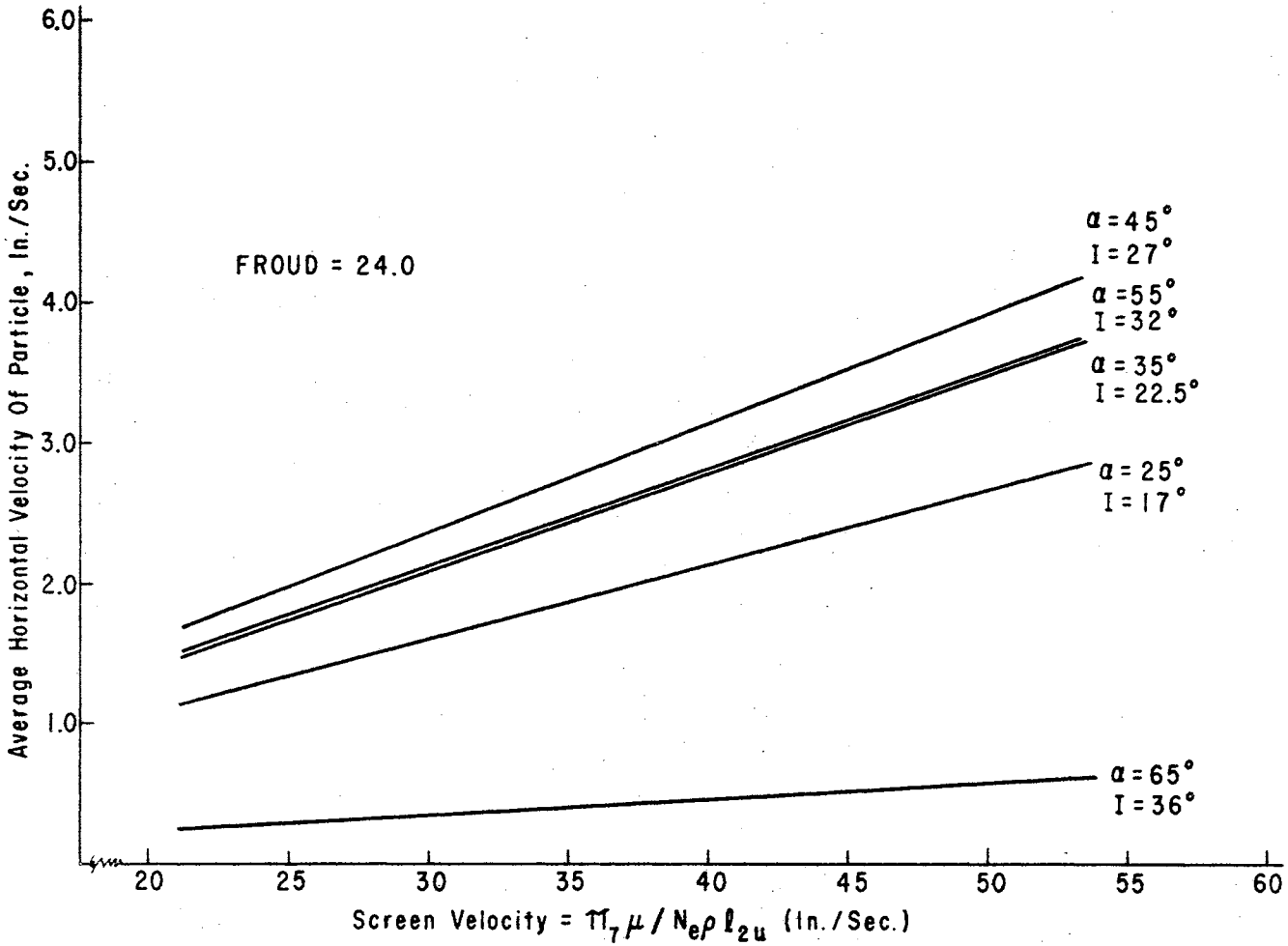

Fig. 15. Average Horizontal Velocity of Particle Versus Screen Velocity, FROUD = 24.0.

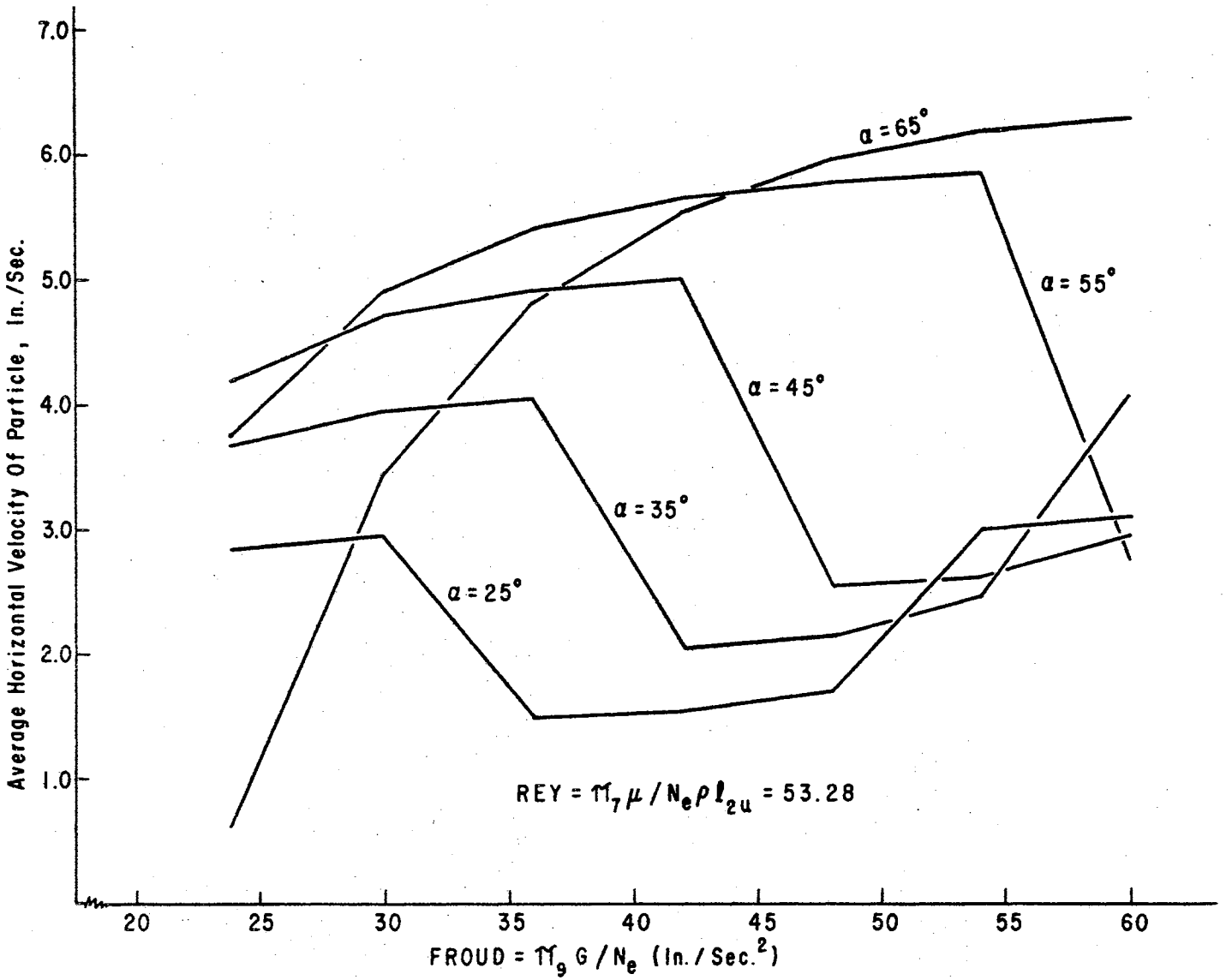

Fig. 16. Average Horizontal Velocity of Particle Versus Π_9 x G/Ne, REY = 53.28.

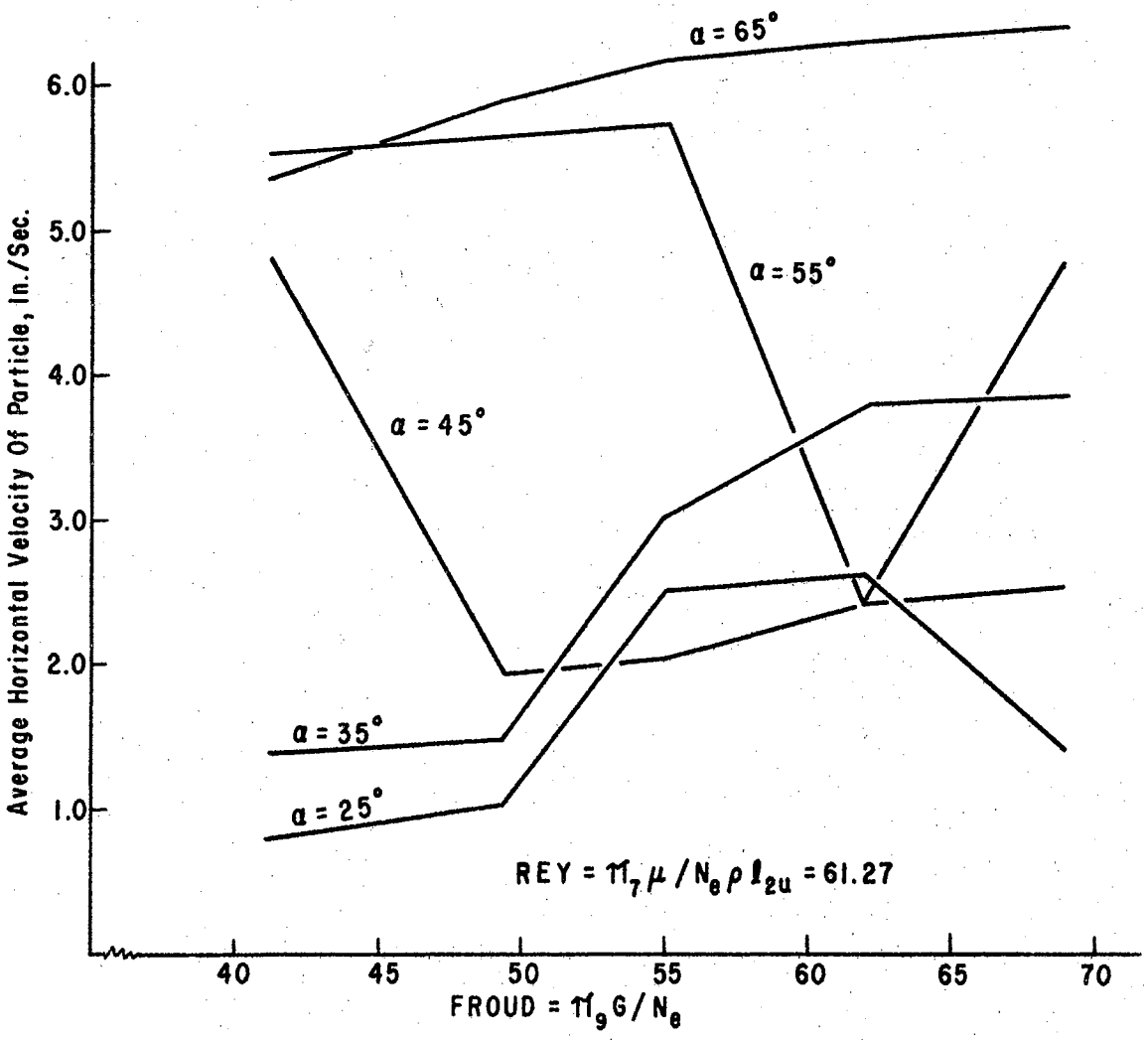

Fig. 17. Average Horizontal Velocity of Particle Versus Π_9 x G/Ne, REY = 61.27.

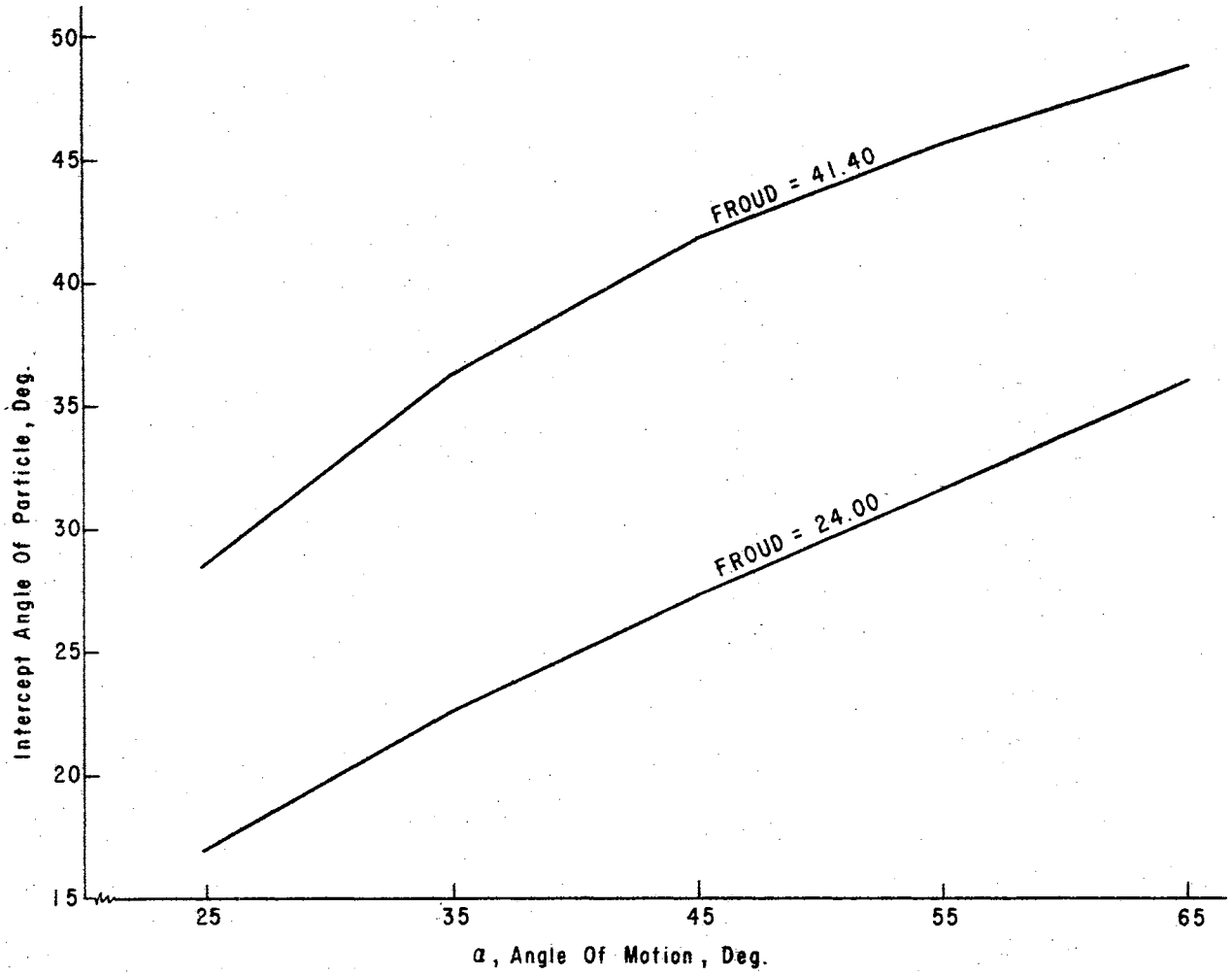

Fig. 18. Intercept Angle Versus Angle of Motion.

CHAPTER IV

APPARATUS AND EQUIPMENT

Vibrating Screen Assembly

Dynamics

From the theoretical considerations developed in Chapter III the following conditions were imposed on the design of the vibrating screen assembly:

1. The square aperture wire screen must remain horizontal while undergoing a complete displacement cycle.
2. Motion imparted to the screen is simple harmonic.
3. The motion must be imparted to the screen at an angle α with respect to the vertical.

In order to select a suitable mechanism to achieve the above requirements a dynamic analysis was made. Fig. 19 represents a follower, member OB, and an eccentric driver, member C, rotating about point D. When $\theta = 0$, the follower contacts the driver at A'. When $\theta = \theta_o$, the follower contacts the driver at A". As C rotates through the angle θ_o, follower OB rotates through the angle ϕ. If $e << L$, then:

$$\text{Tan } \phi \simeq \frac{e \sin \theta}{L + e\,(1-\cos\theta)} \qquad 4 - 1$$

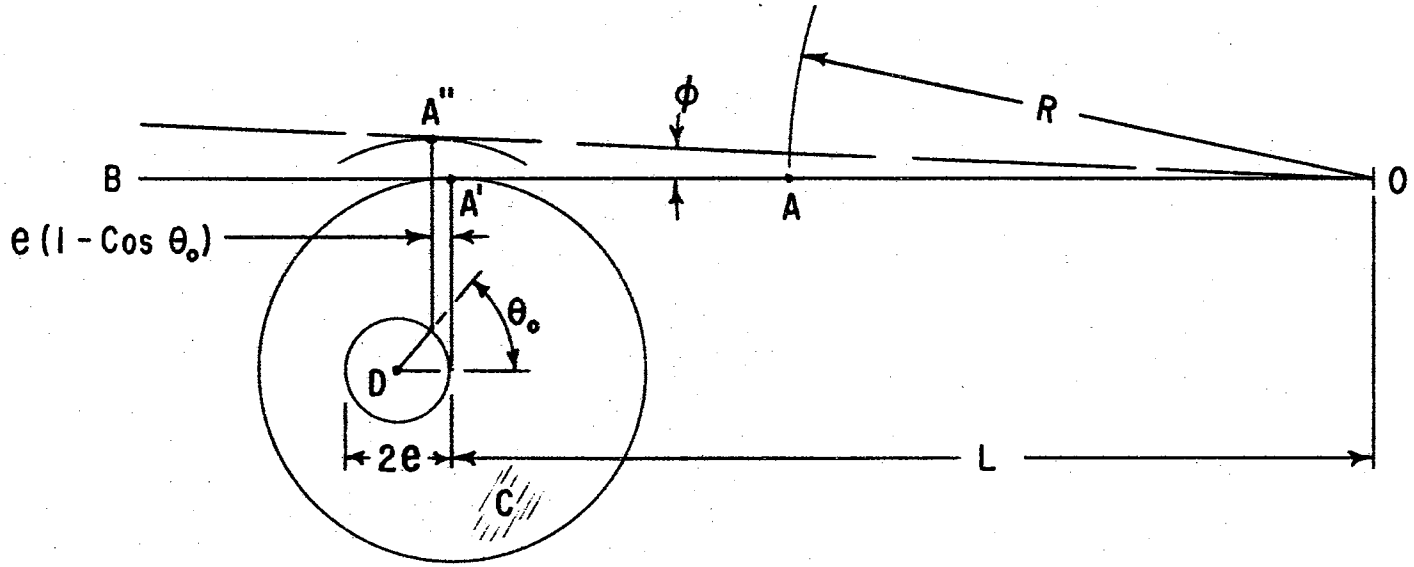

Fig. 19. Schematic of Eccentric Driver and Follower.

Equation 4 - 1 is an approximation because the true point of contact is not A" but at some point slightly to the right of A". Solving for ϕ yields:

$$\phi = \text{Tan}^{-1}\left(\frac{e \sin\theta}{L + e\,(1-\cos\theta)}\right) \qquad 4 - 2$$

Consider the point A on the follower OB. The displacement of this point along a circular patch for small ϕ is:

$$S = R\phi \qquad 4 - 3$$

Then:

$$S = R\,\text{Tan}^{-1}\left(\frac{e \sin\theta}{L + e\,(1-\cos\theta)}\right) \qquad 4 - 4$$

Taking the first and second derivatives of s with respect to θ will give the velocity and acceleration of point A along the path. Performing the differentiations and noting that $\theta = 2\pi ft$ yields:

$$\dot{S} = \frac{ds}{dt} = 2\pi feR\ (L\cos\theta + e\cos\theta - e)\left[L^2 + 2e^2 + 2Le - 2Le\cos\theta - 2e^2\cos\theta\right]^{-1} \qquad 4 - 5$$

$\dot{S}$ = in./sec.

f = frequency of driver (cps)

e = offset of driver, in.

$$\ddot{s} = \frac{d^2 s}{dt^2} = \frac{-4\Pi^2 f^2 Re \sin\theta\,(L + e)}{2e^2+L^2+2Le - (2Le+2e^2)\cos\theta} \quad -$$

$$\frac{8\Pi^2 f^2 e^2 R\ (L\cos\theta + e\cos\theta - e)\ (L\sin\theta + e\sin\theta)}{\left[2e^2 + L^2 + 2Le\ - (2Le + 2e^2)\cos\theta\right]^2} \qquad 4 - 6$$

$\ddot{s}$ = in./sec.^{2}

To achieve true simple harmonic motion, the displacement of the follower would be:

$$\bar{s} = \frac{R}{L}\ e \sin\theta \qquad 4 - 7$$

Differentiating twice yields the acceleration:

$$\ddot{\bar{S}} = 4\Pi^2 f^2 \frac{Re}{L} \sin\theta \qquad 4 - 8$$

If equation 4 - 6 is not appreciably different from equation 4 - 8, then a mechanism of the type shown in Fig. 19 will be acceptable for use in the experimental work.

For comparisons of equations 4 - 6 and 4 - 8 select the following extreme conditions:

e = 0.050 in.

R = 20.0 in.

L = 30.0 in.

f = 40 cps

θ = 90 deg.

Substituting these values into the two equations yield:

$$\ddot{S} = -3{,}152.65 \text{ in./sec.}^2 \qquad 4 - 6$$

$$\ddot{\bar{S}} = -3{,}158.27 \text{ in./sec.}^2 \qquad 4 - 8$$

$$\phi < .167 \text{ deg.}$$

$$\ddot{\bar{S}} - \ddot{S} = 5.62 \text{ in./sec.}^2$$

% variation from simple harmonic motion is:

$$\% = \frac{5.62}{3.158.27} \times 100 = 0.18$$

If additional linkage is attached to the follower OB at point A (Fig. 19) and the entire system reoriented, the arrangement shown in Fig. 20 is obtained. Now O'A' is constrained to follow OA and every point along the line AA' will experience the same displacement, velocity, and acceleration as point A in Fig. 19. α is defined as the angle at which motion is imparted to the screen with respect to the vertical. If α is selected as 45 deg., then the link OA and O'A' will arc through an angle 45 deg. $\pm$ .167 deg. under the extreme conditions which will result in a slight deviation from the desired straight line path. A screen attached to AA' would experience the same motion as A and would remain horizontal as oscillation occured about the angle α.

The acceptability of this linkage ultimately depends on the sensitivity of the instrumentation for recording the motion parameters.

Available were two ± 5g linear accelerometers. One "g" is defined as 385.728 in./sec.^{2} Also available was an oscillograph for recording a permanent trace of the acceleration-time curve. Mounting one accelerometer parallel to link AA' (Fig. 20) and the other one perpendicular to AA' will yield the "X" and "Y" components of acceleration. Considering the arcing effect previously calculated for $\alpha = 45$ deg., sensitivity of recording system can be compared with difference existing between true straight line simple harmonic motion and approximated simple harmonic motion produced by the linkage shown in Fig. 20.

Theoretical motion

$$\ddot{X} = \ddot{Y} = 3{,}158.27 \times \cos 45^\circ = 2{,}233.21 \text{ in./sec.}^2$$

Approximated motion

$$\ddot{Y} = 3{,}152.65 \times \cos (45^\circ + .167^\circ) = 2{,}222.62 \text{ in./sec.}^2$$

$$\ddot{X} = 3{,}152.65 \times \sin (45^\circ + .167^\circ) = 2{,}235.86 \text{ in./sec.}^2$$

$$\frac{2{,}235.86 \text{ in./sec.}^2}{384.7 \text{ in./sec.}^2/g} = 6.06 \text{ g's}$$

Assuming the linear range of the recording system is not exceeded, the system response is:

5g/25 lines of strip chart = .2g/line

One can estimate to 1/2 line which is .1 g

.1 g x 385.728 in./sec.^{2} = 38.57 in./sec.^{2}

If the variation between theoretical motion and approximated is less than 38.57 in./sec.^{2} then it would be impossible to detect it with

the recording system.

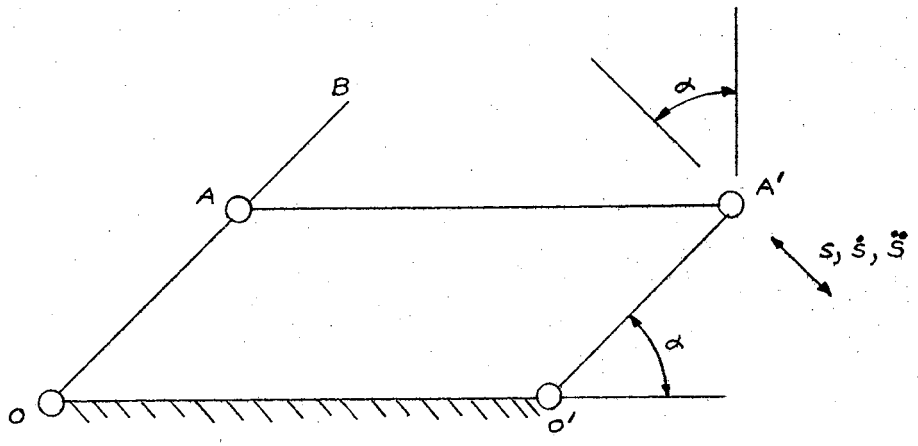

Fig. 20. Schematic of Four-Bar Linkage.

Max. diff. = $\ddot{X}$ theoretical - $\ddot{Y}$ approximate = 10.59 in./sec.^{2}

Since the difference is less than 38.57 in./sec.^{2} it appears that the linkage in Fig. 20 will be suitable for use in the experimental work.

Mechanical Design

A three dimensional schematic of the selected linkage is shown in Fig. 21. The follower assembly is held against the eccentric drive by a tension spring with a variable preload adjustment. Alignment problems are minimized by using the cam-follower drive. To achieve uniform motion at all points in the screen requires that parallel relationships exist between 12, 1'2', 43, 4'3' and 14, 1'4', 23, 2'3'. Self-aligning sealed ball bearings were bolted to a steel base plate at locations

1, 1', 4, and 4' to provide the pivot points for the linkage. Members 11' and 44' were 20-in.-long 3/4" cold rolled shafts which rested in the ball bearings. Members 12, 22', 2'1' and 43, 33', 3'4' were made of steel tubing. Each frame was welded to form a box structure. At points 2, 2', 3, and 3' self-aligning ball bearings were placed to provide the necessary support pivot points for the horizontal frame 2'233'. The horizontal frame had provisions for adjusting the lengths 23 and 2'3' after assembly to permit proper alignment of the entire linkage. The actual linkage with attached screen is shown in Fig. 22. Note the holes in the ends of the shafts which would correspond to 2 and 3 in Fig. 21. Holes were also bored at 1, 1', 2', 3', 4, and 4'. These holes were bored in the shafts with a lathe prior to frame assembly. A gauging link having pins which fit snugly into the bored holes was devised to assist in establishing equal lengths (36 in.) between points 14, 23, 2'3' and 1'4'. A spacing of 20 in. was used between 12, 1'2', 43, and 4'3'. After parallel relationships were established between the links, a piece of steel tubing was bolted to the horizontal frame along 23 and 2'3' to increase rigidity. The screen was then attached to the bolted tubing.

The steel base plate was bolted to three substantial I beam pedestals which in turn were anchored at twelve locations to a concrete test floor.

A schematic of the driver assembly is shown in Fig. 23. Pulley A was keyed to the shaft of a 1/2 HP DC electric motor and pulley B was keyed to the eccentric driver shaft. These pulleys are visible in Fig. 22. A 3/8 in. pitch Worthington positive drive was used and speed ratio from motor to eccentric driver shaft was 1:1.88. Detail of the

eccentric is shown in Fig. 24. The inside piece of the eccentric was press fitted on the driver shaft and then secured with set screws. The outside mating piece was rotated with respect to the inside member to achieve the desired offset. Two set screws were used to secure the outside member to the inside. Eccentricity could be varied from 0.004 in. to approximately 0.150 in. A precision radial ball bearing was press fitted on the outside member of the eccentric. The outer race of the bearing was in contact with a wear plate attached to the follower (oscillating linkage). This arrangement minimized movement between driver and follower.

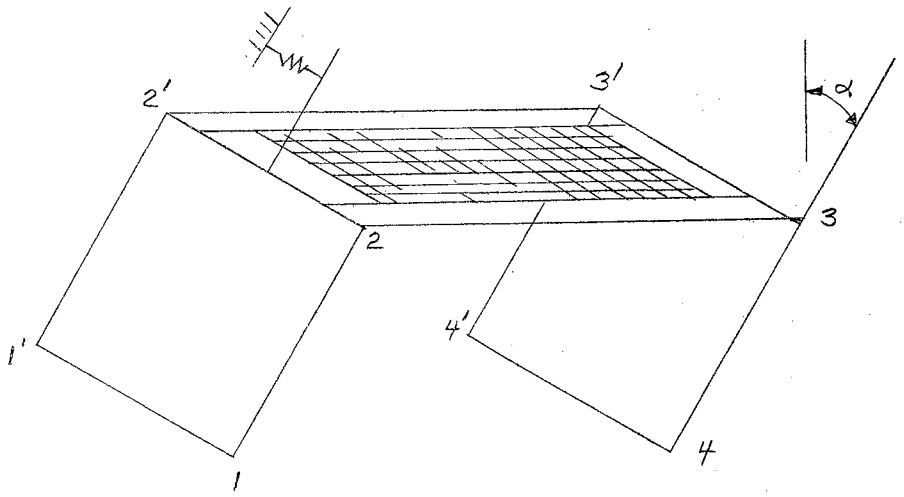

Fig. 21. Three Dimensional Schematic of the Four-Bar Linkage.

Framework for the driver was integral with the I beam floor pedestals. A tension spring with natural frequency above the operating

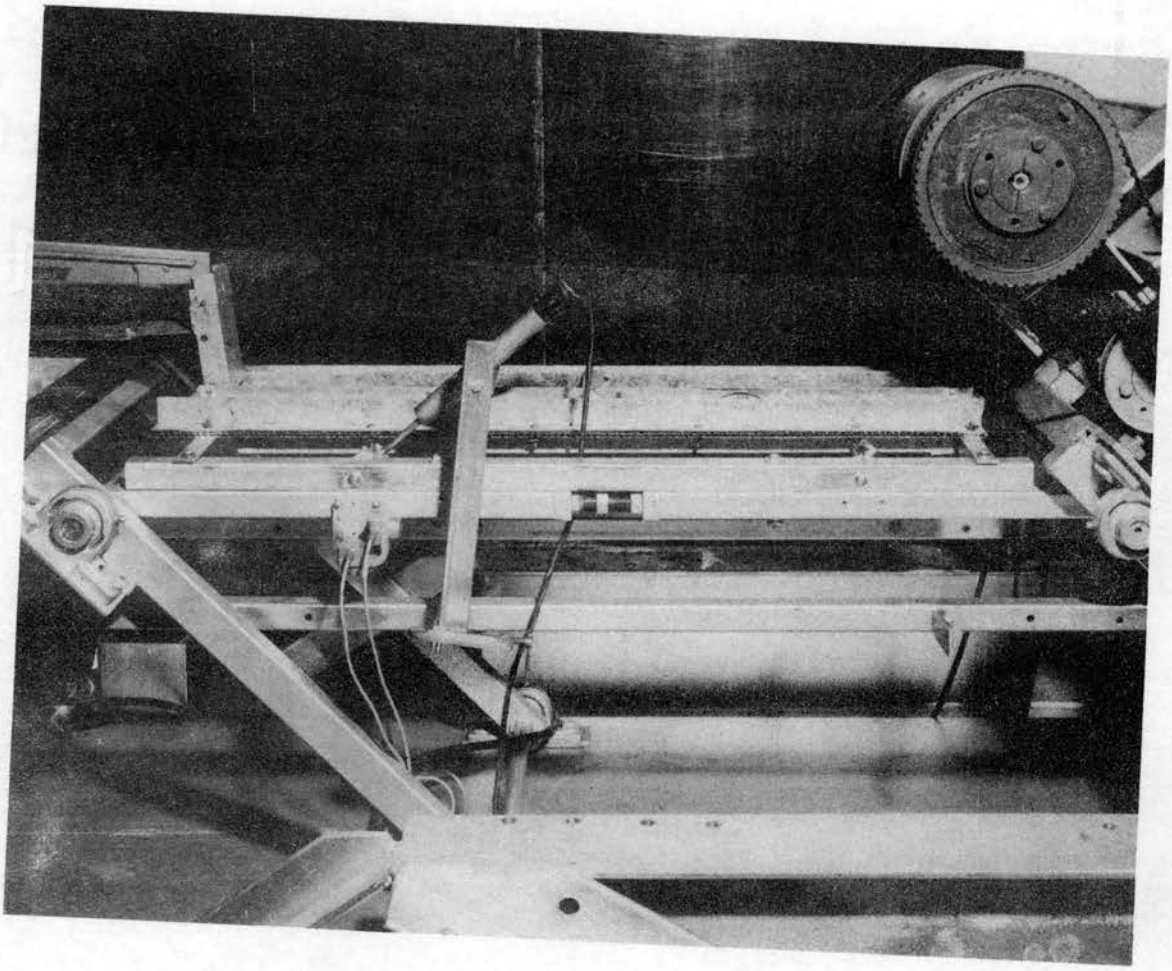

Fig. 22. Vibrating Linkage Assembly.

range held the follower against the driver.

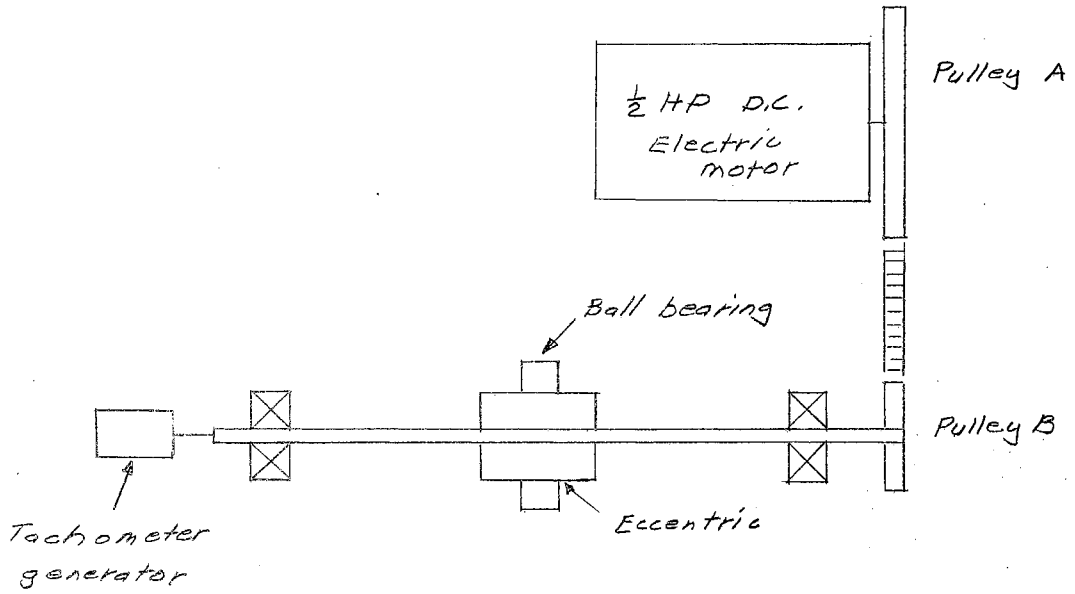

Fig. 23. Schematic of the Driver Assembly.

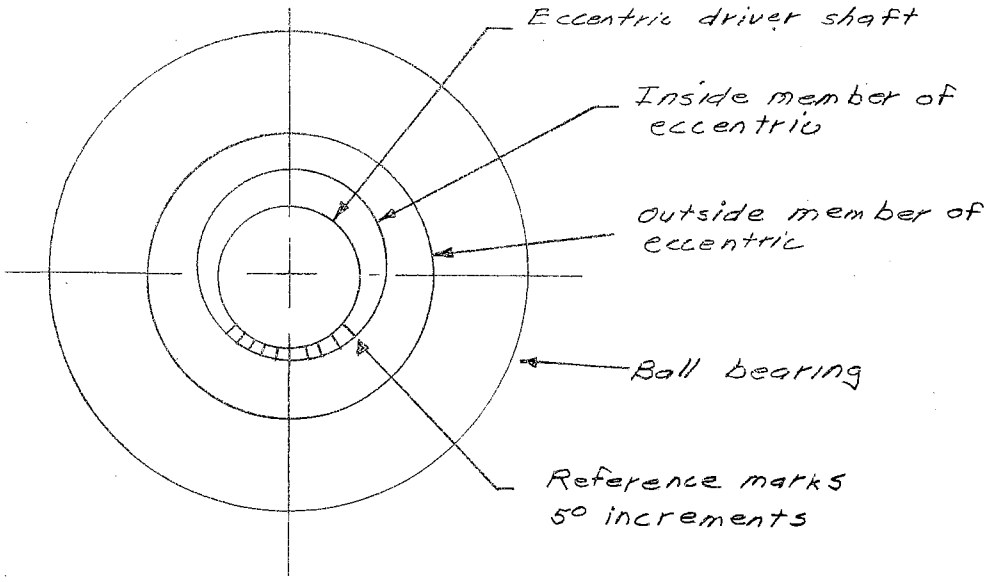

Fig. 24. Schematic of Eccentric.

Screen Assemblies

Eight screens were required for the experimental work. Square mesh steel wire cloth screen with a double crimp weave was used. Screens were 6 in. wide and 27 in. long. After evaluating preliminary experimental tests, the width was reduced to approximately 3 in. by inserting special sheet metal guide strips. The screens are pictured in Chapter V. Right angle strips of 20-gauge sheet metal were formed into upper and lower halves. The halves were bolted together with the screen in between. The bolted assembly was attached to angle iron supports which were bolted to the horizontal frame 233'2, Fig. 21 and Fig. 22.

Divider

A divider constructed from 28-gauge sheet metal was mounted below the screen to divert material passing through the screen into equal length increments down the screen. Fig. 25 shows the divider. Twenty-seven one in. increments were used, thus the material passing through each inch of screen length was collected separately. The last increment was 2 in. It collected material discharged off the screen.

The divider was mounted on horizontal members of a stationary four-bar linkage. The horizontal members were located approximately four in. below the screen and are visible in Fig. 22. This linkage will hereafter be called the accessory carriage. The accessory carriage was isolated from the mountings for the oscillating components to eliminate unwanted vibrations. The carriage could be repositioned as needed when the angle α was changed on the vibrating screen.

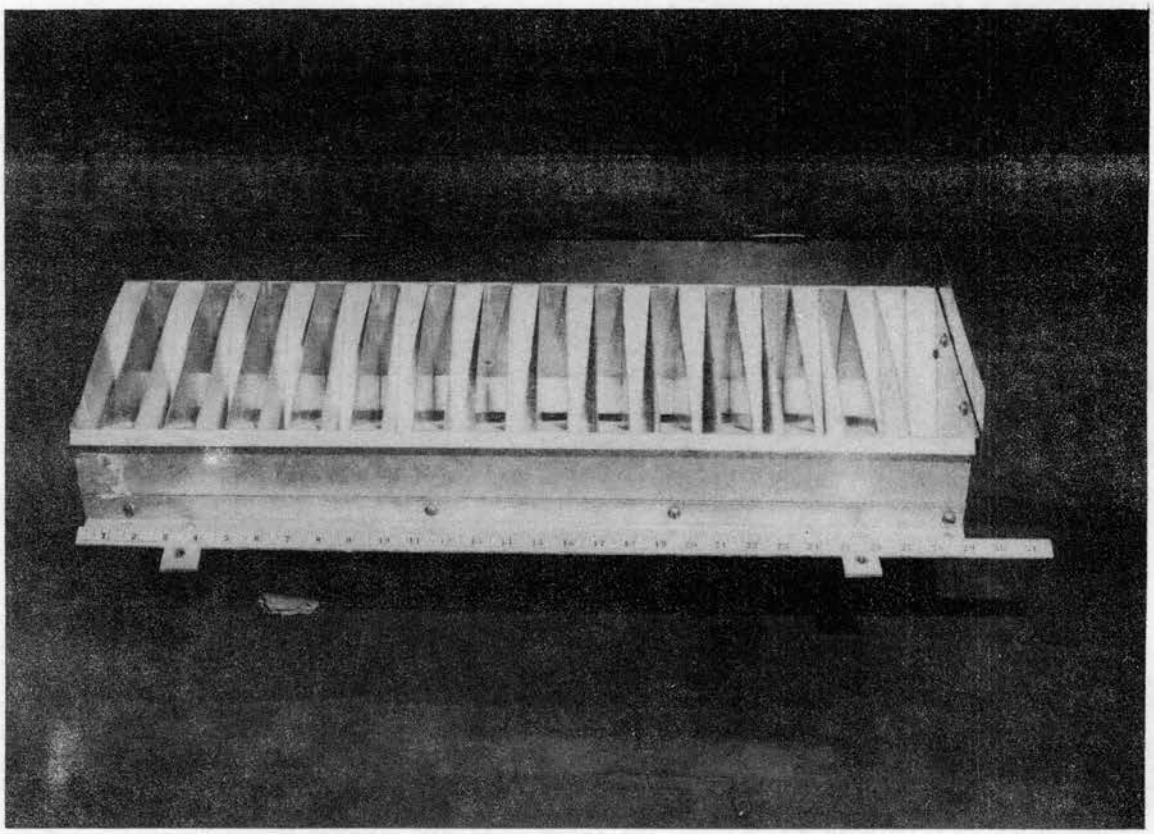

Fig. 25. Divider.

Sampling Tray

A drawer-type sampling tray rested in a slide below the divider. The slide was attached to the accessory carriage. In the tray were two rows of plastic cups for catching twenty-seven fractions of material. Volume of each cup was 10.7 $in.^3$ A metal container caught the discharge off the screen. The sampling tray is shown in Fig. 26. After inserting the tray logitudinally in the slide, movement perpendicular to the screen length could be obtained. This allowed positioning the sampling tray so that material discharging from the divider would not fall into the plastic cups. Moving the tray to another position directed the discharge into the plastic cups and metal container. Thus, a steady state flow condition was reached before a sample was drawn. Rubber flaps were fastened to three sides of the tray to prevent particles from bouncing out.

Metering Devices

Particulate material used in the experimental work was limited to two size classes, undersize particles and oversize particles. The majority of the experimental work involved use of only undersize particles. Undersize particles were metered onto the head end of the screen with the vibratory feeder shown in Fig. 27. A small storage bin and funnel were positioned above the vibrating deck. Two adjustments were available for varying the feed rate. Change in clearance between the funnel and deck was obtained with a screw adjustment. A potentiometer was used to adjust the amplitude of the vibrating tray. The feeder and a voltmeter set on a plywood deck which was bolted to the accessory

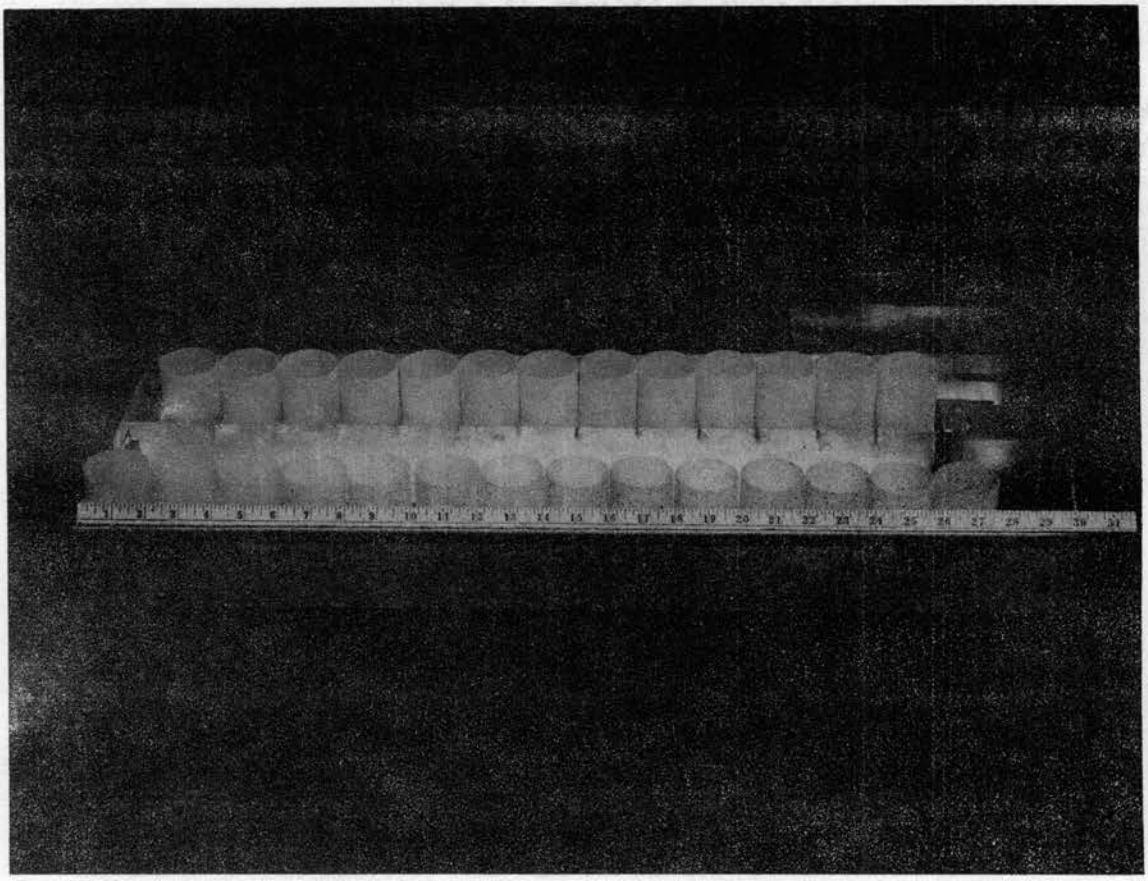

Fig. 26. Sampling Tray and Cups.

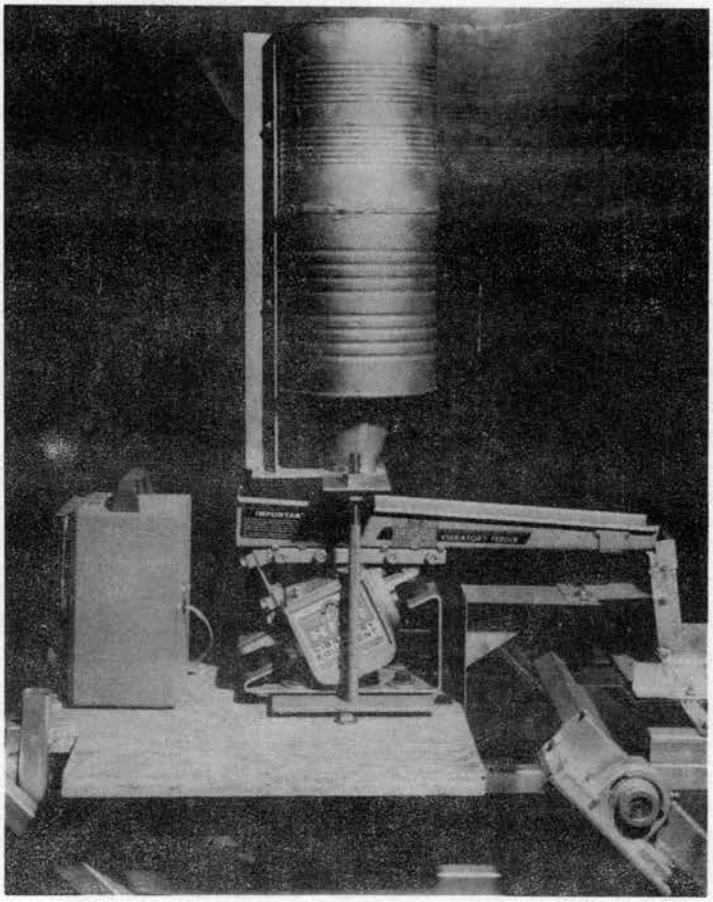

Fig. 27. Vibratory Feeder for Undersize Particles.

carriage. A control box housing the potentiometer was placed below the voltmeter and was supported by the accessory carriage.

Some of the experimental work required introducing undersize and oversize particles simultaneously to the screen. This was achieved by using the arrangement shown in Fig. 28. A second metering device for the oversize particles was positioned above the entrance to the head end of the screen. Flow was varied by changing the size of the discharge aperture. Bridging was minimized by placing a 1/4 in. diameter shaft near the aperture. The shaft was connected with a slight offset to a small high speed electric motor. Sufficient vibration was induced to permit a uniform flow. Plexiglass was put in one end of the small storage bin and the oversize particles are visible in Fig. 28. The individual metering devices permitted independent control of feed rate of undersize and oversize particles. Both size classes were thoroughly mixed before entering the screening area.

Measurement of Particle Characteristics

Size classes of undersize particles were produced with a roll grader. The grader consists of two slightly inclined parallel rotating rolls. The spacing between the rolls increased in 0.010 in. steps down the incline. Initial roll spacing could be varied. A schematic is shown in Fig. 29. A collector under each "step" caught the sized particles. The rolls turned in opposite sense as indicated on the schematic. This facilitated conveying and prevented wedging of particles in the rolls. A Graham Variable Speed Drive powered the rolls. The vibratory feeder shown in Fig. 27 was used to meter material onto the rolls.

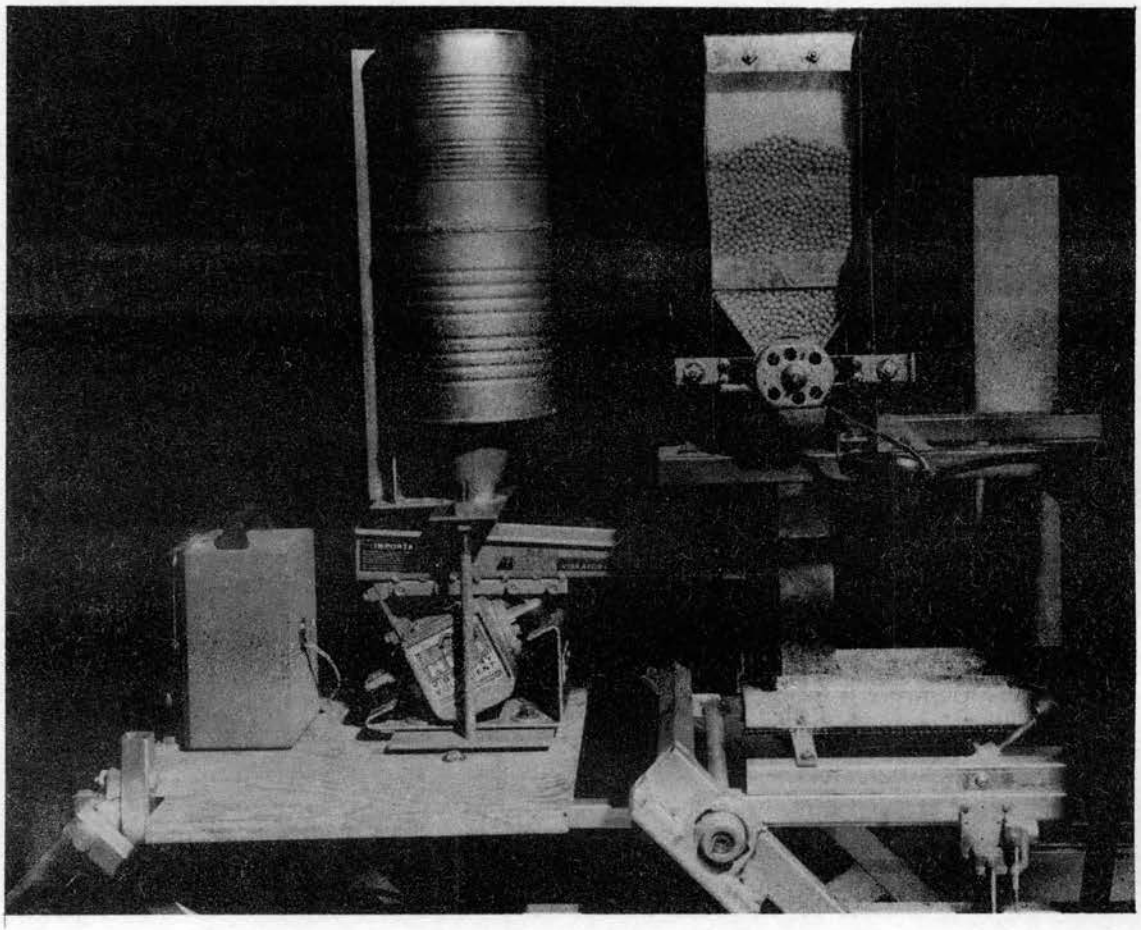

Fig. 28. Feeders for Oversize and Undersize Particles.

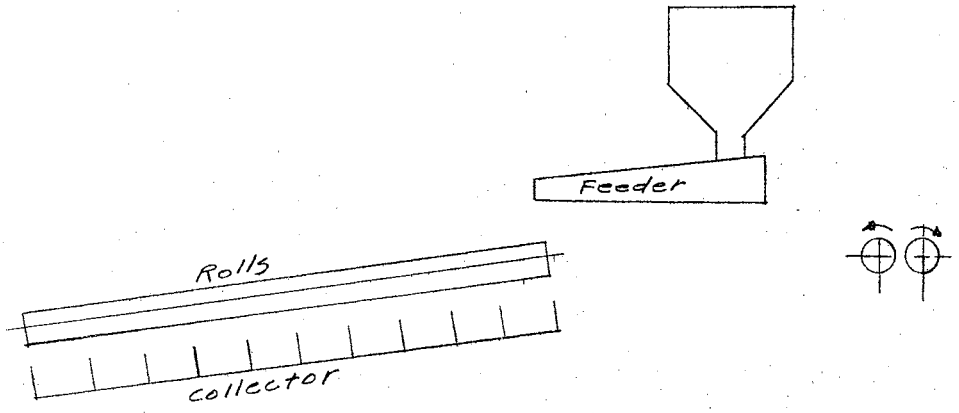

Fig. 29. Schematic of Roll Grader.

Particle length measurements were made with a micrometer and a Wilder Model A Optical Comparator. The comparator projected an image of the particle magnified twenty times on a calibrated grid.

Volume of a known mass of particles was determined by placing the mass in a volume measuring manometer (Fig. 30). Compressing the bellows with the hand crank, forces air out into the manometer raising the mercury level. The apparatus is calibrated by placing known volumes in the chamber and observing the mercury level difference. Mass and volume of particle were used to calculate material density.

Instrumentation

For the experimental work measurement and/or control of the following parameters were required:

1. Frequency of oscillation
2. Amplitude of oscillation
3. Sampling time

4. Voltage of vibratory feeder
5. Acceleration components
6. Mass

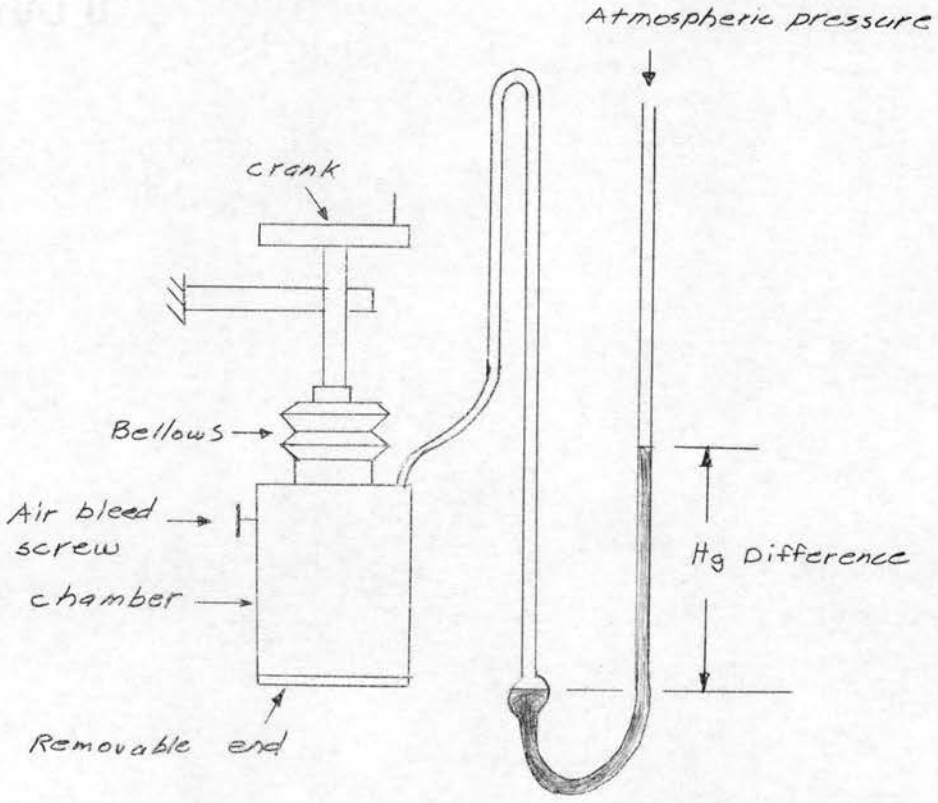

Fig. 30. Volume Measuring Manometer.

A Hewlett-Packard Model 508A tachometer generator and Model 521A electronic counter were used to measure frequency. The tachometer generator was connected to the eccentric driver shaft, Fig. 23 with a flexible connector. The 508A produces 60 counts for each revolution of its drive shaft. Useful shaft speed range is from approximately 15

RPM to 40,000 RPM. The output voltage from the transducer is a linear function of shaft speed. Counts produced by the generator were fed into the 521A counter. With the gate selector switch in the 1 SEC. position the number of electrical events occurring during an accurate one second interval were counted and displayed across the front panel to an accuracy of ± 1 cycle. Approximately every ten seconds a new count was displayed.

Satisfactory speed control was achieved with a Master shunt wound 1/2 HP direct current motor and a Minarik Model SH-56EFB motor speed control. The SH-56EFB converts AC line voltage to DC. Motor speed (90-1725 RPM) was controlled by a variable autotransformer supplying voltage to the armature rectifiers.

A Schaevitz model 1000 S-L linear variable differential transformer was used to measure displacement of the vibrating screen. Transformer housing was held by an adjustable bracket which was C-clamped to the accessory carriage (Fig. 22). The core was secured to the vibrating linkage and oriented perpendicular to OA (Fig. 20 and 22).

Excitation voltage to the differential transformer was supplied by a Daytronic Model 400 A differential transformer amplifier. Output voltage of the 1000 S-L was demodulated and filtered by the 400A. The demodulated and filtered signal was fed into a Dumont Type 401A oscilloscope and a Brush Mark II Recorder. The oscilloscope gave a continuous visual check on the linearity of the system. A permanent trace of displacement versus time was recorded on the Brush recorder. The displacement transducer was calibrated by placing it in a stand and displacing the core a known distance and then adjusting amplifier gain as desired.

Sampling time was recorded with the timer on a Standard Model SG-6

Chrono-Tachometer. Moving the sampling tray to the sampling position actuated a normally open micro switch. This switch started the timer. Moving the tray to the non-sampling position stopped the timer. Smallest time increment which could accurately be read from the dial was .06 sec.

Two CEC (Consolidated Electrodynamics Corporation) Type 4-202-0012 strain gauge accelerometers were oriented at right angles on a triaxial mounting bracket. This bracket was attached to the horizontal member of the vibrating linkage (Fig. 22) so that vertical and horizontal components of acceleration were sensed. Excitation of the accelerometers and subsequent recording of acceleration components on a permanent trace were achieved with a Sanborn Model 321 Duel Channel Carrier-Amplifier Recorder.

The vibratory feeder for metering undersize particles is quite sensitive to changes in line voltage. To minimize the effects of fluxuating voltage, a Stabiline Automatic Voltage Regulator, Type IE 51005 was installed between the AC source and the vibratory feeder control box. Leads from the feeder control box (potentiometer) output were connected to a Heathkit Model V-7A vacuum tube voltmeter (Fig. 27). Thus, the voltage to the feeder could be adjusted as needed.

Balance scales were used for weighing all samples. Mass to the nearest 0.1 gram could be detected.

CHAPTER V

EXPERIMENTAL PROCEDURE

Experimental Design

The pi terms were formulated in Chapter III. In order to restrict the study Π_3, Π_4, Π_5, Π_{12}, Π_{13}, Π_{15}, and Π_{16} were held constant. The dependent variable was Π_1. Independent variables were Π_2, Π_6, Π_7, Π_8, Π_9, Π_{10}, Π_{11}, and Π_{14}. These pi terms are dimensionless and independent as set forth by the Buckingham Pi Theorem.

One of the objectives in this study was to develop a prediction equation for passing undersize particles through the apertures. The general form was $\Pi_1 = f(\Pi_2, \Pi_6, \Pi_7, \Pi_8, \Pi_9, \Pi_{10}, \Pi_{11})$. Due to the large number of independent variables under investigation, the experimental schedule suggested by Murphy (24) was used. One pi term was varied while the others were held constant. Component equations were developed using the least squares method. The mathematical form of the component equations suggested the form for the prediction equation. Then the least squares method was used to formulate the prediction equation. The experimental schedule is shown in TABLE IV.

A second part of the experimental work consisted of mixing undersize and oversize particles in varying proportions. The experimental schedule is shown in TABLE V.

TABLE IV

EXPERIMENTAL SCHEDULE PART I

Π_1	Π_2	Π_6	Π_7	Π_8	Π_9	Π_{10}	Π_{11}
Observed Response	35° 45° 55° 65°	.4705	3.77	0.86	0.05	21.25	.5788
	45°	.1904 .3214 .4705 .7228	3.77	0.86	0.05	21.25	.5788
	45°	.4705	3.35 3.77 4.85 5.15	0.86	0.05	21.25	.5788
	45°	.4705	3.77	.31 - - - * - - 1.26	0.05	21.25	.5788
	45°	.4705	3.77	0.86	.029 .038 .050 .056 .070	21.25	.5788
	45°	.4705	3.77	0.86	0.05	14.16 21.25 28.33 35.41 42.49	.5788
	45°	.4705	3.77	0.86	0.05	21.25	.4315 .5072 .5788 .7182 .8707

*7 levels were run for each replication

TABLE V

EXPERIMENTAL SCHEDULE PART II

Π_1	Π_{14}
Observed Response	0.1270 - - -* - - 0.6631

Value of pi terms held constant:

$\Pi_2 = 45$ $\Pi_3 = 1,223,844$

$\Pi_6 = .4705$ $\Pi_4 = 1.435$

$\Pi_7 = 3.77$ $\Pi_5 = 0.850$

$\Pi_8 = 0.86$ $\Pi_{12} = 2.455$

$\Pi_9 = 0.05$ $\Pi_{13} = 0.998$

$\Pi_{10} = 21.25$ $\Pi_{15} = 0.954$

$\Pi_{11} = .5788$ $\Pi_{16} = 1.421$

*A total of 16 tests were run

Randomization Procedure for Pi Terms

Randomization procedure of the experimental schedule in TABLE IV was developed in accordance with adjustment features in the test equipment. In theory it would have been desirable to completely randomize the pi terms and their respective levels. Practical considerations did not permit this.

The pi terms were run in the order listed in TABLE VI. The response due to Π_{10} was obtained from the same set of observations as Π_7. Each level within each pi term was replicated three times. Levels and replications were completely randomized for Π_7, Π_8, Π_9, amd Π_{10}. Levels were randomized, but not replications for Π_2, Π_6, amd Π_{11}.

TABLE VI

ORDER IN WHICH PI TERMS WERE INVESTIGATED

Order	Pi Term
1	Π_8
2	Π_9
3	Π_7 & Π_{10}
4	Π_6
5	Π_{11}
6	Π_2

For the schedule in TABLE V, Π_{14} was varied by varying Q_o. Since feed rate for Q_o varied appreciably from run to run for the same gate setting, an unequal number of replications were run for each gate setting. This is listed in TABLE VII.

Procedure Used in Conducting a Test

A procedure was developed to insure consistency in recording the

observations necessary to evaluate the pi terms for each test. The precise order is listed below:

1. Adjust eccentricity to desired level.
2. Turn on d.c. electric drive motor and allow speed to stabilize.
3. Adjust motor speed to desired level.
4. Record dynamic displacement of oscillating screen on Brush Recorder.
5. If displacement does not agree with test schedule, stop motor and readjust eccentricity, then proceed to step 2. If displacement is correct proceed to step 6.
6. Record horizontal and vertical components of acceleration. Identify traces.
7. Record total displacement in inches on the data sheet.
8. Adjust voltage on the vibratory feeder to the desired level.
9. If $\Pi_{14} \neq 0$ proceed to step 10. If $\Pi_{14} = 0$ proceed to step 11.
10. Adjust gate stop as required on oversize particle feeder.
11. Visually check to see if frequency is at proper level. If not, adjust accordingly.
12. Energize power switch on Standard Chrono-Tachometer (clock-timer).
13. Turn on vibratory feeder.
14. If $\Pi_{14} \neq 0$ proceed to step 15. If $\Pi_{14} = 0$ proceed to step 16.
15. Turn on oversize particle feeder.
16. When steady state flow condition is reached, slide sampling tray into sampling position.
17. When leading cups become 3/4 full, retract sampling tray to previous position.

18. Observe displayed frequency (RPM) and record on data sheet.
19. Turn off vibratory feeder.
20. If $\Pi_{14} \neq 0$ proceed to step 21. If $\Pi_{14} = 0$ proceed to step 22.
21. Turn off oversize particle feeder.
22. Count and record on data sheet the number of apertures blocked by seeds.
23. Turn off power switch on timer.
24. Record sampling time on data sheet.
25. Reduce motor drive speed to "idle."
26. Remove sampling tray and place on nearby table.
27. Weigh amount collected in each cup and record on data sheet.
28. If $\Pi_{14} \neq 0$ proceed to step 29. If $\Pi_{14} = 0$ proceed to step 30.
29. Separate oversize and undersize particles and weigh both fractions, then record on data sheet.
30. Calculate flow rate using slide rule. If rate is not in predetermined range, test is invalid.
31. Empty tray, replace cups, and insert tray under divider. Place in non-sampling position.
32. Adjust rubber flaps on tray so that particles can not bounce out.
33. Recheck sampling time and set clock to zero.

Procedure for Evaluating Individual Elements in the Experimental Design

Evaluation of the dimensionless ratios required measurement of some of the individual elements in the ratios. Careful consideration was given in selecting the value of the ratios for Π_6 and Π_{11}. This

entailed selecting a suitable material for undersize and oversize particles and then selecting an acceptable set of screens to meet the requirements.

TABLE VII

REPLICATING SCHEDULE FOR PART II

Π_{14} level	Gate Setting in.	No. of Replications
1	1/2	4
2	5/8	2
3	11/16	2
4	3/4	4
5	13/16	1
6	1	3

For undersize particles a geometrical shape other than a sphere seemed desirable from the standpoint of stability. Placing a sphere on a horizontal vibrating screen could induce unwanted rolling of the particle. Grain sorghum appeared to possess the desired stability. Its three characteristic dimensions occur in the approximate ratio of 1:1.4:1.7. Two samples of grain sorghum were obtained and individually processed in the roll grader. Sample size was about 75 lbm. (pounds mass). Sufficient material was drawn at random from each sample to determine the size distribution for each sample. Then the four size

classes having the highest yield in each sample were further analyzed. Ten seeds were selected at random from each size class and three length measurements were made on each seed with a micrometer. Mean lengths and variances were calculated for each size. Thus, eight different size classes were available from which one could be selected for the test work.

Selection of one size class from the eight that were constructed was determined by the availability of commercial screens. Tyler Specifications Tables for woven wire screen were consulted. From these tables a set of screens were found which would meet the conditions imposed by Π_6 and Π_{11}. This set is shown in TABLE VIII. A manufacturer was then located who supplied them as stock items.

TABLE VIII

SPECIFICATIONS FOR WOVEN WIRE SCREEN

Identity	Mesh Openings/in.	Wire Diameter in.	Aperture Size in.	Π_6	Π_{11}
1	3	0.105	0.228	0.46	0.44
2	3 1/2	0.092	0.194	0.47	0.51
3	4	0.080	0.170	0.47	0.59
4	5	0.063	0.137	0.46	0.73
5	6	0.054	0.113	0.48	0.88
6	3 1/2	0.120	0.166	0.72	0.60
7	4 1/2	0.054	0.168	0.32	0.59
8	5	0.032	0.168	0.19	0.59

Numerical values of Π_6 and Π_{11} in TABLE IV are slightly different than in TABLE VIII. The size class of material used in establishing TABLE VIII was later processed in the roll grader a second time to increase the uniformity of the material. At this stage approximately 3 1/4 gallons of test material were available. After that the grain sorghum was visually inspected in small quantities for presence of cracked seeds. These cracked seeds were removed with tweezers. This operation reduced the quantity of experimental material by about 2%. Twenty-five seeds were selected at random from the experimental material and the three characteristic lengths were determined. The minimum dimension, flat side of seed, was measured with a micrometer. The intermediate and maximum dimensions were determined by placing the seed on its flat side under the optical comparator. From these twenty-five observations mean values for the lengths were used in the relevant calculations for TABLE IV.

Screen dimensions as specified by the manufacturer were used in the pi terms affected. Note in TABLE VIII that each screen has an identity number. The eight screens are shown in Fig. 31, 32, and 33. Upon completing the experimental schedule in TABLE IV, a 2 in. piece was removed 10 in. from the head end of screen No. 3. This screen was used in the experimental schedule as outlined in TABLE V. Removal of the section allowed the oversize particles to discharge relatively soon which resulted in a more precise measurement of oversize particle flow rate. Nearly all undersize particles had passed through the aperture before reaching the discharge point.

Plastic balls were selected as the oversize particles. Nominal diameter was 1/4 in. The balls were a pale green which made it easy to

distinguish them from the dark colored grain sorghum. Twenty-five balls were drawn at random from the one gallon sample and two length measurements were made on each ball with the optical comparator. In the experimental work the two size classes were thoroughly mixed prior to entering the screening area. The resulting mixture flowed uniformly down the screen. The experimental materials are shown in Fig. 34. Grain sorghum is on the left and plastic balls on the right.

The vibratory feeder, Fig. 27, was calibrated prior to running the experiment. A graph of voltage setting versus feed rate in lbm./sec. was obtained. Seventeen levels of voltage were replicated three times. The 51 runs were completely randomized. Prior to each run the grain sorghum was thoroughly mixed before filling the hopper. Thus all of the experimental material was used at some time during the calibration test. It was observed that the calibration curve would shift slightly from day to day. To determine the amount of shift, about ten samples were run each morning prior to conducting the main test work.

An attempt was made to calibrate the feeder for the plastic balls. Although uniform flow was achieved for each run, variation in feed rate from run to run was appreciable. In view of this a minimum gate setting of 1/2 in. and a maximum of 1 in. was established. Variation in feed rate of oversize particles from run to run was not detrimental since it was reflected in the independent variable being investigated, Π_{14}.

The volume measuring manometer was calibrated by using 17 known volumes replicated three times. A graph, volume ($in.^3$) versus Hg differential (mm) was made.

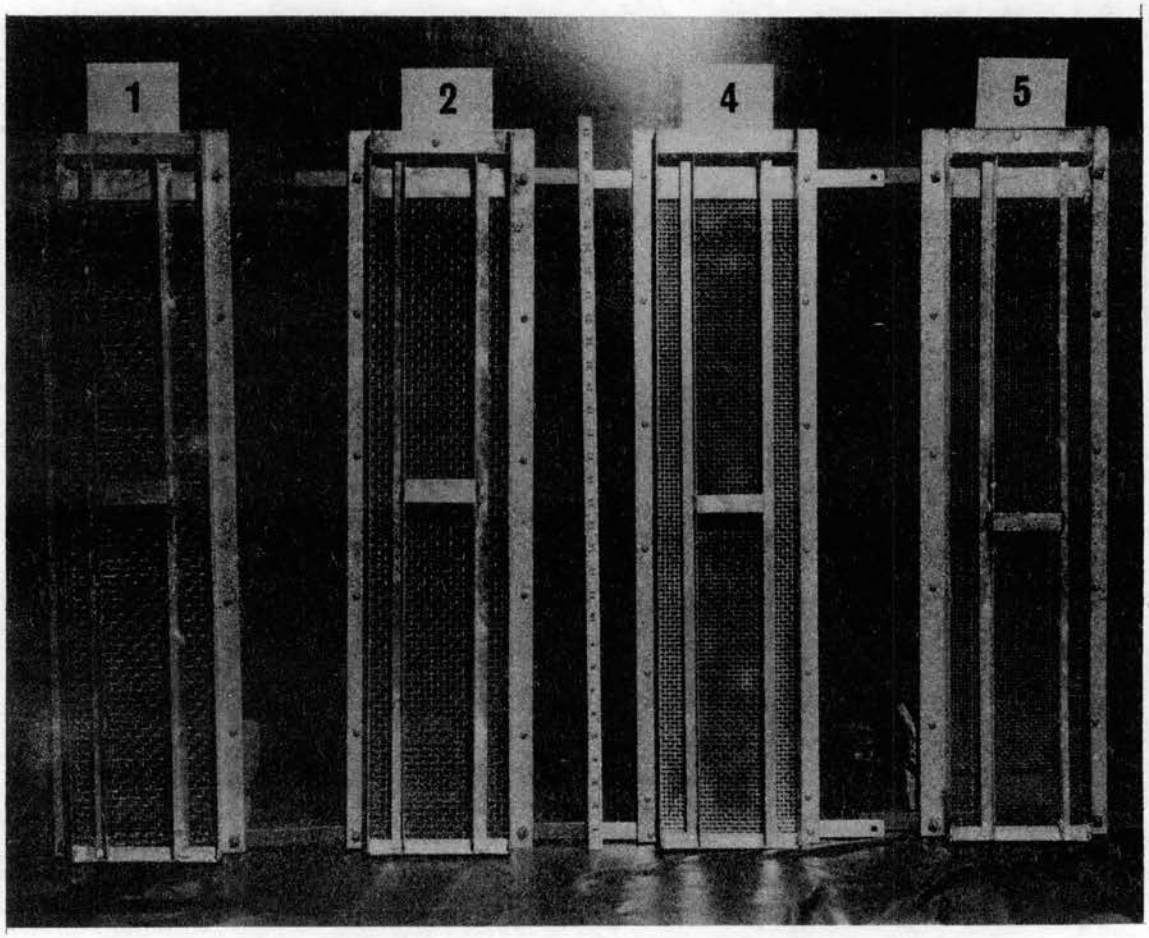

Fig. 31. Screen Assemblies.

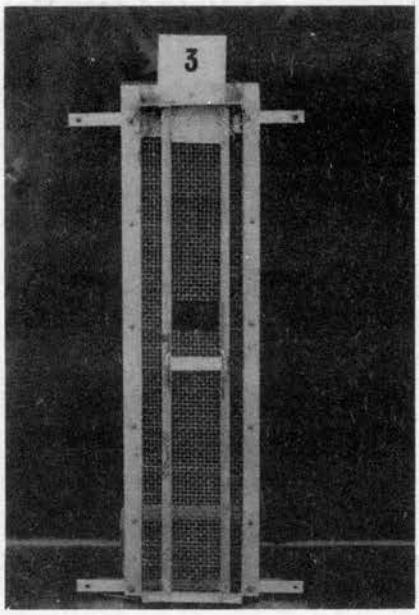

Fig. 32. Screen Assembly.

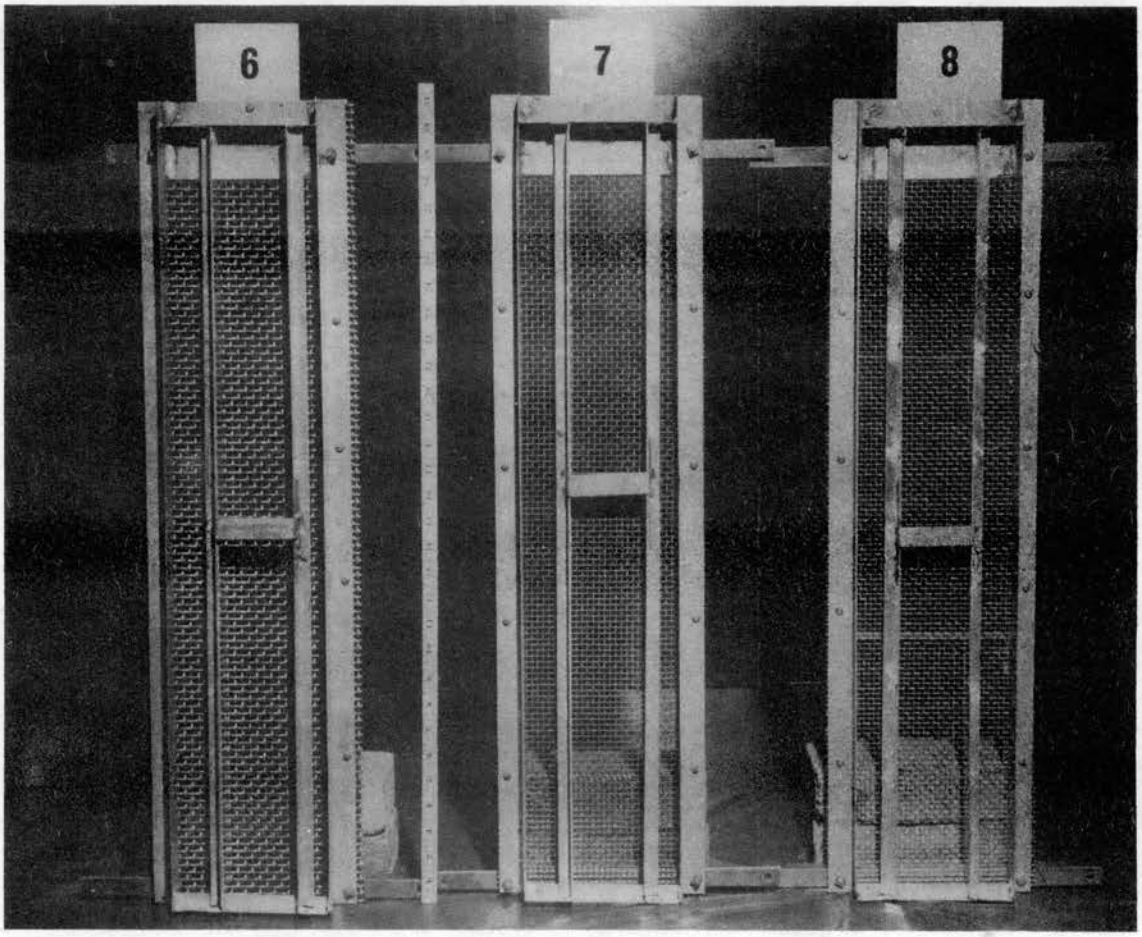

Fig. 33. Screen Assemblies.

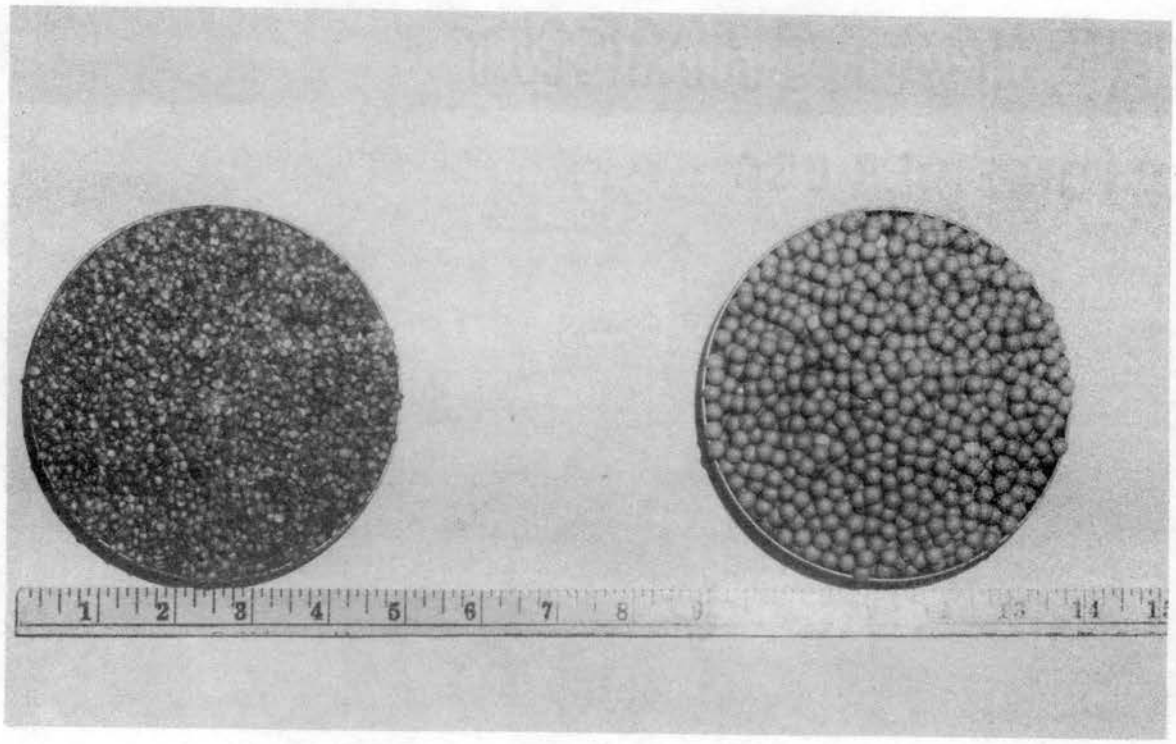

Fig. 34. Undersize and Oversize Particles.

Density of grain sorghum and plastic balls was determined by weighing and measuring the volume of six samples of each material. The materials were thoroughly mixed before drawing the sample.

The linear variable differential transformer was calibrated by placing it in a small test stand. The core was attached to a point gauge. Gain on the amplifier was adjusted so that either .002 in. per chart line or .005 in. per chart line could be achieved. At the end of each day a displacement trace was run at about 2 cps. The following morning another trace was run under the same conditions and the two were compared. If they did not agree the coil was recalibrated in the test stand. Over a period of six weeks, two recalibrations were necessary. About every seven days the coil was placed in the test stand and the calibration checked as an additional precaution.

Preliminary tests gave indication that the two accelerometers did not respond the same under like conditions. To determine where the difference occured, each accelerometer was checked against a test accelerometer in the Mechanical Engineering Laboratories.

The accelerometers were calibrated under static conditions. Accelerometer #3138 was connected to the left channel of the Sanborn Recorder and #3132 was connected to the right channel. #3138 sensed horizontal acceleration and #3132 sensed vertical acceleration. With accelerometers oriented as shown in Fig. 22, reference lines of zero output were established on the strip chart. Each accelerometer was rotated 90 deg. This induced a strain equal to one g of acceleration. Gains on the amplifiers were then adjusted to the desired levels. One should note that this calibration procedure is good only for the condition, G = 1.

Screen motion was evaluated prior to doing the experimental work and additional evaluation was made during the tests. Evaluation under static and dynamic conditions was made.

Four points for sampling screen motion were located and identified as shown in Fig. 35. In Fig. 22 the accelerometers and displacement coil are mounted at location 4.

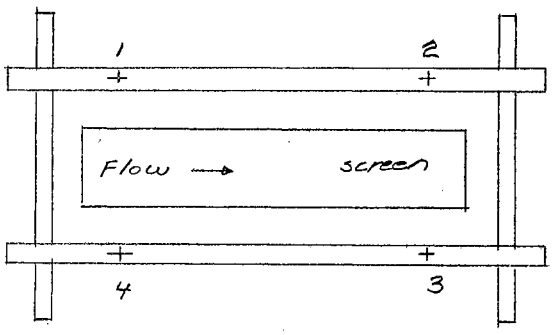

Fig. 35. Four Locations for Sampling Screen Motion.

Static response was evaluated by setting the eccentric at four levels and recording the total vertical displacement at the four sampling locations. An Ames Dial Indicator was used to determine the displacement to the nearest .0005 in. Three replications were run for each dial setting. The 12 tests were completely randomized.

Dynamic response was evaluated by measuring frequency, displacement, and acceleration components. Inertia forces resulted in member deflection which induced displacements appreciably above those obtained for static settings. Therefore it was necessary to run frequency-displace-

ment curves for the various eccentricity settings. From these curves suitable combinations of frequency and displacement were obtained to achieve the levels of Π_7 and Π_9 as required in the experimental schedule. Numerical values of acceleration components did not enter into any of the pi terms. However they were useful in evaluating screen motion before and after linkage adjustments and frame modifications. Acceleration traces were recorded for all formal tests.

A majority of the experimental work was conducted at a frequency of 28.5 cps and amplitude of .024 in. ($\Pi_7 = 3.78$, $\Pi_9 = .05$). For this frequency and amplitude, acceleration components and amplitudes were recorded at the four sampling locations.

CHAPTER VI

PRESENTATION AND ANALYSIS OF DATA

Data Relevant to Undersize and Oversize Particles

After preparing the undersize material as described in Chapter V, twenty-five seeds were drawn at random and three length measurements were made. Results of these measurements are shown in TABLE IX. Dimensions of each seed are presented in Appendix B-I.

TABLE IX

DIMENSIONS OF UNDERSIZE PARTICLES

Length	Mean Value in.	Standard Deviation of Mean in.
l_{1u}	0.1661	0.0107
l_{2u}	0.1412	0.0077
l_{3u}	0.0984	0.0020

An F test at the .5% level indicated that the variance of l_{3u} was significantly smaller than the variance of l_{1u} or l_{2u}. This was expected since the roll grader classified particles based on their

minimum dimension.

Commercial plastic balls were used as the oversize particles in the study. To assess their sphericity, twenty-five balls were selected at random and two length measurements were made. The lengths were perpendicular to each other and in the same plane. Results of these measurements are shown in TABLE X. Dimensions for each ball are presented in Appendix B-II. Mean values for all length measurements were used in calculating pi terms.

TABLE X

DIMENSIONS OF OVERSIZE PARTICLES

Length	Mean Value in.	Standard Deviation of Mean in.
l_{10}	0.2420	0.0040
l_{20}	0.2416	0.0037

The volume measuring manometer was calibrated prior to evaluating the density of the undersize and oversize particles. The calibration curve is presented in Appendix D-I.

Measurements made and used in calculating density of particles are presented in Appendix B-III. Mean density of the undersize particles was 50.3×10^{-3} lbm./in.^{3} Standard deviation of the mean was .0014. Mean density of the oversize particles was 48.0×10^{-3}. Standard

deviation of the mean was .0003.

The calibration curve for the vibratory feeder is presented in Appendix D-II.

Data Relevant to Wire Screens

Initial screen width was 6 in. Preliminary tests indicated that reducing the width would achieve greater compatability between screen capacity and vibratory feeder capacity. Each screen width was reduced to approximately 3 in. Guide strips were positioned so that each screen width was a whole number of apertures. Width of each screen is shown in TABLE XI. Wire diameter and aperture for each screen as

TABLE XI

WIDTH OF TEST SCREENS

Identity	Width/in.
1	2.8125
2	3.0000
3	2.9375
4	2.8750
5	2.6667
6	2.8130
7	2.9375
8	2.7500

specified by the manufacturer were used in calculating the relevant pi terms. An indication of the deviation from the manufacturer specifications was obtained by measuring wire diameter and aperture size at three random locations for each screen size used. Mean values and specifications (nominal) are given in TABLE XII.

TABLE XII

EVALUATION OF SCREEN DIMENSIONS

Identity	Wire Diameter (mean) in.	Aperture (mean) in.	Diameter Nominal in.	Aperture Nominal in.
1	.1043	.2380 x .2253	.105	.228
2	.0917	.1957 x .1837	.092	.194
3	.0803	.1740 x .1690	.080	.170
4	.0627	.1373 x .1413	.063	.137
5	.0543	.1110 x .1097	.054	.113
6	.1190	.1690 x .1677	.120	.166
7	.0533	.1713 x .1757	.054	.168
8	.0317	.1640 x .1677	.032	.168

Analysis of Screen Motion

Theoretical values were calculated for frequency and amplitude in Chapter III. Particles were vigorously ejected from the screen onto the floor when the lower values for frequency and amplitude were used.

Therefore it was necessary to determine a range of smaller values for frequency and amplitude. Minimum and maximum values of the Froude number were established experimentally. Intermediate values were picked which were compatible with acceptable performance of the vibrating screen.

The vibrating screen had two regions of undesirable motion. At 25 cps some cross motion was present. Installation of additional braces on the framework minimized the effect, but no test conditions were selected using 25 cps. The fundamental natural frequency for the vibrating linkage occured at 35 cps. Thus a resonance condition was encountered at this frequency. By quickly accelerating through the natural frequency, the screen could be operated at 40 cps. By modifying certain elements in the linkage, the natural frequency was raised from about 31 cps to 35 cps.

Frequencies and amplitudes which were selected and used are presented in TABLE XIII. Each combination of frequency and amplitude was assigned an identity number. Referral to motion parameters hereafter will be, motion X, where X corresponds to the identity number.

Static response as described in Chapter V was used to check the uniformity of surface displacement for different eccentricities (dial settings) after final adjustments were made. Results of these tests are presented in TABLE XIV. It was concluded that a satisfactory adjustment of the linkage had been achieved.

The two accelerometers were checked against a test accelerometer in the Mechanical Engineering Laboratory. It was found that accelerometer #3138 consistently gave an output which was lower than the input it was sensing. Output of #3132 corresponded to the known input. A correction

factor depending on frequency was applied to all readings taken with #3138. Results of these checks are presented in Appendix B-V.

TABLE XIII

MOTION PARAMETERS USED IN EXPERIMENTAL WORK

Identity	Frequency cps	Amplitude	Π_7	Π_9
2	32.0	.019	3.36	.050
3	28.5	.024	3.78	.050
4	22.0	.040	4.86	.050
5	20.7	.045	5.15	.050
6	16.9	.040	3.77	.029
7	22.0	.031	3.77	.038
3	28.5	.024	3.78	.050
8	33.0	.020	3.64	.056
9	40.0	.017	3.76	.070

Acceleration components and displacements were measured at the four locations previously defined in Fig. 35. These observations were made at a frequency of 28.5 cps and .024 in. amplitude, motion 3. The majority of experimental work was conducted using motion 3. Results of the observations are given in TABLE XV. Note that the "dynamic" amplitude at 28.5 cps was more than twice the "static" amplitude which was measured at a frequency less than one cps. There was evidence to

believe that inertia forces in the linkage members induced displacements above the design values. Variations in acceleration components are noted at the four locations. Determining the exact cause of these differences is most difficult. Variations in member deflections plus some resonances would effect the acceleration response significantly.

TABLE XIV

UNIFORMITY EVALUATION OF SURFACE DISPLACEMENT

Dial Setting	Vertical Displacement of Screen (in.) Location 1	Location 2	Location 3	Location 4
25	.0220	.0220	.0220	.0220
25	.0220	.0220	.0220	.0220
25	.0220	.0220	.0220	.0215
30	.0155	.0150	.0155	.0155
30	.0150	.0150	.0150	.0155
30	.0150	.0155	.0155	.0150
35	.0095	.0095	.0100	.0100
35	.0095	.0100	.0100	.0095
35	.0090	.0090	.0095	.0095
40	.0045	.0045	.0045	.0045
40	.0050	.0050	.0050	.0050
40	.0045	.0050	.0050	.0045

If simple harmonic motion were achieved, each location would have an amplitude of .024 in. Since α was 45 deg., the horizontal and vertical components of acceleration would be equal and have a peak value of 1.414 g's. The observed motion does meet the frequency and amplitude requirements for simple harmonic motion but deviates for the acceleration components. Observed motion was considered as approximated simple harmonic motion.

Acceleration components were measured for each set of motion parameters used and results are shown in TABLE XVI. All observed values of acceleration components were higher than the theoretical values for simple harmonic motion as mentioned previously, deflection of members and resonance would increase these peak accelerations.

TABLE XV

DYNAMIC RESPONSE OF VIBRATING SURFACE AT FOUR LOCATIONS

$\alpha = 45^{o}$ $f = 28.5$ cps

Location	"Static" Amplitude in.	"Dynamic" Amplitude in.	X-Acceleration g's *	Y-Acceleration g's
1	0.0110	0.024	1.85	2.5
2	0.0105	0.022	1.85	2.0
3	0.0105	0.022	1.64	2.2
4	0.0110	0.025	1.64	2.8

*Corrected values

Numerical Evaluation of the Independent Variables

$\Pi_2 = \alpha$ The measured value of the linkage angle in deg.

Π_6 = d/a was calculated by using the screen dimensions specified by the manufacturer.

$\Pi_7 = Ne\rho fAl_{2u}/\mu$ Constant values were used for Ne, ρ, μ, and l_{2u}.

f and A were observed in the experiment.

$Ne = 1/385.728$ lbf./lbm.in./sec.^{2}

$l_{2u} = .1412$

$\mu_{air} = 2.73 \times 10^{-9}$ lb.-sec./in.^{2}

$\rho_{air} = 4.11 \times 10^{-5}$ lbm./in.^{3}

Air conditions used

Temp. 90°F

R.H. 40%

Barometer 29.92 in Hg

Thus $\Pi_7 = \dfrac{4.11 \times 10^{-5} \times .1412}{385.723} \times f \times a$

$\Pi_8 = Q/\rho_u \times f \times a^2$

Q = feed rate/screen width = lbm./sec.-in.

ρ_u = Mean value of six observations = 50.3×10^{-3}

f = Frequency observed in experiment

a = Aperture of screen as specified by the manufacture

$\Pi_9 = Nef^2A/G$

Ne = constant = 1/385.728 lbf./lbm.in./sec.^{2}

G = Constant = 1 at earths surface

f = Frequency observed in experiment

A = Amplitude observed in experiment

$\Pi_{10} = s/l_{2u}$

s = observed in experiment

l_{2u} = mean of 25 observations = .1412 in.

$\Pi_{11} = l_{3u}/a$

l_{3u} = mean of 25 observations = .0984 in.

a = aperture of screen as specified by the manufacture

$\Pi_{14} = Q_o/Q$

Q_o = feed rate of oversize particles observed in experiment per unit width of screen lbm./sec.-in.

Q = feed rate of undersize particles observed in experiment per unit width of screen lbm./sec.-in.

After the experimental work was completed a Fortran program for the IBM 1620 Computer was written to process the raw data. Data recorded for each test was entered on punch cards and was used as input for the program. The raw data collected is presented in Appendix C-I. A coding system was used to identify the data. A series of data pairs are preceded by a header card which was positioned on the center of the page. The three numbers listed are: 1. Number of observations of the independent variable under consideration; 2. Sampling length down screen; 3. An index called KC indicating which pi term was the independent variable. KC assumed the values shown in TABLE XVII. Two rows forming one data pair were used for each test. The first row contains

TABLE XVI

DYNAMIC RESPONSE OF VIBRATING SURFACE FOR TEST CONDITIONS

Identity	α Deg.	Frequency cps	Amplitude in.	Observed X-Acceleration g's	Observed Y-Acceleration g's	Theoretical X-Acceleration g's	Theoretical Y-Acceleration g's
2	45	32.0	.019	2.8	3.2	1.4	1.4
4	45	22.0	.040	2.0	2.2	1.4	1.4
5	45	20.7	.045	2.0	2.5	1.4	1.4
6	45	16.9	.040	1.8	2.0	1.0	1.0
7	45	22.0	.031	1.6	1.8	1.1	1.1
8	45	33.0	.020	2.0	3.4	1.6	1.6
9	45	40.0	.017	2.9	5.2	2.0	2.0
3	35	28.5	.024	1.4	2.8	1.1	1.6
3	45	28.5	.024	1.8	2.4	1.4	1.4
3	55	28.5	.024	2.3	2.0	1.6	1.1
3	65	28.5	.024	2.8	1.4	1.8	.85

eleven pieces of information. In order these are: 1. Fartherest distance in inches down screen undersized particles advanced; 2. Width of screen in inches used in test; 3. Wire diameter of screen in inches; 4. Size of screen aperture in inches; 5. Speed of eccentric driver shaft in RPM; 6. Total screen displacement, 2 x amplitude in inches; 7. Sampling time in minutes; 8. The angle α in degrees; 9. Weight of oversize particles in grams; 10. Pi terms which was the independent variable; 11. A four digit code, the first two digits being the value for α, the third digit the motion identity, and the last digit was the screen identity number. The second row contained ten pieces of information. These were the accumulated weights (grams) of undersize particles which had passed through the screen for 1 in., 2 in., ... 10 in., of screen length. If particle travel exceeded 10 in. the "over flow" was added to the tenth location. If all undersize particles passed through the screen before ten in. of travel, zeros were entered in the remaining locations.

Presentation of the raw data for Π_{10} equal to the independent variable was altered slightly. The header card contained the number of observations and the index KC. The sampling length down screen was entered as the tenth piece of data on the first card of each data pair.

Output of the raw data program is presented in Appendix C-II. First, pi terms held constant were tabulated in row form. Π_7, Π_8, and Π_9 which varied slightly from test to test are expressed as a mean value and a standard deviation. Below, the left column is the value of the independent pi term. Second column is the observed response of the system. The remaining columns are the individual values from which the mean values and standard deviations were calculated. All calculations

were made using eight significant figures. Output was truncated, F form, during printout.

The raw data program was also used to punch out cards containing the independent variable and dependent variable. This output was used as data for regression analysis of the component equations.

TABLE XVII

CODING OF RAW DATA

KC	Independent Pi Term
1	Π_2
2	Π_6
3	Π_7
4	Π_8
5	Π_9
6	Π_{10}
7	Π_{11}
8	Π_{14}

Presentation of Component Equations

Initial analysis of the component equations consisted of plotting the data on arithmetic coordinates, semi-log, and log-log. P versus Π_{14} indicated a straight line on log-log. All other component equations

appeared to be of the form $y = a + bx + cx^d$ where d could be integer or non-integer and positive or negative. An existing computer program using the least square method was altered to accommodate the model. An estimate of d was obtained graphically. This was used in conjunction with an iterative procedure incorporated into the regression program. The value of a, b, c, and d which gave the best fit were computed. In an attempt to simplify the model, d was selected as 2 and the regression analysis was rerun. Results indicated that the simpler model was satisfactory. The values for a, b, c, and d for each component equation are presented in TABLE XVIII.

TABLE XVIII

COEFFICIENTS FOR COMPONENT EQUATIONS

Model $P = a + b\Pi + c\Pi^d$

R^2 = Per cent Variation in P accounted for by knowing Π

Π	a	b	c	d	R^2
2	.79817130E-00	.46957603E-02	-.41747340E-04	2	.537
6	.91875280E-00	.24773286E-00	-.58010749E-00	2	.965
7	.66524220E-00	.10366910E-00	-.99758431E-02	2	.829
8	.95997560E-00	.18423061E-00	-.36343453E-00	2	.943
9	.84798840E-00	.10171208E+02	-.17596452E+03	2	.984
10	.11912983E+01	-.33976180E-02	-.91445396E+02	-2	.998
11	-.64241820E-00	.65183182E+01	-.66299276E+01	2	.998

It was hypothesized that Π_1 versus Π_{14} was of the form $y = ax^d$. This was transformed to logs and a linear regression analysis made. This was an acceptable model. Results of regression analysis were:

$$\Pi_1 = .289\ \Pi_{14}^{-.607}$$

$$R^2 = .978$$

The component equations and experimental data are plotted in Fig. 36, 37, 38, 39, 40, 41, 42, and 43. A relatively low value for R^2 was obtained for Π_1 versus Π_2. However this makes little difference since a small change in response is noted for the range of Π_2 investigated. The type of response obtained in Π_1 versus Π_6 is the result of the two phenomena occuring in the physical system. As Π_6 increases, the area of the aperture (open area) decreases in a linear fashion for each inch of screen length. Thus, one would expect the response to decrease. Increasing Π_6 required that the feed rate to the screen be increased to maintain a constant value of Π_8. This had the effect of increasing the depth of material entering the screen. The greater depth tended to distribute material further down the screen which would decrease the response for the level of Π_{10} selected. Study of the literature plus other considerations suggests the decrease in response is exponential in nature.

A relatively low R^2 was achieved for Π_1 versus Π_7. Again this makes little difference since a small change in response was obtained for the range of Π_7 investigated.

For the pi terms having greatest effect on response, the lowest R^2 was .943 which was obtained for Π_1 versus Π_8. Inspection of Fig. 39 shows individual observations deviated more from the regression line

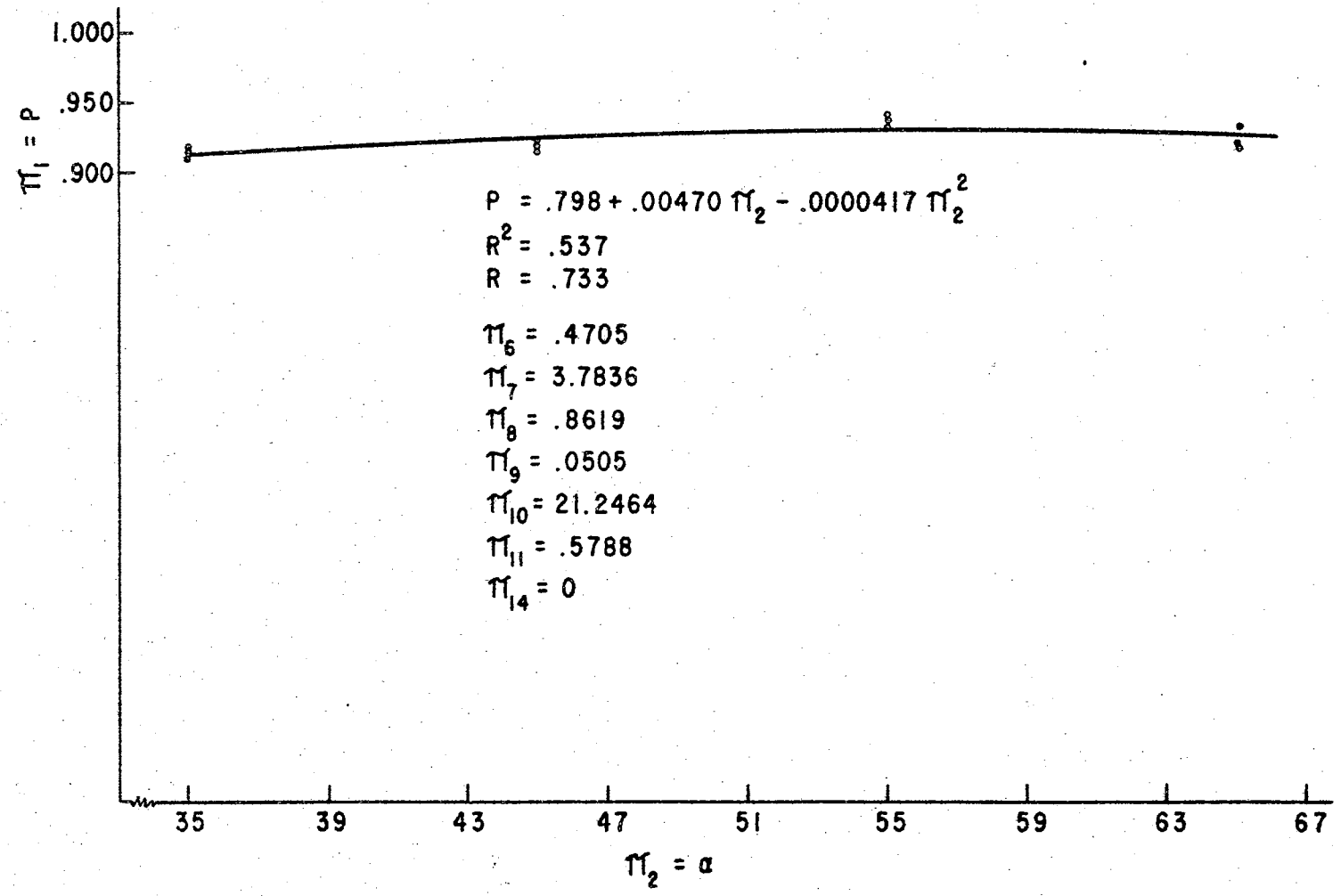

Fig. 36. Π_1 versus Π_2.

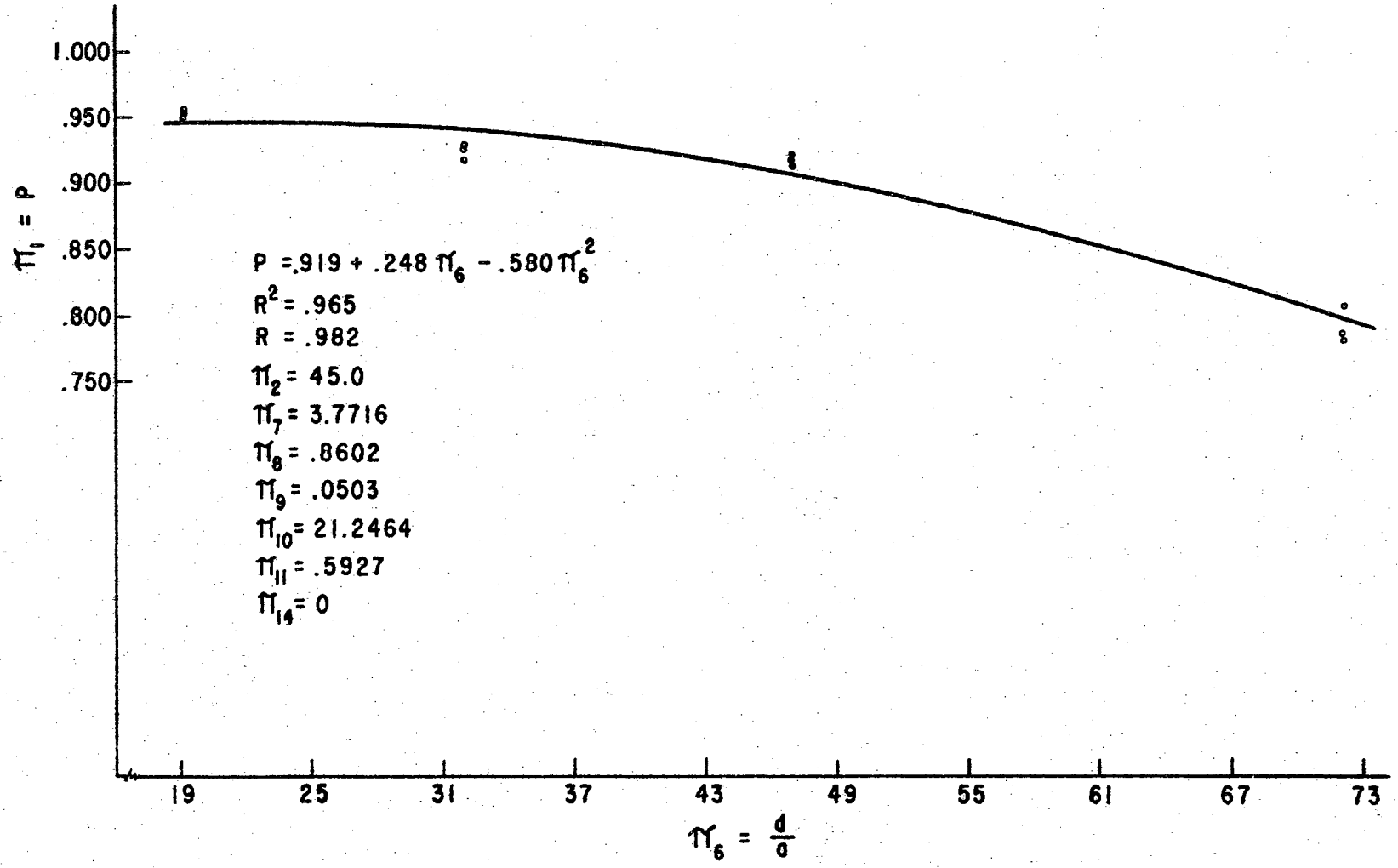

Fig. 37. Π_1 versus Π_6.

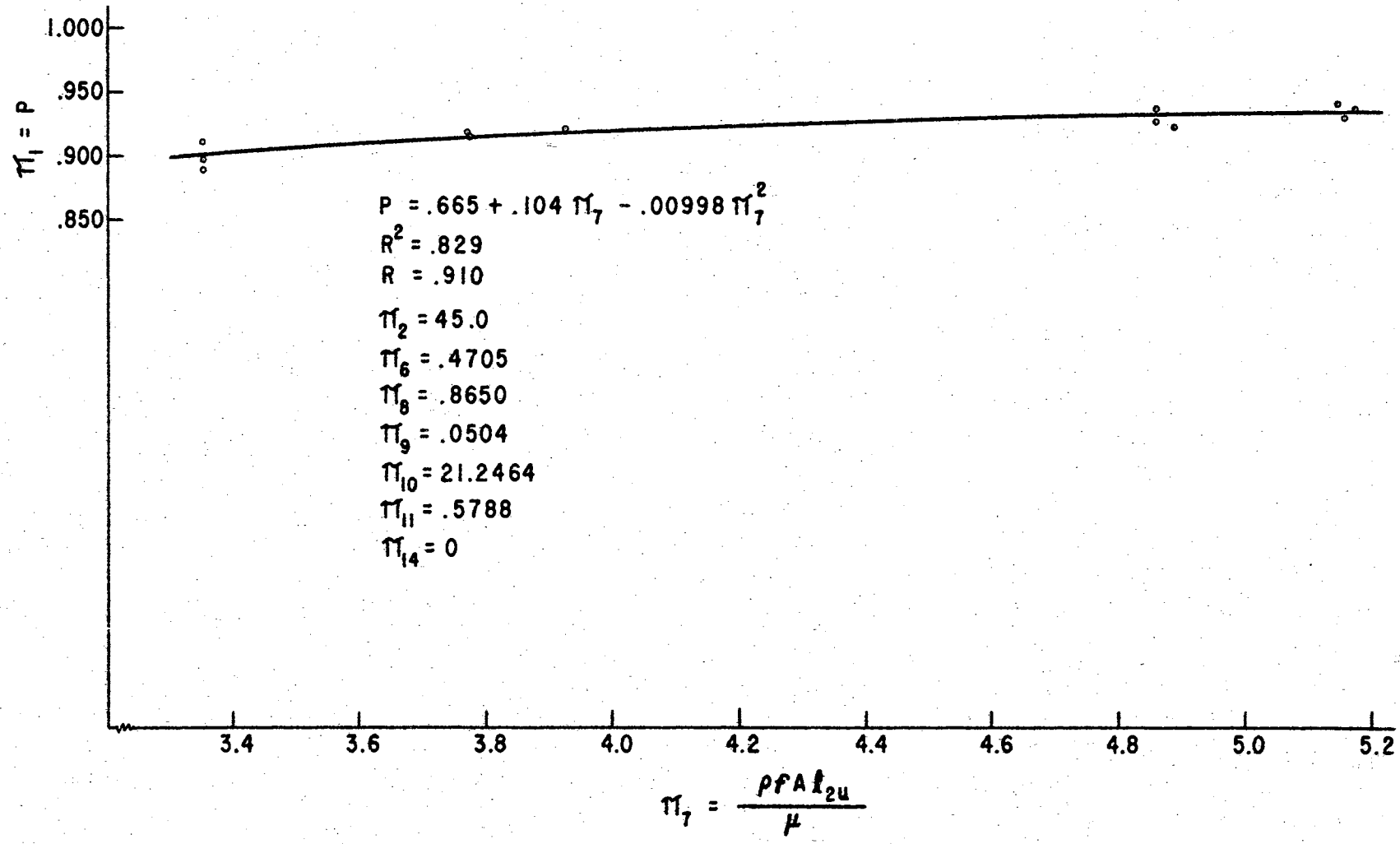

Fig. 38. Π_1 versus Π_7.

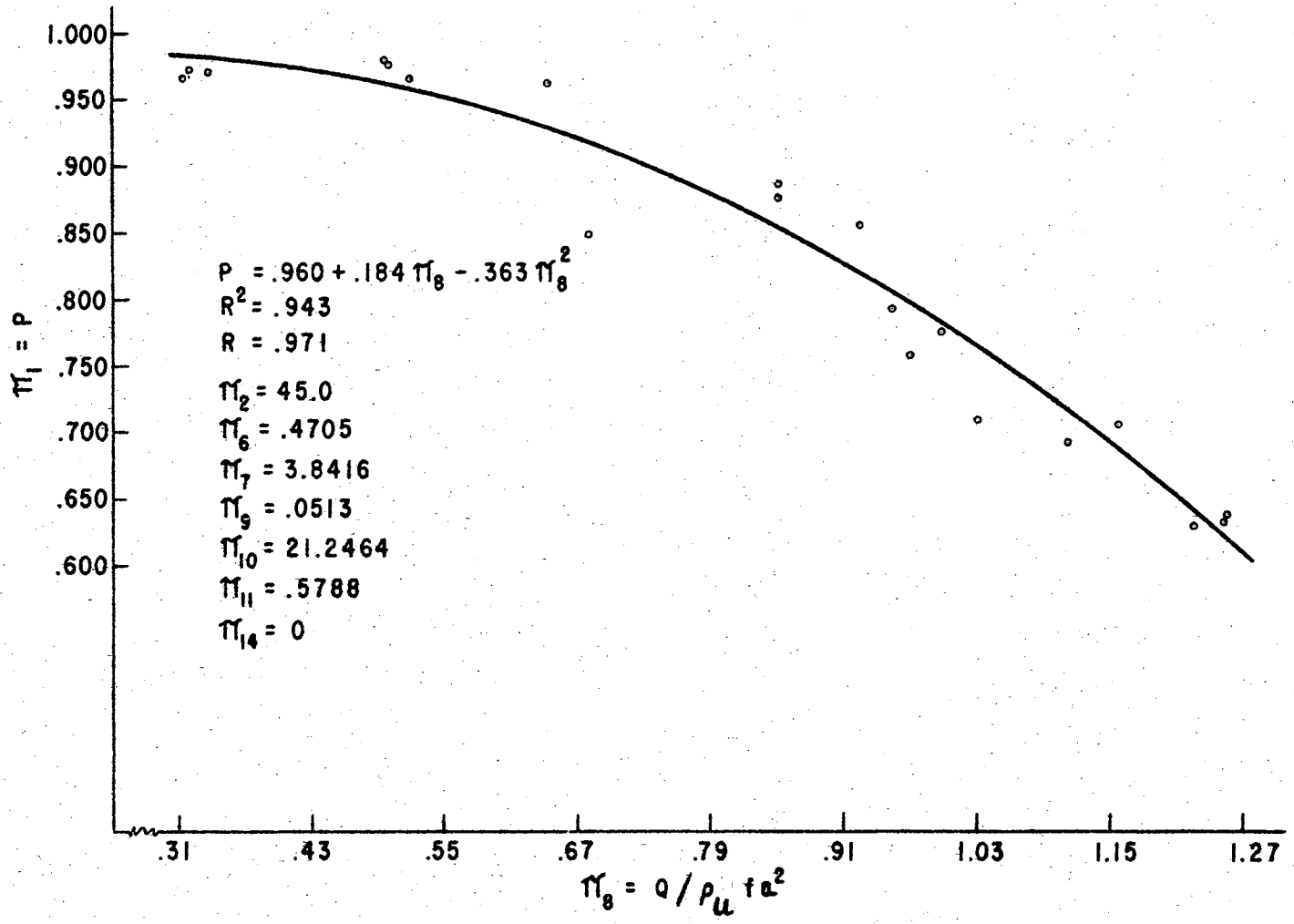

Fig. 39. Π_1 versus Π_8.

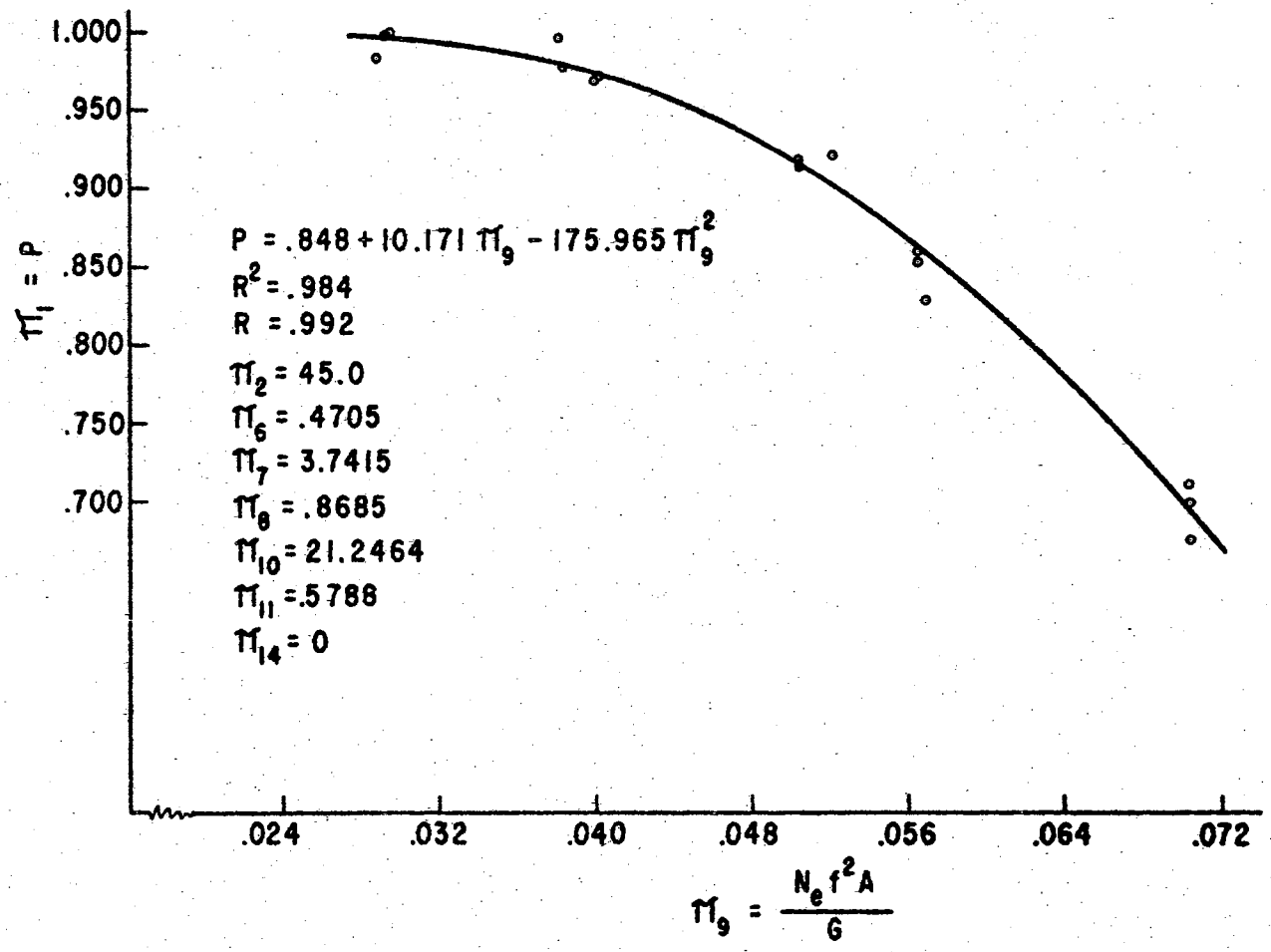

Fig. 40. Π_1 versus Π_9.

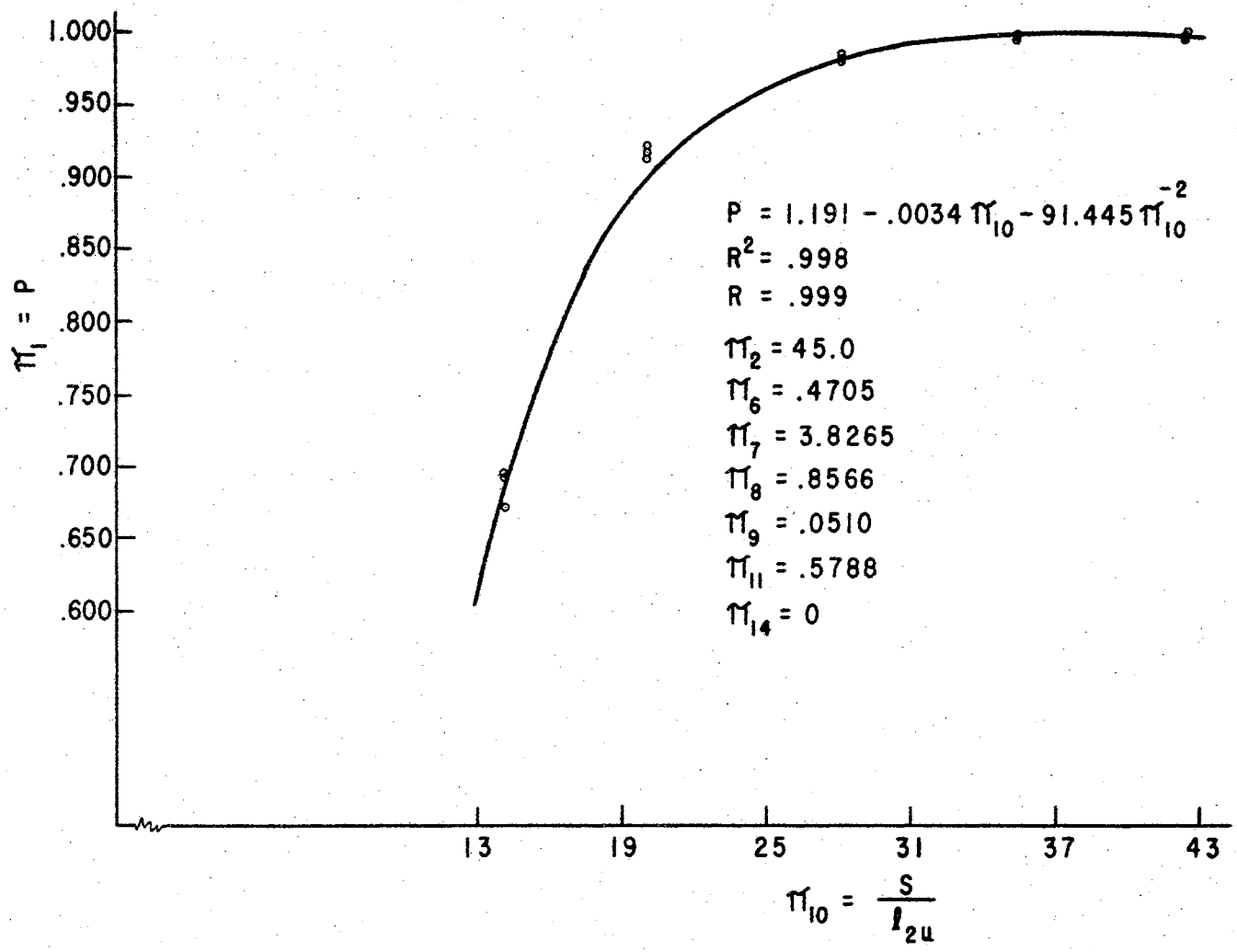

Fig. 41. Π_1 versus Π_{10}.

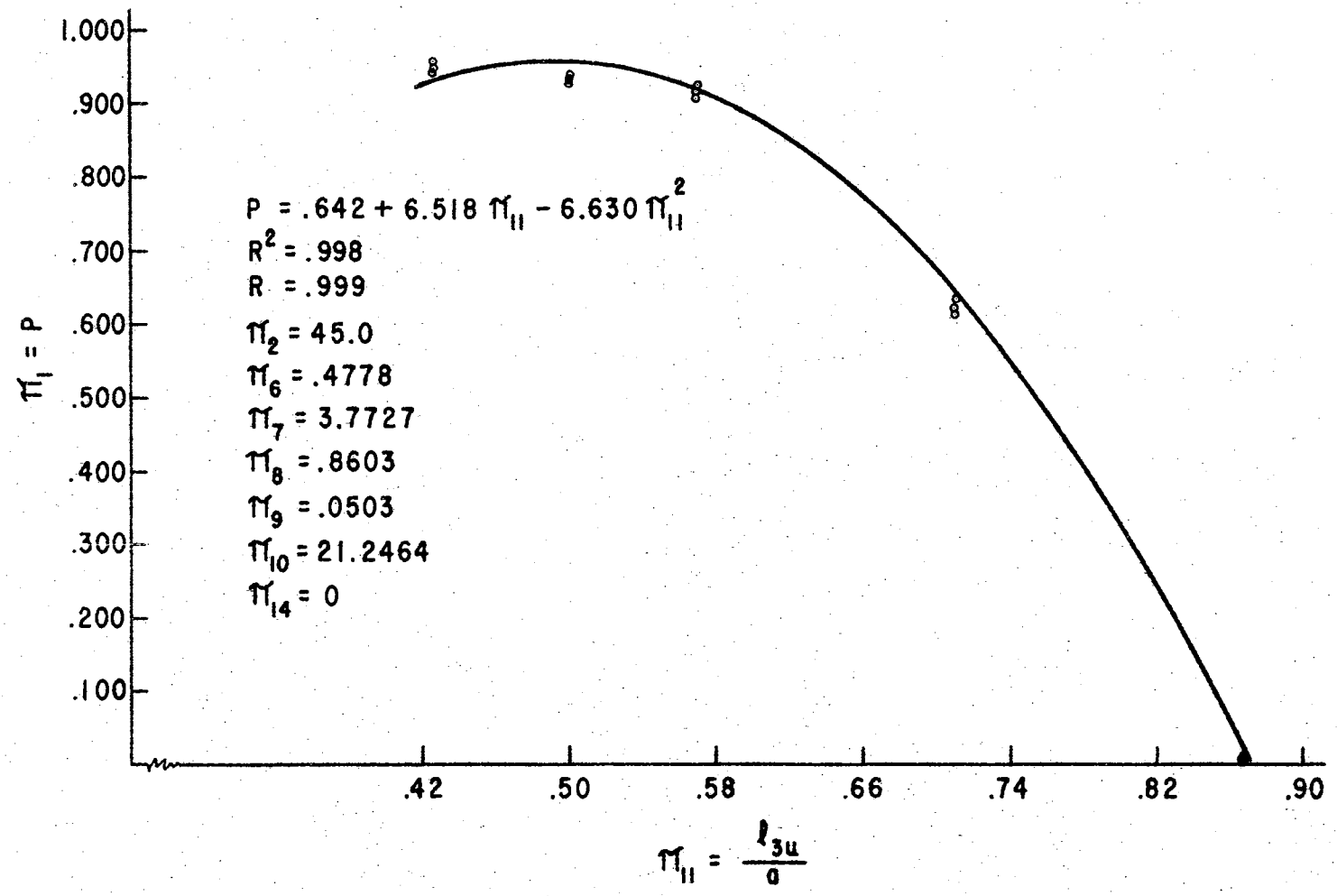

Fig. 42. Π_1 versus Π_{11}.

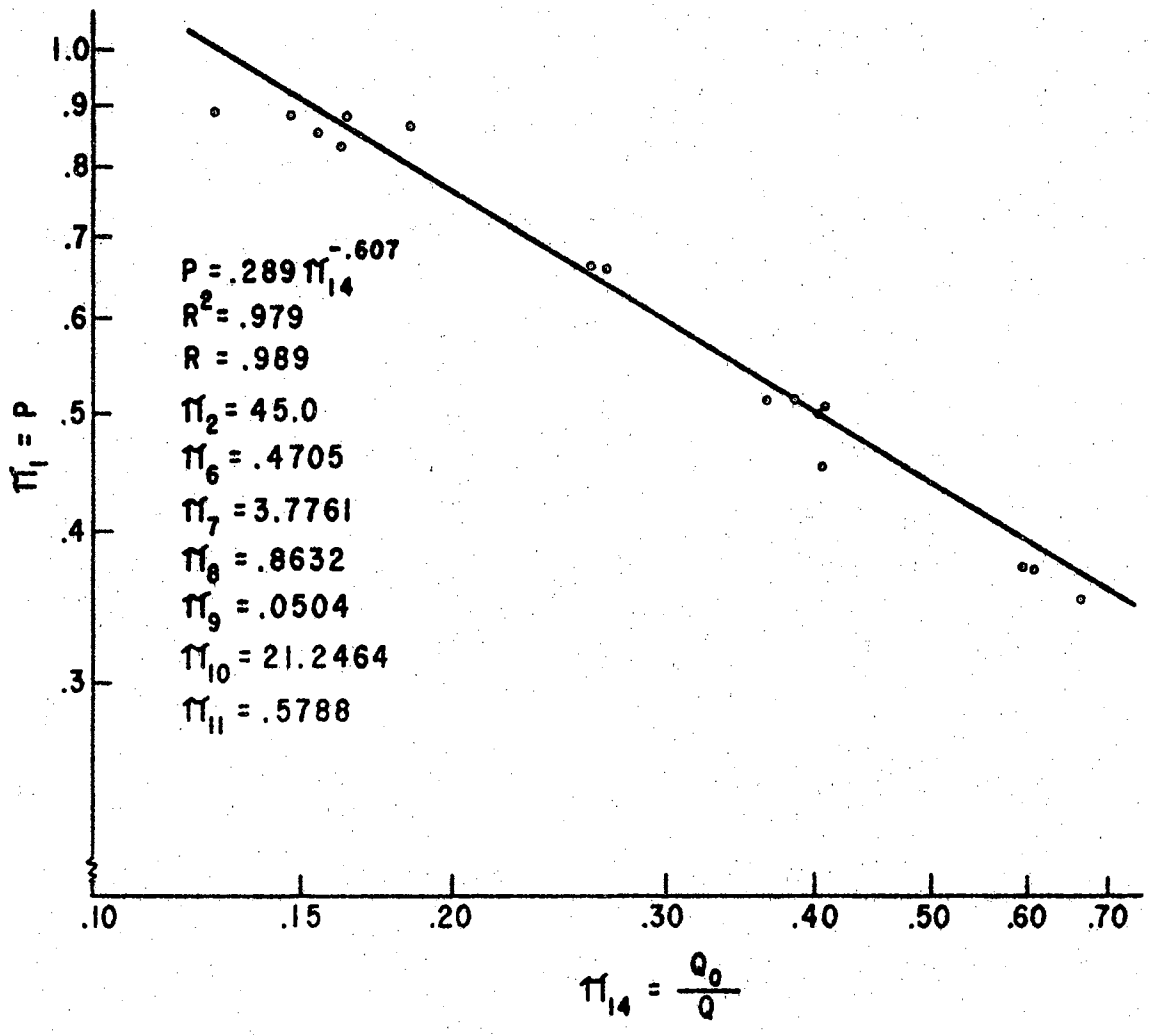

Fig. 43. Π_1 versus Π_{14}.

as compared to the other component equations. Π_8 was varied by changing the feed rate to the screen. Increasing Π_8 increased depth of material on the screen, which in turn distributed material further down the screen. This decreased the response as was expected.

Froude number appears to be an excellent means of characterizing the screen motion. At the lower end of the range investigated, relative movement between particles and screen was small. At the upper end of the range, particle movement was brisk. Increasing the Froude number has the effect of distributing material further down the screen thus decreasing the response for the level of Π_{10} under consideration.

Π_{10} was varied by changing the sampling distance S down the screen. As Π_{10} increased the response increased. This is plausible since a distance down screen can be reached beyond which no undersize particles pass. It is of interest to note that the length of screen needed to achieve a specified level of response can be determined by this dimensionless ratio.

The range of response due to varying Π_{11} was at least 2.9 times the range for any of the other pi terms. Thus l_{3u}/a was a highly significant variable. Experimental procedure was altered for obtaining the response at $\Pi_{11} = .7182$ and $\Pi_{11} = .8707$. At the .7 level, particles lodged in the apertures and eventually blocked all openings. To minimize the blocking, sampling time was decreased. At the end of the tests approximately 50% of the screen area was ineffective. For $\Pi_{11} = .8$, aperture blocking was not serious but very few undersize particles passed through the apertures. To prevent excessive layering of particles, sampling time was reduced.

The observed response due to Π_{11} provides insights to some inter-

esting possibilities for size classing particles. It is apparent that poor response is obtained when the particles are only slightly smaller than the aperture. On the other hand little is to be gained for values of Π_{11} less than .50. Performing a given sizing operation might be most efficient by using several screens of different aperture size rather than one screen. By judicious selection of aperture size and screen length, Π_{11} could be maintained near the .5 level which would provide optimum condition for particle passage. One must remember the observed response was for one size class of undersize particles. To implement this concept would require knowledge of the response of composite mixtures of different size classes of undersize and oversize particles.

The final phase of the experimental work consisted of mixing undersize and oversize particles. As the ratio of oversize to undersize increased, the response decreased in an exponential manner for the level of Π_{10} selected. This is reasonable to expect since oversize particles block out apertures and tend to convey the undersize particles further down the screen. For $\Pi_{14} = 0.6$, depth of particles at the screen entrance was approximately 1 in.

Development of the Prediction Equation

An objective of this study was to develop a prediction equation of the form $\Pi_1 = f(\Pi_2, \Pi_6, \Pi_7, \Pi_8, \Pi_9, \Pi_{10}, \Pi_{11})$.

The first model hypothesized was: $\Pi_1 = C_1 + C_2\Pi_2 + C_3\Pi_6 +$

$$C_4\Pi_7 + C_5\Pi_8 + C_6\Pi_9 + C_7\Pi_{10} + C_8\Pi_{11} + C_9\Pi_2^2\Pi_6^2\Pi_7^2\Pi_8^2\Pi_9^2\Pi_{10}^{-2}\Pi_{11}^2 \qquad 6 - 1$$

Basis for this hypothesis was that the component equation contained terms which were linear in arithmetic coordinates and terms which were linear in logarithmic coordinates.

A computer program employing the least squares method was used to evaluate the model. One hundred and two experimental observations were used in forming the prediction equation. 85.4% (R^2 x 100) of the variation in Π_1 was accounted for by knowing Π_2, Π_6, Π_7, Π_8, Π_9, Π_{10}, and Π_{11}. The equation obtained was then used to calculate predicted values for each of the 102 observations. Deviation of the predicted response from the observed response was expressed as a + or - per cent deviation. 86.1% of the predicted values deviated less than $\pm$ 10% from the observed response. 58.9% of the predicted values deviated less than $\pm$ 5%. Model I was tolerable but in an attempt to find a better mathematical model a second model was investigated. Model II was hypothesized as:

$$\Pi_1 = C_1 + C_2\Pi_2 + C_3\Pi_2^2 + C_4\Pi_6 + C_5\Pi_6^2 + C_6\Pi_7 + C_7\Pi_7^2 + C_8\Pi_8 + C_9\Pi_8^2 + C_{10}\Pi_9 + C_{11}\Pi_9^2 + C_{12}\Pi_{10} + C_{13}\Pi_{10}^2 + C_{14}\Pi_{11} + C_{15}\Pi_{11}^2 \qquad 6 - 2$$

One hundred and two observations were used in the least squares program to evaluate Model II. For this model 98% (R^2 x 100) of the variation in Π_1 was accounted for by knowing Π_2, Π_6, Π_7, Π_8, Π_9, Π_{10}, and Π_{11}. Model II prediction equation was then used to calculate predicted values for each of the 102 observations. Predicted values were compared with observed values. 93.14% of the predicted values deviated less than

± 10% from the observed response. 91.18% of the predicted values deviated less than ± 5%. It was concluded that Model II satisfactorially represented the response of the system under investigation. The value of the coefficients for the prediction equation are given in TABLE IXX. Numerical evaluation of the prediction equation is presented in Appendix C-III.

TABLE IXX

COEFFICIENTS FOR MODEL II PREDICTION EQUATION

Coefficient	Numerical Value
C_1	-.91159020E-00
C_2	-.63099464E-02
C_3	.76858091E-04
C_4	-.58851930E-01
C_5	-.23026625E-00
C_6	-.83348270E-01
C_7	.13077284E-01
C_8	.59216929E-00
C_9	-.61024423E-00
C_{10}	.30397990E+01
C_{11}	-.10534173E+03
C_{12}	.52918966E-01
C_{13}	-.76819983E-03
C_{14}	.61202131E+01
C_{15}	-.63257509E+01

Prediction Equation Test

During the experimental work a limited number of tests were run for use in checking the prediction equation. Frequency and amplitude in the Froude number were recombined to give the same numerical values for motions 3, 7, and 8. The manner in which this was done is shown in TABLE XX. Motions 7A, 3B, and 8C were replicated three times. The

TABLE XX

MOTION PARAMETERS SELECTED FOR TESTING PREDICTION EQUATION

Identity	Frequency cps	Amplitude in.	Π_9
7	22.0	.031	.038
3	28.5	.024	.050
8	33.0	.020	.056
7A	19.8	.037	.038
3B	26.9	.027	.050
8C	30.2	.024	.056

nine texts were completely randomized. Raw data is presented in Appendix C-IV. Calculations of the pi terms are presented in Appendix C-V. Values of the independent pi terms for the nine tests were used in evaluating the prediction equation. The predicted values of the response P, were compared with the observed values. Results are

presented in TABLE XXI. Based on these limited observations the prediction equation appears to be valid.

TABLE XXI

RESULTS OF PREDICTION EQUATION TEST

P OBS	P CAL	DIFF	PERCENT
.9836	.9801	-.0034	-.348
.9765	.9743	-.0021	-.225
.9826	.9906	.0080	.815
.9206	.9068	-.0137	-1.490
.9193	.9003	-.0190	-2.067
.9224	.9093	-.0130	-1.417
.8773	.8446	-.0327	-3.730
.8819	.8543	-.0275	-3.125
.8738	.8469	-.0269	-3.078

Comparing Theory with Experimental Results

As mentioned earlier in this chapter, the range of theoretical values calculated for frequency and amplitude in Chapter III were too high. The values actually used in the experimental work were subjected to the same theoretical analysis as those in Chapter III. The calculations are presented in Appendix A-II. For the values of frequency and amplitude used, theoretical calculations were not made for: motion 6 for α = 35, 45, and 55, motions 2, 3, 4, 5, 7 and 8 for α = 65. Theoretical calculations were not made because the condition of equation 3 - 7 was not met. This merely indicates that particles were undergoing sliding effects rather than executing small hops. No theory

was developed for the sliding region. Graphical results are presented in Fig. 44, 45, and 46.

A qualitative response of the system due to increasing Π_7 was hypothesized in Chapter III. This hypothesis is consistent with theoretical calculations for the test conditions used (Fig. 44). The actual response obtained in the experiment is shown in Fig. 35. A slight increase in response was observed for increasing Π_7. The net response must be the combined effect of response due to: 1. drag forces; 2. decreased layering effect; 3. increase in distribution of particles down the screen. Visual observations of material movement on the screen suggests that drag effects of air on the particles were not significant in this system. Only for high Froude numbers were the particles appreciably projected into the air and even then the probability of them achieving terminal velocity seemed unlikely. Thus it appears that the decreased layering effect increased the response more than the decrease in response due to the increased distribution of material down the screen. There is some evidence to support the qualitative hypothesis concerning an increase in Π_7.

Theoretical average horizontal velocity versus Froude number is shown in Fig. 45 for the test conditions used. These calculations are compatible with the hypothesis set forth in Chapter III concerning an increase in Π_9. The actual response of Π_1 is shown in Fig. 40. An appreciable decrease in Π_1 was obtained for increasing Π_9. Therefore there is evidence to support the qualitative hypothesis set forth.

Study of Fig. 36 reveals only a slight increase in response due to increasing α. Only limited comments are in order concerning this response. In Fig. 46 one notes an increase in the intercept angle

between particles and screen for increasing α. Theoretically a decrease in response would be expected for an increase in intercept angle. It is not unlikely that the intercept angle looses its identity due to scattering effects and intra particle intersection.

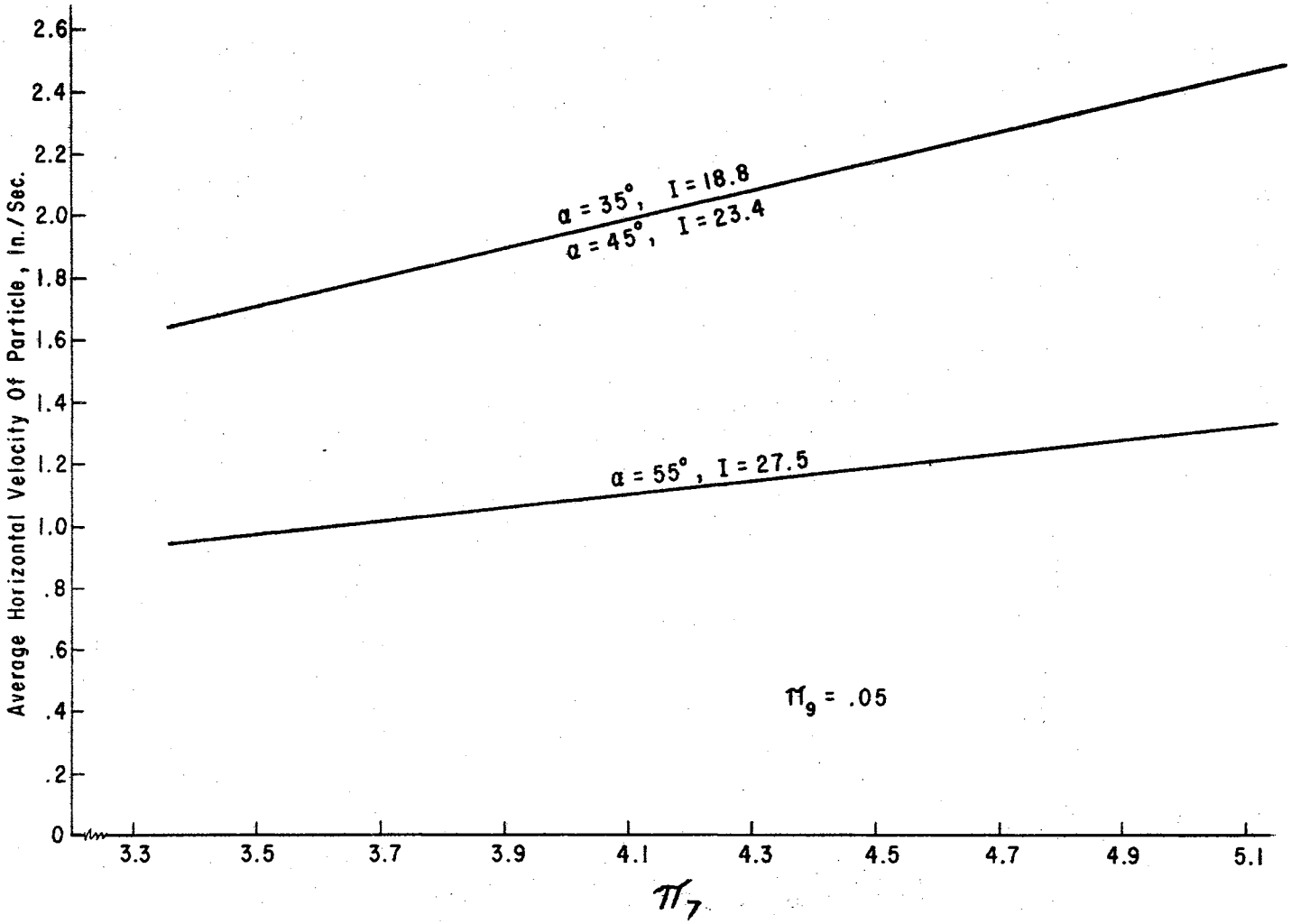

Fig. 44. Average Horizontal Velocity of Particle Versus Π_7.

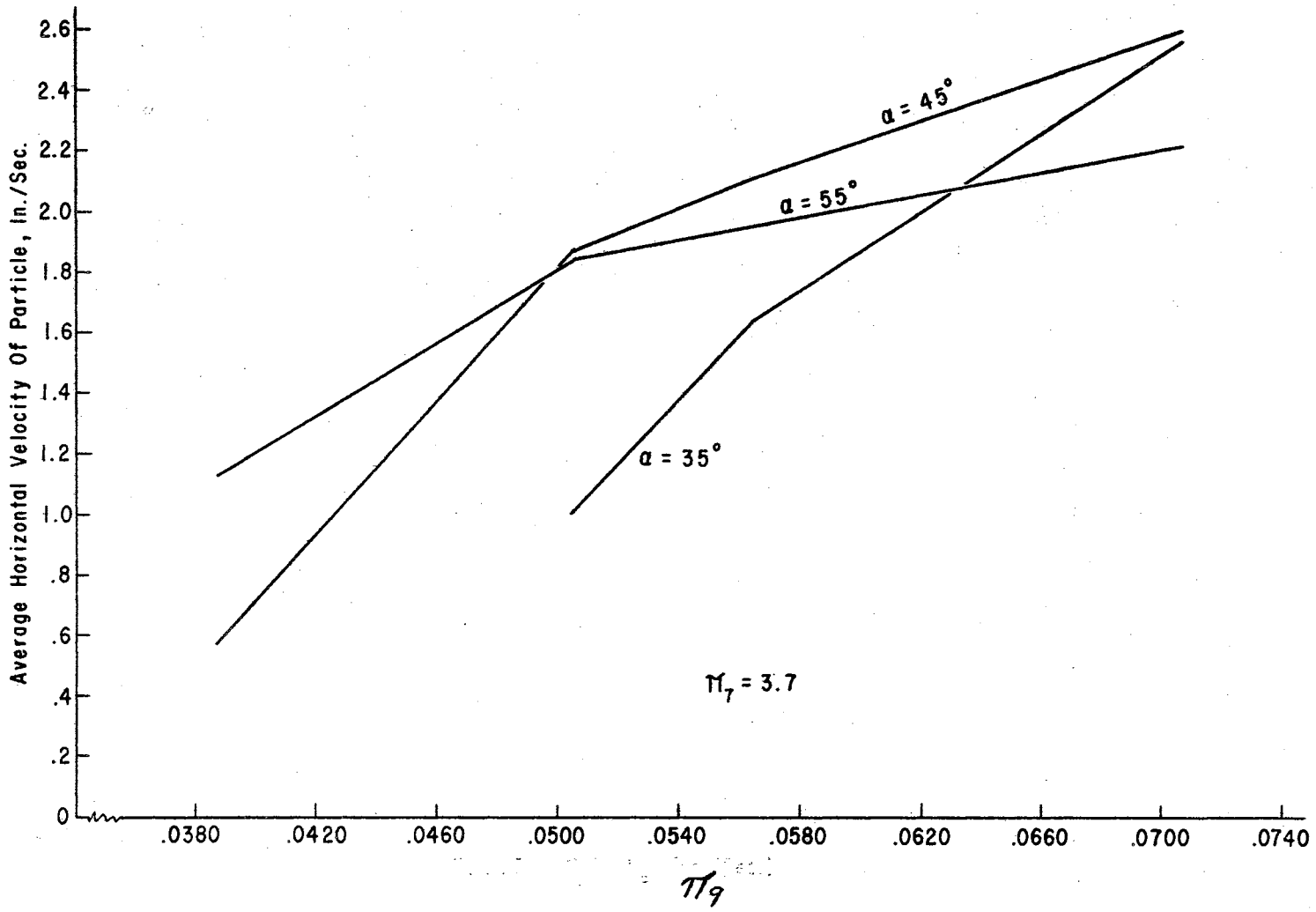

Fig. 45. Average Horizontal Velocity of Particle Versus Π_9.

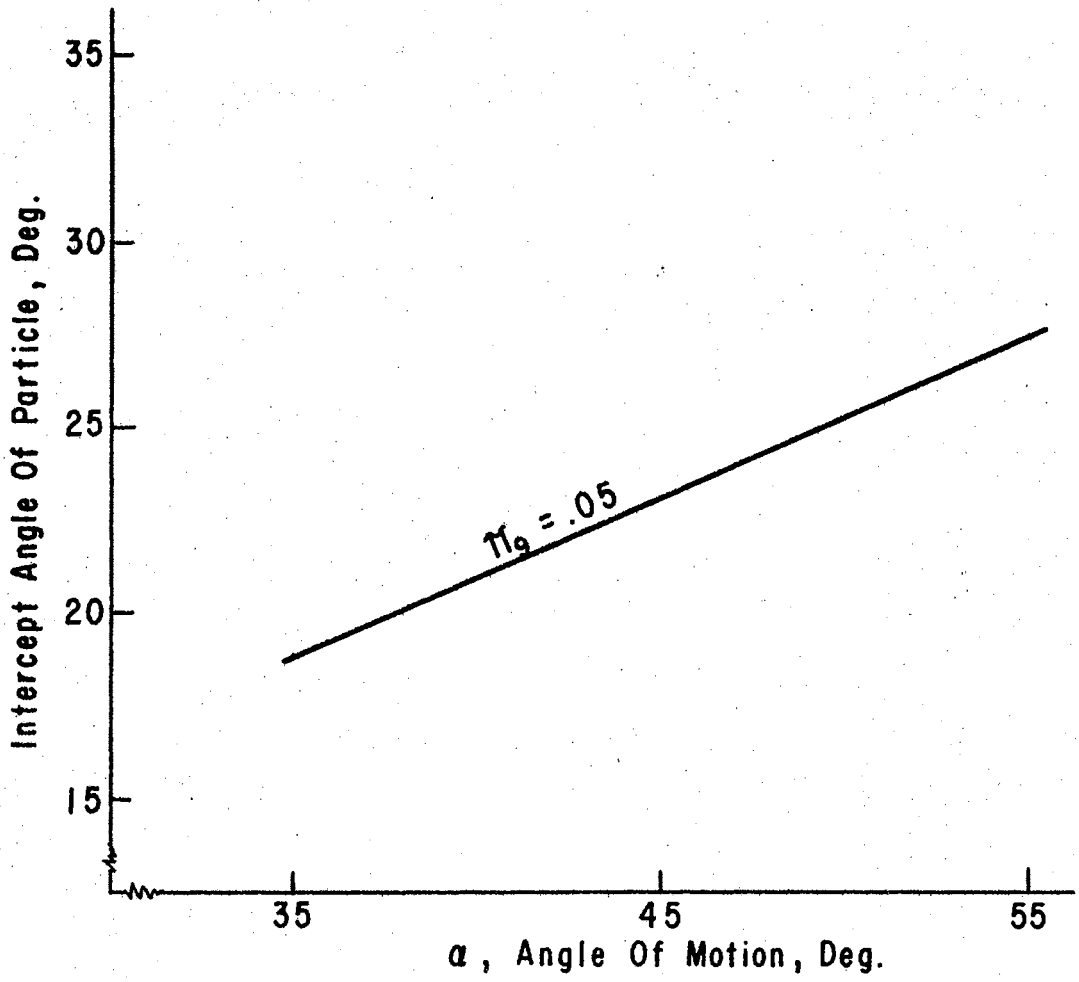

Fig. 46. Intercept Angle Versus Angle of Motion.

CHAPTER VII

MODEL PREDICTING SEPARATION IN A MULTI-SCREEN SYSTEM

Prediction equation 6 - 2, was developed by using one screen. Consideration should be given to a system composed of several screens. This suggests that screens of different length, wire diameter, and aperture size could be used to achieve a more efficient separation as compared to a single screen.

The system shown in Fig. 47 was selected for demonstrating how the prediction equation for one screen can be extended to several screens in series. The Q's are the feed rates in.lbm./sec./in. and the S's are the

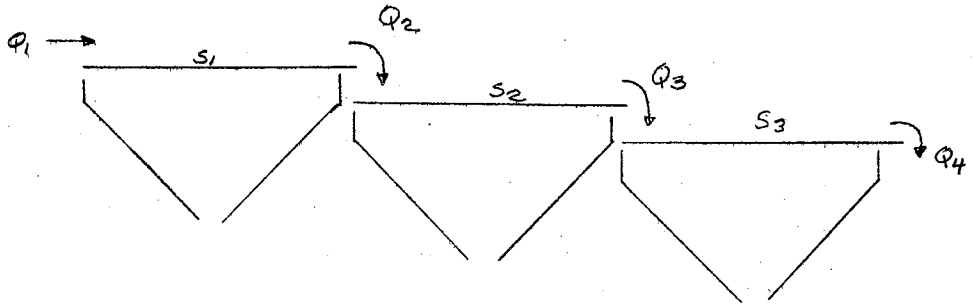

Fig. 47. Multi-Screen System.

screen lengths in inches. Restrictions placed on the system were:

1. All screens were of unit width; 2. All screens were connected to a common drive. The following relations exist between the three screens:

Q_1 = Specified input to system

$$Q_2 = (1 - P_1)\, Q_1 \qquad 7 - 1$$

$$Q_3 = (1 - P_1)\,(1 - P_2)\, Q_1 \qquad 7 - 2$$

$$Q_4 = (1 - P_1)\,(1 - P_2)\,(1 - P_3)\, Q_1 \qquad 7 - 3$$

where P_1, P_2, and $P_3 = \Pi_1$ for the respective screens. To maximize equation 6 - 2 implies:

$$\partial \Pi_1 / \partial \Pi_x = 0 \qquad 7 - 4$$

x = 2, 6, 7, 8, 9, 10, and 11

The general form of the derivative is:

$$\partial \Pi_1 / \partial \Pi_x = a + 2b\Pi_x \qquad 7 - 5$$

Setting equation 7 - 5 = 0 yields:

$$\Pi_x \text{ (max.)} = -a/2b \qquad 7 - 6$$

Maximizing each pi term yields:

$$\Pi_2 \text{ (max.)} = -C_2/2C_3 \simeq 41.0 \qquad 7 - 7$$

$$\Pi_6 \text{ (max.)} = -C_4/2C_5 \simeq -.13 \qquad 7 - 8$$

$$\Pi_7 \text{ (max.)} = -C_6/2C_7 \simeq 3.2 \qquad 7 - 9$$

$$\Pi_8 \text{ (max.)} = -C_8/2C_9 \simeq .49 \qquad 7 - 10$$

$$\Pi_9 \text{ (max.)} = -C_{10}/2C_{11} \simeq .015 \qquad 7\text{-}11$$

$$\Pi_{10} \text{ (max.)} = -C_{12}/2C_{13} \simeq 34.4 \qquad 7\text{-}12$$

$$\Pi_{11} \text{ (max.)} = -C_{14}/2C_{15} \simeq .48 \qquad 7\text{-}13$$

Π_6 (max.) is a valid mathematical solution but has no meaning in the physical system since Π_6 cannot assume negative values. Π_9 (max.) is not in the range of values for which the predication equation was developed. By judicious use of some of these maximized values, a partial optimization of the system can be achieved by using these maximized values in equation 6 - 2.

Model Analysis

The exact procedure for applying the prediction equation to the multi-screen system is presented in three phases, one for each screen.

Screen 1:

Input

Π_2 = Design value

Π_6 = Design value

Π_7 = Design value

Π_8 = Design value

Π_9 = Design value

Π_{10} = Design value

Π_{11} = Design value

1. Calculate $\Pi_1 = P_1$ using equation 6 - 2.
2. Calculate aperture size (a_1) using Π_{11}.
3. Calculate wire diameter (d_1) using Π_6.
4. Calculate screen length using Π_{10}.
5. Calculate frequency using Π_7 and Π_9.
6. Calculate amplitude using Π_7.
7. Calculate Q_1 using Π_8.
8. Calculate Q_2 using equation 7 - 1.

Screen 2:

Input

Π_2 = Same as screen 1.

Π_6 = Design value.

Π_7 = Same as screen 1.

Π_8 = Optimum value equation 7 - 10.

Π_9 = Same as screen 1.

Π_{10} = Design value or optimum value, whichever is smallest.

Π_{11} = Design value

1. Calculate $\Pi_1 = P_2$ using equation 6 - 2.
2. Calculate aperture size (a_2) using Π_{11}.
3. Calculate wire diameter (d_2) using Π_6.
4. Calculate screen length using smallest value for Π_{10}.
5. Calculate Q_3 using equation 7 - 2.

Screen 3:

Input

Π_2 = Same as screen 1.

Π_6 = Design value.

Π_7 = Same as screen 1.

Π_8 = Optimum value equation 7 - 10.

Π_9 = Same as screen 1.

Π_{10} = Design value or optimum value, whichever is smallest.

Π_{11} = Design value

1. Calculate $\Pi_1 = P_3$ using equation 6 - 2.
2. Calculate aperture size (a_3) using Π_{11}.
3. Calculate wire diameter (d_3) using Π_6.
4. Calculate screen length using smallest value of Π_{10}.
5. Calculate Q_4 using equation 7 - 3.
6. Calculate the value of P for the system using the relation:

   $P_{SYSTEM} = (Q_1 - Q_4)/Q_1$

A computer program was written to evaluate the model. Listing of Fortran statements is presented in Appendix E-I. Experimental data was used as input to screen 1. Partial optimization was achieved by using equation 7 - 10. Ratio of aperture size of screen 2 to screen 1 and screen 3 to screen 2 was specified as input. Maximum screen length L2 and L3 was specified as input for screens 2 and 3. If the length was greater than the optimum value as determined by equation 7 - 12, the optimum value was used. If specified screen length was less than the optimum value, the specified value was used.

Four sample calculations are presented in Appendix B-II. Π_2 was

equal to 45 deg. for the calculations presented. It must be recognized that usefulness of the model analysis is limited because the prediction equation is valid only for one size class of undersize particles. However a concept has been presented which can be expanded and applied to prediction equations which do contain parameters describing particle size and weight distributions.

CHAPTER VIII

SUMMARY AND CONCLUSIONS

Summary

The objectives of this study were to: 1. Establish basic relationships between particles and a single screen system using dimensional analysis and theoretical considerations; 2. Develop the necessary equations to predict particle passage for one size class of undersize particles for the system under consideration; 3. Extend the use of the prediction equation to a multi-screen system.

A horizontal screen subjected to simple harmonic motion was the hypothetical screening system. Two size classes of particles, undersize and oversize were considered. Important parameters in the system were identified in TABLE II and were combined into dimensionless ratios in accordance with the Buckingham Pi Theorem. Π_1 was designated as the dependent variable. The remaining fifteen pi terms were treated as independent variables. To restrict the area of investigation, the eight independent variables thought to be of greatest importance were selected for study. The remaining seven independent variables were held constant for all experimental work. The dimensionless ratios thought to be most important were:

1. $\Pi_2 = \alpha$
2. $\Pi_6 = d/a$

3. $\Pi_7 = N e \rho f A l_{2u} / \mu$

4. $\Pi_8 = Q / \rho_u f a^2$

5. $\Pi_9 = N e f^2 A / G$

6. $\Pi_{10} = S / l_{2u}$

7. $\Pi_{11} = l_{3u} / a$

8. $\Pi_{14} = Q_o / Q$

Π_7 which is a form of Reynolds number and Π_9 which is a form of the Froude number were used in conjunction with analytical considerations to develop a hypothesis concerning the qualitative response of the system.

Grain sorghum was selected as the undersize particles. One size class was constructed by processing the seeds in a roll (size) grader. Commercial plastic balls were selected as the one size class of oversize particles.

A four-bar linkage driven by an eccentric was used to impart approximated simple harmonic motion to the horizontal screen. The test screens were 6 in. wide and 27 in. long. Screen widths were reduced to about 3 in. after conducting preliminary test work.

The test schedule as outlined in TABLE IV was followed so that the experimental data could be used to develop a prediction equation of the form:

$$\Pi_1 = f(\Pi_2, \Pi_6, \Pi_7, \Pi_8, \Pi_9, \Pi_{10}, \Pi_{11})$$

The response of Π_1 as effected by changes in Π_{14} was determined by the test schedule shown in TABLE V. All test conditions were replicated three times. Randomization procedures are presented in Chapter V.

Component equations for the dependent variable and each independent variable were developed by using the least squares method. Mathematical models which gave satisfactory results were:

$$\Pi_1 = a + b\Pi_x + C\Pi_x^2 \qquad x = 2, 6, 7, 8, 9, \text{ and } 11$$

$$\Pi_1 = a + b\Pi_x + C\Pi_x^{-2} \qquad x = 10$$

$$\Pi_1 = a\Pi_x^b \qquad x = 14$$

A dimensionless homogeneous prediction equation was formulated using the least squares method. Form of the equation was:

$$\Pi_1 = C_1 + C_2\Pi_2 + C_3\Pi_2^2 + C_4\Pi_6 + C_5\Pi_6^2 + C_6\Pi_7 + C_7\Pi_7^2 + C_8\Pi_8 + C_9\Pi_8^2 + C_{10}\Pi_9 + C_{11}\Pi_9^2 + C_{12}\Pi_{10} + C_{13}\Pi_{10}^2 + C_{14}\Pi_{11} + C_{15}\Pi_{11}^2$$

Numerical value of the constants are given in TABLE IXX. One hundred and two observations were used to develop the equation. 98% of the variation in Π_1 was accounted for by knowing Π_2, Π_6, Π_7, Π_8, Π_9, Π_{10}, and Π_{11}. 93.14% of the predicted values deviated less than $\pm$ 10% from the observed response. 91.18% of the predicted values deviated less than $\pm$ 5%.

A limited number of tests were run to check the prediction equation. Frequency and amplitude in the Froude number were recombined to give the

same numerical values for three motion conditions. The predicted values were compared with the observed. All predicted values varied less than ± 3.8% from the observed response.

Theoretical calculations involving frequency and amplitude do indicate the qualitative response of the system when varying Π_7 and Π_9.

A model was developed for extending the use of the prediction equation from one screen to three screens in series. The model has limited usefulness but does provide a concept which will have application to other prediction equations which might be developed in future investigations.

Conclusions

Basic relationships between one size class of undersize particles, one size class of oversize particles, and a single screen system were established by use of dimensional analysis, theoretical considerations, and experimental observations. The relationships investigated were:

	Range
$\Pi_6 = d/a$	.19 - .73
$\Pi_8 = Q/\rho_u f a^2$	.31 - 1.3
$\Pi_9 = Nef^2A/G$	.028 - .070
$\Pi_{10} = S/l_{2u}$	14.1 - 42.5
$\Pi_{11} = l_{3u}/a$	.43 - .87
$\Pi_{14} = Q_o/Q$	.12 - .66

Changes in Π_2 did not have appreciable effect on the system response. The free flowing nature of the particles plus interaction effects between particles may have rendered this parameter unimportant for the range of values investigated.

In the design of a screening system, Π_6 should be made as small as possible to obtain greatest response. The minimum value is dependent on structural limitations.

Π_7 which is a form of Reynolds number, did not have appreciable influence on Π_1 for the size of particles used. Visual observation of particle movement suggested minimum drag effect. The variation in response obtained was probably due to some combination of experimental error, layering, and scattering effects.

Π_8 can be designated as the flow parameter. It is the ratio of volume flow of undersize particles per unit time to the volume swept out by the apertures per unit time. This ratio adequately relates feed rate, screen motion, and aperture size. It appears to assume even greater importance when establishing compatibility for a multi-screen system.

Π_9 is a form of the Froude number and is an excellent means for describing the screen motion. For $\Pi_9 > .08$, particle movement on a horizontal screen is exceptionally brisk.

To optimize space requirements, a given screen should be just long enough to achieve the desired response. Π_{10} provides the criteria necessary to obtain this optimization.

The observed response due to Π_{11} provides insights to some interesting possibilities for size classing particles. Performing a given sizing operation may be most efficient by using several screens

of different aperture size rather than using one screen.

The appreciable decrease in response due to an increase in Π_{14} indicates that oversize particles have pronounced effects on the undersize particles for the conditions investigated.

The approach used in analyzing a multi-screen system provides the basis for possible future investigations. Consider two screens in series. Passing a mixture of oversize and undersize particles over screen one removes some of the undersize particles. Thus the value of Π_{14} for screen two will be larger which would lower the response for the second screen. However, accompanying this is a reduction in the feed rate to the second screen. This decreases Π_8 which would increase the response. By careful selection of frequency and aperture size for screen two, Π_8 would have greater influence than Π_{14}.

Suggestions for Future Investigations

This study has resulted in the formulation of basic concepts which are applicable to size classing systems employing perforated surfaces. To realize greater benefits from this study would require additional work consisting of:

1. Developing prediction equations which would include in addition to equation 6 - 2, effects due to varying proportion of different size classes of particles, different shape factor of particles, and possible moisture effects.

2. Developing structural design criteria for screen assembly and mounting so that the smallest d/a ratio can be utilized.

3. Developing criteria for minimizing or eliminating particle lodging in apertures for those particles which are about the same size

as the aperture.

4. Developing additional optimizing techniques for multi-screen systems.

BIBLIOGRAPHY

1. Allen, G. F. "Screen and Pneumatic Classification." Industrial and Engineering Chemistry, Vol. 12, p. 39-44, Dec., 1962.

2. Allen, M. "Kill Static in Lab Screening." Chemical Engineering, Vol. 65, p. 176, Sept. 22, 1958.

3. Berg, R. H. and G. M. Kovac. "Here's How to Clinch Vital Particle-Size Control: Coulter Counter." Food Engineering, Vol. 32, p. 40-3, May, 1960.

4. Bodziony, J. "On a Certain Hypothesis Concerning the Process of Screening of Granular Bodies." Acad Polonaise des Sciences Bul ser des Sciences Techniques, Vol. 8, N. 2, p. 99-106, 1960.

5. Chemical Engineering, "Fast Action for Fast Screening; Cirlyptic Screens." Vol. 67, p. 102, June 13, 1960.

6. Chepil, W. S. "Compact Rotary Sieve and the Importance of Dry Sieving in Physical Soil Analysis." Soil Science Society of America Proceedings, Vol. 26, p. 4-6, Jan., 1962.

7. Crowley, R. "Particle Size Analysis in Flour Milling." Progress Through Research, Vol. 11, No. 4, p. 10-12, 1957.

8. Dallavalle, J. M. Micromeritics. Second Edition. New York: Pitman Publishing Corporation, 1948, p. 110-113.

9. Eck, K. and W. Walter. "How to Specify Industrial Sifters." Industrial and Engineering Chemistry, Vol. 52, N. 9, p. 53A-4A, 56A, Sept., 1960.

10. Elsken, J. C. and G. A. Ehinger. "New High-Capacity Stationary Screens." Chemical Engineering Progress, Vol. 59, N. 1; p. 76-80, Jan., 1963.

11. Engineer, "Vibrating Screen Separator." Vol. 212, p. 1011, Dec. 15, 1961.

12. Faul, H. and G. L. Davis. "Mineral Separation with Asymmetric Vibrators." American Mineralogist, Vol. 44, p. 1076-82, Sept., 1959.

13. Fink, J. E. "How to Reduce Screen Blinding." Engineering and Mining Journal, Vol. 159, p. 102-4, Dec., 1950.

14. Food Engineering. "Better Separation, Better Starch; Specially Designed Cyclonic Unit Picks Off Light Material in New Operation to Reduce Gluten." Vol. 29, p. 63-4, Jan., 1957.

15. Food Engineering. "Solids Separation, Sifters, Screens, Graders, Reels, Centrifuges, Classifiers." Vol. 33, p. 63-70, April, 1961.

16. Food Engineering. "Advances in Processing Methods." Vol. 34, p. 44, Feb., 1962.

17. Fowler, R. T. and S. C. Lim. "Influence of Various Factors Upon Effectiveness of Separation of Finely Divided Solids by Vibrating Screen." Chemical Engineering Science, Vol. 10, N. 3, p. 163-70, May, 1959.

18. Fowler, R. T. and S. C. Lim. "Prediction of Effectiveness of Separation of Granular Solids by Vibrating Screen." Australian Chemical Engineering, Vol. 2, N. 2, p. 9-13, Feb., 1961.

19. Gaudin, A. M. Principles of Mineral Dressing., New York: McGraw Hill, 1939.

20. Harmond, J. E., Brandenburg, N. R. and D. E. Booster. "Seed Cleaning by Electrostatic Separation." Agricultural Engineering Journal, Vol. 42, N. 1, Jan., 1961.

21. Irani, R. R. and C. F. Callis. "Accurate Particle Size Distribution with Electroformed Sieves." Analytical Chemistry, Vol. 31, p. 2026-8, Dec., 1959.

22. Langhaar, H. L. Dimensional Analysis and Theory of Models. New York: Wiley, 1957.

23. Moore, L. "Getting Better Screening; Gyratory Screens." Food Engineering, Vol. 31, p. 80, March, 1959.

24. Murphy, G. Similitude in Engineering. New York: The Ronald Press, 1950.

25. Northcott, E. and F. N. Oberg. "Applications of Electrostatics to Concentration of Coarse Pebble Phosphate." Mining Engineering, Vol. 10, Trans., p. 1084-6, Oct., 1958.

26. Product Engineering. "Sonic Vibrating Filter Requires Less Power." Vol. 29, p. 22-3, Sept. 22, 1958.

27. Sinden, A. D. "Vibratory Screening Topics." Automation. Vol. 9, p. 67-9, Jan., 1962.

28. Slater, C. and L. Cohen. "A Centrifugal Particle Size Analyzer." Journal of Scientific Instruments, Vol. 39, N. 12, p. 614-17, Dec., 1962.

29. South African Mining and Engineering Journal. "Latest Advances in Screening Technique." Vol. 71, N. 3513, p. 1363-5, June 3, 1960.

30. South African Mining and Engineering Journal. "Jar-Bar Grizzly Feeder." Vol. 73, N. 3633, p. 617-18, Sept. 21, 1962.

31. Sullivan, J. F. "Resonant Vibrating Screens for the Mining Industry." Mining Congress Journal, Vol. 48, p. 26-30, Sept., 1962.

32. Utley, H. F. "Progressive Producer Installs New Type of Screen." Pit and Quarry, Vol. 50, p. 94-5, May, 1958.

33. Vandenhoeck, P. "Pneumatic Classifiers Reclaim Phosphate." Farm Chemicals, Vol. 123, p. 60-2, Sept., 1960.

APPENDIX A

THEORETICAL CALCULATIONS FOR SELECTED FREQUENCIES AND AMPLITUDES

THEORETICAL CALCULATIONS FOR TEST CONDITIONS

Explanation of Tables

A - I

ALPHA = Angle with respect to the vertical at which motion is imparted to the horizontal screen. deg.

F = Frequency. cps.

A = Amplitude. in.

G = Maximum acceleration in mechanism. g's.

VEL = Average horizontal velocity of particle. in./sec.

I = Angle with respect to the vertical at which particle impacts surface. deg.

REY = Π_7 $\mu/Nepl_{2u}$

FROUD = Π_9 G/Ne

A - II

REY = Reynolds number (Π_7).

FROUD = Froude number (Π_9).

APPENDIX A-I

THEORETICAL CALCULATIONS FOR SELECTED FREQUENCIES AND AMPLITUDES

ALPHA 25.0

F	A	G	VEL	I	REY	FROUD
20.0	.0600	2.46	2.86	16.97	53.28	24.00
25.0	.0480	3.07	2.98	21.05	53.28	30.00
30.0	.0400	3.69	1.52	25.25	53.28	36.00
35.0	.0342	4.30	1.56	28.89	53.27	41.99
40.0	.0300	4.92	1.74	30.16	53.28	48.00
45.0	.0266	5.54	3.01	20.82	53.27	53.99
50.0	.0240	6.15	3.12	22.20	53.28	60.00
20.0	.0600	2.46	2.86	16.97	53.28	24.00
25.0	.0384	2.46	2.29	16.97	42.62	24.00
30.0	.0266	2.46	1.91	16.97	35.51	23.99
35.0	.0195	2.46	1.63	16.97	30.44	23.99
40.0	.0150	2.46	1.43	16.97	26.64	24.00
45.0	.0118	2.46	1.27	16.97	23.67	23.99
50.0	.0096	2.46	1.14	16.97	21.31	24.00

APPENDIX A-I Continued

ALPHA 35.0

F	A	G	VEL	I	REY	FROUD
20.0	.0600	2.46	3.74	22.51	53.28	24.00
25.0	.0480	3.07	3.99	27.51	53.28	30.00
30.0	.0400	3.69	4.08	32.28	53.28	36.00
35.0	.0342	4.30	2.07	36.87	53.27	41.99
40.0	.0300	4.92	2.15	40.41	53.28	48.00
45.0	.0266	5.54	2.46	40.28	53.27	53.99
50.0	.0240	6.15	4.10	29.78	53.28	60.00
20.0	.0600	2.46	3.74	22.51	53.28	24.00
25.0	.0384	2.46	2.99	22.51	42.62	24.00
30.0	.0266	2.46	2.49	22.51	35.51	23.99
35.0	.0195	2.46	2.14	22.51	30.44	23.99
40.0	.0150	2.46	1.87	22.51	26.64	24.00
45.0	.0118	2.46	1.66	22.51	23.67	23.99
50.0	.0096	2.46	1.49	22.51	21.31	24.00

APPENDIX A-I Continued

ALPHA 45.0

F	A	G	VEL	I	REY	FROUD
20.0	.0600	2.46	4.22	27.30	53.28	24.00
25.0	.0480	3.07	4.75	32.60	53.28	30.00
30.0	.0400	3.69	4.95	37.57	53.28	36.00
35.0	.0342	4.30	5.04	42.33	53.27	41.99
40.0	.0300	4.92	2.55	46.57	53.28	48.00
45.0	.0266	5.54	2.62	49.85	53.27	53.99
50.0	.0240	6.15	2.80	51.59	53.28	60.00
20.0	.0600	2.46	4.22	27.30	53.28	24.00
25.0	.0384	2.46	3.38	27.30	42.62	24.00
30.0	.0266	2.46	2.81	27.30	35.51	23.99
35.0	.0195	2.46	2.41	27.30	30.44	23.99
40.0	.0150	2.46	2.11	27.30	26.64	24.00
45.0	.0118	2.46	1.87	27.30	23.67	23.99
50.0	.0096	2.46	1.69	27.30	21.31	24.00

APPENDIX A-I Continued

ALPHA 55.0

F	A	G	VEL	I	REY	FROUD
20.0	.0600	2.46	3.77	31.57	53.28	24.00
25.0	.0480	3.07	4.95	36.73	53.28	30.00
30.0	.0400	3.69	5.45	41.64	53.28	36.00
35.0	.0342	4.30	5.69	46.03	53.27	41.99
40.0	.0300	4.92	5.79	50.12	53.28	48.00
45.0	.0266	5.54	5.86	53.72	53.27	53.99
50.0	.0240	6.15	2.96	56.85	53.28	60.00
20.0	.0600	2.46	3.77	31.57	53.28	24.00
25.0	.0384	2.46	3.02	31.57	42.62	24.00
30.0	.0266	2.46	2.51	31.57	35.51	23.99
35.0	.0195	2.46	2.15	31.57	30.44	23.99
40.0	.0150	2.46	1.88	31.57	26.64	24.00
45.0	.0118	2.46	1.67	31.57	23.67	23.99
50.0	.0096	2.46	1.51	31.57	21.31	24.00

APPENDIX A-I Continued

ALPHA 65.0

F	A	G	VEL	I	REY	FROUD
20.0	.0600	2.46	.63	36.02	53.28	24.00
25.0	.0480	3.07	3.46	40.81	53.28	30.00
30.0	.0400	3.69	4.85	45.20	53.28	36.00
35.0	.0342	4.30	5.59	49.15	53.27	41.99
40.0	.0300	4.92	6.00	52.62	53.28	48.00
45.0	.0266	5.54	6.22	55.82	53.27	53.99
50.0	.0240	6.15	6.34	58.71	53.28	60.00
20.0	.0600	2.46	.63	36.02	53.28	24.00
25.0	.0384	2.46	.50	36.02	42.62	24.00
30.0	.0266	2.46	.42	36.02	35.51	23.99
35.0	.0195	2.46	.36	36.02	30.44	23.99
40.0	.0150	2.46	.31	36.02	26.64	24.00
45.0	.0118	2.46	.28	36.02	23.67	23.99
50.0	.0096	2.46	.25	36.02	21.31	24.00

APPENDIX A-I Continued

ALPHA 25.0

F	A	G	VEL	I	REY	FROUD
30.0	.0460	4.24	1.79	28.61	61.27	41.40
35.0	.0394	4.95	2.03	29.91	61.27	48.29
40.0	.0345	5.66	3.51	21.01	61.27	55.20
45.0	.0306	6.37	3.60	22.89	61.27	62.09
50.0	.0276	7.07	2.41	25.08	61.27	69.00
30.0	.0460	4.24	1.79	28.61	61.27	41.40
35.0	.0337	4.24	1.53	28.61	52.51	41.39
40.0	.0258	4.24	1.34	28.61	45.95	41.40
45.0	.0204	4.24	1.19	28.61	40.84	41.39
50.0	.0165	4.24	1.07	28.61	36.76	41.40

APPENDIX A-I Continued

ALPHA 35.0

F	A	G	VEL	I	REY	FROUD
30.0	.0460	4.24	2.38	36.44	61.27	41.40
35.0	.0394	4.95	2.48	40.52	61.27	48.29
40.0	.0345	5.66	4.01	31.47	61.27	55.20
45.0	.0306	6.37	4.80	30.26	61.27	62.09
50.0	.0276	7.07	4.89	32.44	61.27	69.00
30.0	.0460	4.24	2.38	36.44	61.27	41.40
35.0	.0337	4.24	2.04	36.44	52.51	41.39
40.0	.0258	4.24	1.78	36.44	45.95	41.40
45.0	.0204	4.24	1.58	36.44	40.84	41.39
50.0	.0165	4.24	1.43	36.44	36.76	41.40

APPENDIX A-I Continued

ALPHA 45.0

F	A	G	VEL	I	REY	FROUD
30.0	.0460	4.24	5.79	41.92	61.27	41.40
35.0	.0394	4.95	2.94	46.81	61.27	48.29
40.0	.0345	5.66	3.04	50.38	61.27	55.20
45.0	.0306	6.37	3.42	50.90	61.27	62.09
50.0	.0276	7.07	5.78	39.20	61.27	69.00
30.0	.0460	4.24	5.79	41.92	61.27	41.40
35.0	.0337	4.24	4.96	41.92	52.51	41.39
40.0	.0258	4.24	4.34	41.92	45.95	41.40
45.0	.0204	4.24	3.86	41.92	40.84	41.39
50.0	.0165	4.24	3.47	41.92	36.76	41.40

APPENDIX A-I Continued

ALPHA 55.0

F	A	G	VEL	I	REY	FROUD
30.0	.0460	4.24	6.52	45.66	61.27	41.40
35.0	.0394	4.95	6.67	50.34	61.27	48.29
40.0	.0345	5.66	6.75	54.42	61.27	55.20
45.0	.0306	6.37	3.43	57.72	61.27	62.09
50.0	.0276	7.07	3.54	60.17	61.27	69.00
30.0	.0460	4.24	6.52	45.66	61.27	41.40
35.0	.0337	4.24	5.59	45.66	52.51	41.39
40.0	.0258	4.24	4.89	45.66	45.95	41.40
45.0	.0204	4.24	4.35	45.66	40.84	41.39
50.0	.0165	4.24	3.91	45.66	36.76	41.40

APPENDIX A-I Continued

ALPHA 65.0

F	A	G	VEL	I	REY	FROUD
30.0	.0460	4.24	6.37	48.78	61.27	41.40
35.0	.0394	4.95	6.91	52.82	61.27	48.29
40.0	.0345	5.66	7.19	56.43	61.27	55.20
45.0	.0306	6.37	7.33	59.67	61.27	62.09
50.0	.0276	7.07	7.41	62.49	61.27	69.00
30.0	.0460	4.24	6.37	48.78	61.27	41.40
35.0	.0337	4.24	5.46	48.78	52.51	41.39
40.0	.0258	4.24	4.77	48.78	45.95	41.40
45.0	.0204	4.24	4.24	48.78	40.84	41.39
50.0	.0165	4.24	3.82	48.78	36.76	41.40

APPENDIX A-II

THEORETICAL CALCULATIONS FOR TEST CONDITIONS

ALPHA 35.0

F	A	G	VEL	I	REY	FROUD
32.0	.0190	1.99	1.64	18.88	3.36	.050
28.5	.0240	2.00	1.84	18.96	3.78	.050
22.0	.0400	1.98	2.36	18.78	4.86	.050
20.7	.0450	1.97	2.49	18.73	5.14	.049
22.0	.0310	1.53	1.13	15.38	3.76	.038
28.5	.0240	2.00	1.84	18.96	3.78	.050
33.0	.0200	2.23	1.95	20.78	3.64	.056
40.0	.0170	2.79	2.21	25.21	3.75	.070

ALPHA 45.0

F	A	G	VEL	I	REY	FROUD
32.0	.0190	1.99	1.64	23.40	3.36	.050
28.5	.0240	2.00	1.86	23.36	3.78	.050
22.0	.0400	1.98	2.36	23.26	4.86	.050
20.7	.0450	1.97	2.48	23.17	5.14	.049
22.0	.0310	1.53	.58	19.41	3.76	.038
28.5	.0240	2.00	1.86	23.36	3.78	.050
33.0	.0200	2.23	2.11	25.37	3.64	.056
40.0	.0170	2.79	2.59	30.20	3.75	.070

APPENDIX A-II Continued

ALPHA 55.0

F	A	G	VEL	I	REY	FROUD
32.0	.0190	1.99	.92	27.59	3.36	.050
28.5	.0240	2.00	1.05	27.58	3.78	.050
22.0	.0400	1.98	1.29	27.44	4.86	.050
20.7	.0450	1.97	1.33	27.42	5.14	.049
28.5	.0240	2.00	1.05	27.58	3.78	.050
33.0	.0200	2.23	1.64	29.68	3.64	.056
40.0	.0170	2.79	2.56	34.41	3.75	.070

ALPHA 65.0

F	A	G	VEL	I	REY	FROUD
40.0	.0170	2.79	1.36	38.56	3.75	.070

APPENDIX B

DIMENSIONS OF UNDERSIZE PARTICLES

DIMENSIONS OF OVERSIZE PARTICLES

PARTICLE DENSITY CALCULATIONS

ACCELEROMETER TESTS

APPENDIX B-I

DIMENSIONS OF UNDERSIZE PARTICLES

Particle	l_{1u} in.	l_{2u} in.	l_{3u} in.
1	.175	.143	.097
2	.160	.137	.097
3	.168	.150	.099
4	.156	.137	.099
5	.177	.140	.099
6	.165	.132	.095
7	.162	.156	.096
8	.178	.139	.100
9	.179	.150	.100
10	.159	.148	.097
11	.168	.140	.098
12	.176	.150	.099
13	.146	.137	.096
14	.160	.131	.096
15	.185	.158	.102
16	.150	.134	.096
17	.153	.139	.099
18	.184	.150	.101
19	.166	.135	.101
20	.174	.141	.102
21	.171	.144	.099
22	.167	.130	.100
23	.161	.138	.095
24	.153	.135	.100
25	.159	.135	.097

APPENDIX B-II

DIMENSIONS OF OVERSIZE PARTICLES

Particle	l_{10} in.	l_{20} in.
1	.243	.244
2	.250	.250
3	.241	.241
4	.239	.240
5	.231	.231
6	.243	.244
7	.240	.240
8	.241	.240
9	.242	.243
10	.242	.239
11	.245	.245
12	.245	.245
13	.240	.240
14	.240	.239
15	.242	.242
16	.249	.249
17	.247	.244
18	.239	.238
19	.243	.243
20	.241	.240
21	.242	.240
22	.237	.240
23	.240	.241
24	.240	.240
25	.248	.242

APPENDIX B-III

PARTICLE DENSITY CALCULATIONS

Zero reading = 149 mm Hg

Sample	Reading mm Hg	Diff. mm Hg	Wt. Grams	Vol. $in.^3$	Density $lbm./in.^3$
		Oversize Particles			
1	215	66	51.0	2.350	.0477
2	215	66	51.0	2.350	.0477
3	213	64	50.5	2.300	.0483
4	215	66	51.2	2.350	.0481
5	216	67	51.7	2.375	.0480
6	214	65	50.6	2.325	.0482
		Undersize Particles			
1	220	71	54.9	2.470	.0490
2	211	62	52.9	2.250	.0520
3	220	71	55.0	2.470	.0490
4	211	62	52.9	2.250	.0520
5	217	68	53.8	2.400	.0496
6	216	67	52.9	2.325	.0503

APPENDIX B-IV

ACCELEROMETER TESTS

Accelerometer No.	Frequency cps	Input g's	Output g's	% Low
3132	20	1.0	1.00	0
3132	20	2.0	2.00	0
3132	40	1.0	1.00	0
3138	20	1.0	0.80	20.0
3138	20	2.0	1.80	10.0
3138	25	1.0	0.95	5.0
3138	30	1.0	0.95	5.0
3138	30	2.0	1.95	2.5
3138	40	1.0	0.95	5.0
3138	40	2.0	1.95	2.5

APPENDIX C

RAW DATA

COMPONENT EQUATION DATA

EVALUATION OF MODEL II PREDICTION EQUATION

RAW DATA FOR TESTING PREDICTION EQUATION

COMPONENT EQUATION DATA
FOR
TESTING PREDICTION EQUATION

Explanation of Tables

C - I & C - IV

The header contains three numbers: 1. Number of observations of the independent variable; 2. Sampling length down screen - in.; 3. The index KC, indicating which pi term is the independent variable. KC assumes the values shown below:

KC	Pi Term
1	Π_2
2	Π_6
3	Π_7
4	Π_8
5	Π_9
6	Π_{10}
7	Π_{11}
8	Π_{14}

Two rows form one data pair. The first row contains eleven pieces of information. In order these are: 1. Fartherest distance in inches down screen undersize particles advanced; 2. Width of screen in inches; 3. Wire diameter of screen in inches; 4. Screen aperture in inches; 5. Speed of eccentric driver shaft in RPM; 6. Total screen displacement, 2 x amplitude in inches; 7. Sampling time in minutes; 8. The angle α in degrees; 9. Weight of oversize particles in grams;

10. Pi term which was the independent variable; 11. A four digit code, the first two digits being the value for α, the third digit the motion identity, and the last digit is the screen identity number.

The second row contains ten pieces of information. These are the accumulated weights (grams) of undersize particles which passed through the screen for 1 in., 2 in., ... 10 in., of screen length. If particle travel exceeded 10 in. the "over flow" was added to the tenth location.

Raw data for Π_{10} equal to the independent variable was altered slightly. The header card contains the number of observations and the index KC. The sampling length down screen was entered as the tenth piece of data on the first card of each data pair.

C - III

P OBS = Observed value of Π_1.

P CAL = Calculated value of Π_1 using the Model II prediction equation.

PERCENT = Deviation of predicted value from the observed value of Π_1.

APPENDIX C-I

RAW DATA

12 3 1

```
7 2.9375 .080 .170 1706. .048 .110  35.0    .0  2 3533
84.8 200.4 281.0 302.1 306.2 306.7 306.8    .0    .0    .0

7 2.9375 .080 .170 1707. .047 .108  35.0    .0  2 3533
87.5 199.2 278.2 301.4 305.2 305.7 306.0    .0    .0    .0

7 2.9375 .080 .170 1708. .047 .106  35.0    .0  2 3533
86.8 201.0 282.1 303.6 307.1 307.8 307.9    .0    .0    .0

8 2.9375 .080 .170 1707. .048 .109  45.0    .0  2 4533
98.2 213.9 282.3 302.3 306.4 307.6 307.9 308.0    .0    .0

8 2.9375 .080 .170 1709. .048 .110  45.0    .0  2 4533
90.8 207.8 283.2 303.6 307.5 308.5 309.1 309.2    .0    .0

7 2.9375 .080 .170 1705. .050 .104  45.0    .0  2 4533
92.7 206.6 274.0 292.0 295.9 297.0 297.5    .0    .0    .0

7 2.9375 .080 .170 1709. .048 .102  55.0    .0  2 5533
85.8 201.5 271.3 286.0 288.3 288.7 288.8    .0    .0    .0

7 2.9375 .080 .170 1713. .048 .100  55.0    .0  2 5533
81.5 195.8 265.5 280.0 282.6 283.1 283.2    .0    .0    .0

7 2.9375 .080 .170 1707. .048 .095  55.0    .0  2 5533
77.9 189.6 261.4 277.1 279.0 279.5 279.6    .0    .0    .0

6 2.9375 .080 .170 1710. .048 .103  65.0    .0  2 6533
73.7 185.8 270.4 288.0 289.2 289.5   .0     .0    .0    .0

6 2.9375 .080 .170 1712. .048 .100  65.0    .0  2 6533
75.3 187.8 269.3 290.6 292.3 292.5   .0     .0    .0    .0

6 2.9375 .080 .170 1707. .049 .110  65.0    .0  2 6533
75.8 188.5 289.0 312.5 314.3 314.4   .0     .0    .0    .0
```

APPENDIX C-I Continued

12 3 2

```
 8 2.7500 .032 .168 1711. .047 .114  45.0    .0  6 4538
128.0 243.7 284.4 294.6 298.6 299.0 299.4 299.6    .0    .0

 8 2.7500 .032 .168 1711. .047 .118  45.0    .0  6 4538
129.2 249.7 292.7 302.7 305.8 307.3 307.6 307.8    .0    .0

 8 2.7500 .032 .168 1711. .047 .112  45.0    .0  6 4538
128.6 243.0 283.0 292.7 295.6 296.7 297.0 297.2    .0    .0

 8 2.9375 .054 .168 1707. .048 .121  45.0    .0  6 4537
110.4 228.2 303.6 325.1 329.6 330.6 331.0 331.4    .0    .0

 9 2.9375 .054 .168 1710. .048 .123  45.0    .0  6 4537
127.4 244.7 317.2 335.3 340.1 341.4 341.6 341.8 341.9    .0

 8 2.9375 .054 .168 1709. .048 .126  45.0    .0  6 4537
129.3 250.6 320.0 338.2 342.7 344.3 344.9 345.1    .0    .0

 8 2.9375 .080 .170 1707. .048 .109  45.0    .0  6 4533
 98.2 213.9 282.3 302.3 306.4 307.6 307.9 308.0    .0    .0

 8 2.9375 .080 .170 1709. .048 .110  45.0    .0  6 4533
 90.8 207.8 283.2 303.6 307.5 308.5 309.1 309.2    .0    .0

 7 2.9375 .080 .170 1705. .050 .104  45.0    .0  6 4533
 92.7 206.6 274.0 292.0 295.9 297.0 297.5    .0    .0    .0

 9 2.8130 .120 .166 1709. .048 .150  45.0    .0  6 4536
 93.7 206.0 314.8 376.3 393.9 398.1 399.3 399.7 399.8    .0

 9 2.8130 .120 .166 1708. .048 .157  45.0    .0  6 4536
 99.0 212.1 331.2 388.9 404.0 408.3 409.5 409.9 410.1    .0

 9 2.8130 .120 .166 1709. .048 .175  45.0    .0  6 4536
101.0 221.1 350.7 421.5 440.8 446.1 447.5 447.9 448.1    .0
```

APPENDIX C-I Continued

12 3 3

```
 8 2.9375 .080 .170 1917. .038 .112  45.0    .0  7 4523
104.2 222.7 329.5 359.3 364.5 366.2 366.5 366.6   .0    .0

 8 2.9375 .080 .170 1919. .038 .114  45.0    .0  7 4523
 95.2 216.4 318.2 349.1 356.2 357.9 358.1 358.2   .0    .0

 7 2.9375 .080 .170 1919. .038 .102  45.0    .0  7 4523
 93.7 206.9 301.2 324.9 329.1 330.0 330.1   .0    .0    .0

 8 2.9375 .080 .170 1707. .048 .109  45.0    .0  7 4533
 98.2 213.9 282.3 302.3 306.4 307.6 307.9 308.0   .0    .0

 8 2.9375 .080 .170 1709. .048 .110  45.0    .0  7 4533
 90.8 207.8 283.2 303.6 307.5 308.5 309.1 309.2   .0    .0

 7 2.9375 .080 .170 1705. .050 .104  45.0    .0  7 4533
 92.7 206.6 274.0 292.0 295.9 297.0 297.5   .0    .0    .0

 9 2.9375 .080 .170 1318. .080 .137  45.0    .0  7 4543
119.0 233.0 277.9 291.2 294.6 295.7 296.2 296.4 296.5   .0

 9 2.9375 .080 .170 1326. .080 .137  45.0    .0  7 4543
117.8 231.4 283.0 298.8 304.0 305.2 305.7 306.0 306.1   .0

 9 2.9375 .080 .170 1319. .080 .131  45.0    .0  7 4543
120.1 228.5 274.9 288.9 293.2 294.7 295.4 295.7 295.8   .0

 9 2.9375 .080 .170 1242. .090 .146  45.0    .0  7 4553
127.7 242.5 283.5 295.5 299.0 300.1 300.7 300.9 301.2   .0

 9 2.9375 .080 .170 1248. .090 .149  45.0    .0  7 4553
129.4 247.3 293.8 306.9 311.0 312.4 313.0 313.3 313.6   .0

 9 2.9375 .080 .170 1244. .090 .138  45.0    .0  7 4553
122.3 230.3 273.8 286.6 290.9 292.6 293.4 293.5 293.8   .0
```

APPENDIX C-I Continued

21 3 4

```
 7 2.9375 .080 .170 1710. .048 .213  45.0    .0  8 4533
120.1 196.0 216.4 221.8 223.8 224.2 224.4    .0    .0    .0

 6 2.9375 .080 .170 1708. .049 .138  45.0    .0  8 4533
125.0 204.7 226.0 230.3 231.3 231.7    .0    .0    .0    .0

 7 2.9375 .080 .170 1709. .049 .127  45.0    .0  8 4533
123.8 227.2 261.5 268.6 270.5 271.2 271.3    .0    .0    .0

 8 2.9375 .080 .170 1711. .048 .150  45.0    .0  8 4533
122.1 246.2 371.0 413.4 421.9 423.5 423.8 423.9    .0    .0

 9 2.9375 .080 .170 1710. .048 .154  45.0    .0  8 4533
122.0 247.3 374.3 457.7 481.0 486.4 487.8 488.3 488.6    .0

 8 2.9375 .080 .170 1708. .050 .138  45.0    .0  8 4533
119.7 244.8 373.3 482.2 519.1 526.9 528.8 529.3    .0    .0

 9 2.9375 .080 .170 1709. .049 .109  45.0    .0  8 4533
 87.4 185.3 290.5 391.0 439.0 451.7 454.7 455.8 456.2    .0

 7 2.9375 .080 .170 1704. .047 .199  45.0    .0  8 4533
125.0 190.5 206.1 210.3 211.2 211.5 211.7    .0    .0    .0

 6 2.9375 .080 .170 1706. .047 .134  45.0    .0  8 4533
126.0 202.3 219.8 223.3 223.8 224.1    .0    .0    .0    .0

 7 2.9375 .080 .170 1709. .050 .122  45.0    .0  8 4533
122.0 222.0 254.6 263.0 265.2 265.5 265.8    .0    .0    .0

 7 2.9375 .080 .170 1707. .048 .148  45.0    .0  8 4533
122.0 245.2 369.7 408.0 415.6 417.0 417.5    .0    .0    .0

 8 2.9375 .080 .170 1708. .048 .153  45.0    .0  8 4533
119.5 245.5 372.9 461.5 485.5 490.8 492.2 492.4    .0    .0

 9 2.9375 .080 .170 1709. .048 .154  45.0    .0  8 4533
118.5 242.7 371.4 480.0 515.4 523.0 524.9 525.1 525.4    .0

 9 2.9375 .080 .170 1710. .048 .112  45.0    .0  8 4533
 92.1 189.0 295.6 399.8 449.5 463.0 466.2 467.1 467.6    .0
```

APPENDIX C-I Continued

```
 6 2.9375 .080 .170 1708. .050 .189  45.0    .0  8 4533
118.2 188.0 206.6 211.2 212.5 213.0   .0    .0   .0    .0

 7 2.9375 .080 .170 1710. .049 .136  45.0    .0  8 4533
121.2 205.0 227.3 233.0 234.8 235.3 235.5    .0   .0    .0

 7 2.9375 .080 .170 1707. .050 .120  45.0    .0  8 4533
122.9 225.7 229.7 267.8 270.2 270.8 270.9    .0   .0    .0

 7 2.9375 .080 .170 1711. .050 .106  45.0    .0  8 4533
 83.0 186.3 278.4 314.0 322.1 324.1 324.7    .0   .0    .0

 8 2.9375 .080 .170 1709. .049 .136  45.0    .0  8 4533
101.0 220.9 348.6 420.8 442.6 447.5 449.0 449.6   .0    .0

 9 2.9375 .080 .170 1708. .050 .119  45.0    .0  8 4533
 90.0 190.1 303.4 396.1 430.3 437.3 438.8 439.6 439.9    .0

 9 2.9375 .080 .170 1711. .050 .126  45.0    .0  8 4533
 98.3 208.2 323.4 441.1 498.1 511.7 515.7 516.6 516.9    .0
```

APPENDIX C-I Continued

15 3 5

```
 4 2.9375 .080 .170 1013. .080 .135  45.0     .0  9 4563
105.0 212.4 228.6 229.0    .0    .0    .0     .0    .0    .0

 4 2.9375 .080 .170 1011. .080 .131  45.0     .0  9 4563
 89.5 205.0 232.6 232.8    .0    .0    .0     .0    .0    .0

 5 2.9375 .080 .170 1015. .078 .189  45.0     .0  9 4563
 99.6 214.4 330.8 337.2 337.3    .0    .0     .0    .0    .0

 5 2.9375 .080 .170 1323. .061 .148  45.0     .0  9 4573
 94.9 212.6 306.0 312.9 313.3    .0    .0     .0    .0    .0

 5 2.9375 .080 .170 1320. .061 .118  45.0     .0  9 4573
 81.3 193.6 252.8 253.3 253.6    .0    .0     .0    .0    .0

 6 2.9375 .080 .170 1316. .064 .121  45.0     .0  9 4573
 82.2 197.7 264.3 272.4 273.3 273.4    .0     .0    .0    .0

 8 2.9375 .080 .170 1707. .048 .109  45.0     .0  9 4533
 98.2 213.9 282.3 302.3 306.4 307.6 307.9  308.0    .0    .0

 8 2.9375 .080 .170 1709. .048 .110  45.0     .0  9 4533
 90.8 207.8 283.2 303.6 307.5 308.5 309.1  309.2    .0    .0

 7 2.9375 .080 .170 1705. .050 .104  45.0     .0  9 4533
 92.7 206.6 274.0 292.0 295.9 297.0 297.5     .0    .0    .0

 9 2.9375 .080 .170 1983. .040 .111  45.0     .0  9 4583
 94.7 209.2 312.2 350.4 360.0 362.3 363.2  363.5 363.7    .0

 9 2.9375 .080 .170 1983. .040 .105  45.0     .0  9 4583
 93.7 203.4 302.8 340.8 350.3 353.1 354.0  354.4 354.8    .0

10 2.9375 .080 .170 1987. .040 .122  45.0     .0  9 4583
107.3 231.2 340.2 387.7 402.8 407.7 409.8  410.6 411.2 411.3

10 2.9375 .080 .170 2397. .034 .109  45.0     .0  9 4593
 96.3 201.9 313.3 386.2 415.5 427.7 433.7  436.8 438.2 441.1

10 2.9375 .080 .170 2399. .034 .119  45.0     .0  9 4593
 98.3 210.8 335.0 419.0 453.7 466.2 472.5  475.2 476.3 478.5

10 2.9375 .080 .170 2396. .034 .124  45.0     .0  9 4593
102.9 220.6 341.7 429.0 471.2 488.5 495.6  499.4 501.7 506.1
```

APPENDIX C-I Continued

15 6

```
8 2.9375 .080 .170 1707. .048 .109 45.    .0 2  10 4533
98.2 213.9 282.3 302.3 306.4 307.6 307.9 308.0    .0    .0

8 2.9375 .080 .170 1709. .048 .110 45.    .0 2  10 4533
90.8 207.8 283.2 303.6 307.5 308.5 309.1 309.2    .0    .0

7 2.9375 .080 .170 1705. .050 .104 45.    .0 2  10 4533
92.7 206.6 274.0 292.0 295.9 297.0 297.5    .0    .0    .0

8 2.9375 .080 .170 1707. .048 .109 45.    .0 3  10 4533
98.2 213.9 282.3 302.3 306.4 307.6 307.9 308.0    .0    .0

8 2.9375 .080 .170 1709. .048 .110 45.    .0 3  10 4533
90.8 207.8 283.2 303.6 307.5 308.5 309.1 309.2    .0    .0

7 2.9375 .080 .170 1705. .050 .104 45.    .0 3  10 4533
92.7 206.6 274.0 292.0 295.9 297.0 297.5    .0    .0    .0

8 2.9375 .080 .170 1707. .048 .109 45.    .0 4  10 4533
98.2 213.9 282.3 302.3 306.4 307.6 307.9 308.0    .0    .0

8 2.9375 .080 .170 1709. .048 .110 45.    .0 4  10 4533
90.8 207.8 283.2 303.6 307.5 308.5 309.1 309.2    .0    .0

7 2.9375 .080 .170 1705. .050 .104 45.    .0 4  10 4533
92.7 206.6 274.0 292.0 295.9 297.0 297.5    .0    .0    .0

8 2.9375 .080 .170 1707. .048 .109 45.    .0 5  10 4533
98.2 213.9 282.3 302.3 306.4 307.6 307.9 308.0    .0    .0

8 2.9375 .080 .170 1709. .048 .110 45.    .0 5  10 4533
90.8 207.8 283.2 303.6 307.5 308.5 309.1 309.2    .0    .0

7 2.9375 .080 .170 1705. .050 .104 45.    .0 5  10 4533
92.7 206.6 274.0 292.0 295.9 297.0 297.5    .0    .0    .0

8 2.9375 .080 .170 1707. .048 .109 45.    .0 6  10 4533
98.2 213.9 282.3 302.3 306.4 307.6 307.9 308.0    .0    .0

8 2.9375 .080 .170 1709. .048 .110 45.    .0 6  10 4533
90.8 207.8 283.2 303.6 307.5 308.5 309.1 309.2    .0    .0

7 2.9375 .080 .170 1705. .050 .104 45.    .0 6  10 4533
92.7 206.6 274.0 292.0 295.9 297.0 297.5    .0    .0    .0
```

APPENDIX C-I Continued

15 3 7

```
 6 2.8125 .105 .228 1707. .048 .060  45.0     .0 11 4531
100.0 208.7 278.6 290.0 291.3 291.5    .0     .0     .0     .0

 6 2.8125 .105 .228 1710. .048 .067  45.0     .0 11 4531
112.0 225.4 316.8 334.7 336.0 336.0    .0     .0     .0     .0

 6 2.8125 .105 .228 1707. .048 .069  45.0     .0 11 4531
112.3 229.7 322.2 338.2 340.0 340.3    .0     .0     .0     .0

 6 3.0000 .092 .194 1709. .048 .086  45.0     .0 11 4532
112.3 227.0 305.1 324.0 327.4 328.0    .0     .0     .0     .0

 7 3.0000 .092 .194 1707. .048 .089  45.0     .0 11 4532
120.8 241.7 319.7 337.1 340.0 340.6 340.8     .0     .0     .0

 7 3.0000 .092 .194 1714. .048 .094  45.0     .0 11 4532
122.0 247.3 328.6 349.0 352.3 353.0 353.2     .0     .0     .0

 8 2.9375 .080 .170 1707. .048 .109  45.0     .0 11 4533
 98.2 213.9 282.3 302.3 306.4 307.6 307.9 308.0     .0     .0

 8 2.9375 .080 .170 1709. .048 .110  45.0     .0 11 4533
 90.8 207.8 283.2 303.6 307.5 308.5 309.1 309.2     .0     .0

 7 2.9375 .080 .170 1705. .050 .104  45.0     .0 11 4533
 92.7 206.6 274.0 292.0 295.9 297.0 297.5     .0     .0     .0

10 2.8750 .063 .137 1707. .048 .037  45.0     .0 11 4534
 15.6  31.2  42.8  50.6  54.3  56.3  58.0  59.1  60.2  67.2

10 2.8750 .063 .137 1706. .048 .038  45.0     .0 11 4534
 15.3  30.4  41.9  49.1  53.4  56.0  57.5  58.4  59.3  67.1

10 2.8750 .063 .137 1714. .048 .040  45.0     .0 11 4534
 15.4  30.7  43.9  51.5  56.0  58.6  60.3  61.7  62.7  71.0

10 2.6700 .054 .113 1709. .047 .190  45.0     .0 11 4535
   .2    .4    .6    .9   1.0   1.2   1.3   1.5   1.8 207.7

10 2.6700 .054 .113 1709. .047 .199  45.0     .0 11 4535
   .1    .6    .7    .8   1.0   1.3   1.5   1.7   2.0 233.0

10 2.6700 .054 .113 1711. .047 .200  45.0     .0 11 4535
   .2    .4    .7    .9   1.1   1.4   1.7   1.8   2.0 239.3
```

APPENDIX C-I Continued

16 3 8

```
 7 2.9375 .080 .170 1712. .048 .115  45.0  42.2 14 4533
86.3 200.0 296.0 327.5 331.8 332.0 332.2   .0   .0   .0

 6 2.9375 .080 .170 1704. .048 .125  45.0  58.2 14 4533
97.0 212.9 316.4 354.2 357.9 358.0   .0   .0   .0   .0

 7 2.9375 .080 .170 1710. .048 .128  45.0  57.0 14 4533
95.2 211.8 316.9 362.7 368.0 368.3 368.5   .0   .0   .0

 6 2.9375 .080 .170 1705. .048 .121  45.0  51.9 14 4533
95.0 211.3 314.8 352.2 355.2 355.4   .0   .0   .0   .0

 6 2.9375 .080 .170 1711. .048 .131  45.0  68.5 14 4533
99.5 215.8 323.1 367.5 372.0 372.4   .0   .0   .0   .0

 7 2.9375 .080 .170 1711. .048 .138  45.0  63.3 14 4533
100.7 216.9 327.3 385.9 392.7 393.2 393.3   .0   .0   .0

10 2.9375 .080 .170 1707. .048 .170  45.0 128.3 14 4533
115.0 232.9 317.0 381.8 427.1 457.4 474.2 479.9 480.7 480.9

10 2.9375 .080 .170 1704. .048 .173  45.0 129.4 14 4533
120.5 239.6 328.8 399.4 448.5 477.7 491.2 495.3 495.9 496.2

10 2.9375 .080 .170 1708. .048 .210  45.0 237.4 14 4533
124.4 233.4 295.8 340.4 375.7 413.5 460.1 520.1 557.2 581.8

10 2.9375 .080 .170 1706. .048 .203  45.0 237.6 14 4533
123.9 231.4 296.5 341.2 373.6 403.1 441.3 507.8 562.3 587.0

10 2.9375 .080 .170 1705. .048 .208  45.0 213.4 14 4533
126.2 238.8 302.1 346.2 381.9 420.7 468.5 532.8 571.3 589.0

10 2.9375 .080 .170 1708. .048 .208  45.0 234.2 14 4533
126.7 239.8 313.0 363.0 400.4 435.6 481.0 547.1 587.9 607.6

10 2.9375 .080 .170 1710. .048 .223  45.0 265.7 14 4533
124.3 233.4 296.9 340.4 375.0 410.1 460.5 541.1 605.8 654.6

10 2.9375 .080 .170 1708. .048 .206  45.0 345.0 14 4533
112.1 180.6 216.6 244.8 272.6 298.0 330.0 382.7 441.4 578.2
```

APPENDIX C-I Continued

```
10 2.9375 .080 .170 1708. .048 .215  45.0 363.5 14 4533
115.7 184.6 223.1 251.7 277.7 304.0 338.9 396.1 461.4 599.3

10 2.9375 .080 .170 1709. .048 .222  45.0 410.6 14 4533
115.5 185.0 220.0 244.4 269.8 297.8 331.0 385.3 447.8 619.2
```

APPENDIX C-II

COMPONENT EQUATION DATA

PI 6	.4705		
PI 7	3.7836	STD DEV	.0609
PI 8	.8619	STD DEV	.0145
PI 9	.0505	STD DEV	.0007
PI 10	21.2464		
PI 11	.5788		
PI 14	.0000		

PI 2	P	PI 7	PI 8	PI 9
35.0000	.9159	3.7719	.8440	.0503
35.0000	.9091	3.6955	.8569	.0493
35.0000	.9162	3.6977	.8780	.0493
45.0000	.9165	3.7741	.8546	.0503
45.0000	.9159	3.7786	.8491	.0504
45.0000	.9210	3.9268	.8661	.0523
55.0000	.9394	3.7786	.8553	.0504
55.0000	.9375	3.7874	.8535	.0507
55.0000	.9349	3.7741	.8901	.0503
65.0000	.9340	3.7808	.8485	.0505
65.0000	.9206	3.7852	.8820	.0506
65.0000	.9192	3.8528	.8644	.0514

APPENDIX C-II Continued

PI 2	45.0000		
PI 7	3.7716	STD DEV	.0588
PI 8	.8602	STD DEV	.0115
PI 9	.0503	STD DEV	.0007
PI 10	21.2464		
PI 11	.5927		
PI 14	.0000		

PI 6	P	PI 7	PI 8	PI 9
.1904	.9492	3.7042	.8673	.0495
.1904	.9509	3.7042	.8608	.0495
.1904	.9522	3.7042	.8757	.0495
.3214	.9161	3.7741	.8481	.0503
.3214	.9277	3.7808	.8593	.0505
.3214	.9272	3.7786	.8472	.0504
.4705	.9165	3.7741	.8546	.0503
.4705	.9159	3.7786	.8491	.0504
.4705	.9210	3.9268	.8661	.0523
.7228	.7873	3.7786	.8818	.0504
.7228	.8076	3.7764	.8647	.0504
.7228	.7826	3.7786	.8471	.0504

APPENDIX C-II Continued

PI 2	45.0000		
PI 6	.4705		
PI 8	.8650	STD DEV	.0140
PI 9	.0504	STD DEV	.0006
PI 10	21.2464		
PI 11	.5788		
PI 14	.0000		

PI 7	P	PI 8	PI 9
3.3554	.8987	.8815	.0502
3.3589	.8883	.8453	.0503
3.3589	.9124	.8706	.0503
3.7741	.9165	.8546	.0503
3.7786	.9159	.8491	.0504
3.9268	.9210	.8661	.0523
4.8568	.9372	.8477	.0500
4.8863	.9245	.8699	.0506
4.8605	.9293	.8838	.0501
5.1488	.9412	.8575	.0499
5.1737	.9368	.8706	.0504
5.1571	.9319	.8835	.0501

APPENDIX C-II Continued

PI 2	45.0000		
PI 6	.4705		
PI 7	3.8416	STD DEV	.0824
PI 9	.0513	STD DEV	.0011
PI 10	21.2464		
PI 11	.5788		
PI 14	.0000		

PI 8	P	PI 7	PI 9
.3180	.9643	3.7808	.0505
.5075	.9753	3.8550	.0514
.6453	.9638	3.8573	.0515
.8527	.8752	3.7830	.0505
.9578	.7660	3.7808	.0505
1.1593	.7052	3.9337	.0525
1.2643	.6367	3.8573	.0515
.3223	.9735	3.6890	.0491
.5061	.9808	3.6933	.0492
.6581	.9578	3.9360	.0525
.8531	.8855	3.7741	.0503
.9727	.7573	3.7764	.0504
1.0306	.7068	3.7786	.0504
1.2605	.6321	3.7808	.0505
.3406	.9699	3.9337	.0525
.5228	.9651	3.8595	.0515
.6827	.8479	3.9314	.0524
.9242	.8574	3.9406	.0527
.9986	.7753	3.8573	.0515
1.1173	.6897	3.9337	.0525
1.2378	.6256	3.9406	.0527

APPENDIX C-II Continued

PI 2	45.0000		
PI 6	.4705		
PI 7	3.7415	STD DEV	.0798
PI 8	.8685	STD DEV	.0225
PI 10	21.2464		
PI 11	.5788		
PI 14	.0000		

PI 9	P	PI 7	PI 8
.0295	.9982	3.7329	.8645
.0294	.9991	3.7255	.9074
.0289	.9807	3.6467	.9077
.0384	.9766	3.7173	.8260
.0382	.9968	3.7089	.8405
.0399	.9667	3.8795	.8864
.0503	.9165	3.7741	.8546
.0504	.9159	3.7786	.8491
.0523	.9210	3.9268	.8661
.0566	.8583	3.6536	.8530
.0566	.8534	3.6536	.8797
.0568	.8271	3.6610	.8759
.0703	.7102	3.7540	.8716
.0704	.7001	3.7571	.8653
.0702	.6751	3.7524	.8794

APPENDIX C-II Continued

PI 2	45.0000		
PI 6	.4705		
PI 7	3.8265	STD DEV	.0734
PI 8	.8566	STD DEV	.0073
PI 9	.0510	STD DEV	.0009
PI 11	.5788		
PI 14	.0000		

PI 10	P	PI 7	PI 8	PI 9
14.1643	.6944	3.7741	.8546	.0503
14.1643	.6720	3.7786	.8491	.0504
14.1643	.6944	3.9268	.8661	.0523
21.2464	.9165	3.7741	.8546	.0503
21.2464	.9159	3.7786	.8491	.0504
21.2464	.9210	3.9268	.8661	.0523
28.3286	.9814	3.7741	.8546	.0503
28.3286	.9818	3.7786	.8491	.0504
28.3286	.9815	3.9268	.8661	.0523
35.4107	.9948	3.7741	.8546	.0503
35.4107	.9945	3.7786	.8491	.0504
35.4107	.9946	3.9268	.8661	.0523
42.4929	.9987	3.7741	.8546	.0503
42.4929	.9977	3.7786	.8491	.0504
42.4929	.9983	3.9268	.8661	.0523

APPENDIX C-II Continued

PI 2	45.0000		
PI 6	.4778		
PI 7	3.7727	STD DEV	.0533
PI 8	.8603	STD DEV	.0188
PI 9	.0503	STD DEV	.0006
PI 10	21.2464		
PI 14	.0000		

PI 11	P	PI 7	PI 8	PI 9
.4315	.9557	3.7741	.8531	.0503
.4315	.9428	3.7808	.8791	.0505
.4315	.9468	3.7741	.8661	.0503
.5072	.9301	3.7786	.8662	.0504
.5072	.9380	3.7741	.8707	.0503
.5072	.9303	3.7896	.8509	.0507
.5788	.9165	3.7741	.8546	.0503
.5788	.9159	3.7786	.8491	.0504
.5788	.9210	3.9268	.8661	.0523
.7182	.6369	3.7741	.8641	.0503
.7182	.6244	3.7719	.8406	.0503
.7182	.6183	3.7896	.8411	.0507
.8707	.0028	3.6998	.8223	.0494
.8707	.0030	3.6998	.8807	.0494
.8707	.0029	3.7042	.8989	.0495

APPENDIX C-II Continued

PI 2	45.0000		
PI 6	.4705		
PI 7	3.7761	STD DEV	.0056
PI 8	.8632	STD DEV	.0158
PI 9	.0504	STD DEV	.0001
PI 10	21.2464		
PI 11	.5788		

PI 14	P	PI 7	PI 8	PI 9
.1270	.8910	3.7852	.8711	.0506
.1625	.8837	3.7675	.8677	.0501
.1546	.8599	3.7808	.8691	.0505
.1460	.8857	3.7697	.8893	.0502
.1839	.8676	3.7830	.8577	.0505
.1609	.8321	3.7830	.8599	.0505
.2667	.6591	3.7741	.8555	.0503
.2607	.6626	3.7675	.8690	.0501
.4080	.5084	3.7764	.8374	.0504
.4047	.5051	3.7719	.8750	.0503
.3623	.5129	3.7697	.8574	.0502
.3854	.5151	3.7764	.8829	.0504
.4058	.4535	3.7808	.8862	.0505
.5966	.3746	3.7764	.8484	.0504
.6065	.3722	3.7764	.8425	.0504
.6631	.3552	3.7786	.8425	.0504

APPENDIX C-III

EVALUATION OF MODEL II PREDICTION EQUATION

P OBS	P CAL	DIFF	PERCENT
.9159	.9068	-.0090	-.987
.9091	.9074	-.0017	-.192
.9162	.8971	-.0190	-2.077
.9165	.9001	-.0164	-1.791
.9159	.9017	-.0141	-1.545
.9210	.8821	-.0388	-4.221
.9394	.9127	-.0266	-2.837
.9375	.9118	-.0256	-2.731
.9349	.8971	-.0378	-4.043
.9340	.9444	.0104	1.119
.9206	.9281	.0074	.807
.9192	.9317	.0125	1.365
.9492	.9499	.0006	.071
.9509	.9529	.0019	.209
.9522	.9459	-.0062	-.655
.9161	.9304	.0142	1.559
.9277	.9241	-.0036	-.388
.9272	.9300	.0027	.295
.9165	.9001	-.0164	-1.791
.9159	.9017	-.0141	-1.545
.9210	.8821	-.0388	-4.221
.7873	.7844	-.0029	-.380
.8076	.7929	-.0146	-1.819
.7826	.8004	.0178	2.275
.8987	.8840	-.0147	-1.644
.8883	.8999	.0116	1.307
.9124	.8884	-.0240	-2.633
.9165	.9001	-.0164	-1.791
.9159	.9017	-.0141	-1.545
.9210	.8821	-.0388	-4.221
.9372	.9375	.0003	.034
.9245	.9241	-.0003	-.039
.9293	.9204	-.0089	-.958
.9412	.9474	.0062	.659
.9368	.9390	.0021	.229
.9319	.9344	.0025	.269
.9643	.9651	.0007	.081
.9753	.9759	.0005	.053
.9638	.9601	-.0037	-.387
.8752	.8993	.0241	2.757
.7660	.8458	.0797	10.410
.7052	.6920	-.0132	-1.880
.6367	.6053	-.0314	-4.942

APPENDIX C-III Continued

P OBS	P CAL	DIFF	PERCENT
.9735	.9751	.0015	.161
.9808	.9902	.0094	.962
.9578	.9506	-.0072	-.752
.8855	.9007	.0152	1.724
.7573	.8379	.0806	10.643
.7068	.8010	.0941	13.318
.6321	.6153	-.0168	-2.658
.9699	.9566	-.0133	-1.374
.9651	.9744	.0093	.965
.8479	.9459	.0980	11.566
.8574	.8503	-.0070	-.822
.7753	.8148	.0395	5.098
.6897	.7254	.0357	5.185
.6256	.6223	-.0033	-.534
.9982	1.0068	.0086	.865
.9991	.9861	-.0129	-1.301
.9807	.9865	.0058	.594
.9766	.9869	.0102	1.047
.9968	.9815	-.0153	-1.535
.9667	.9545	-.0121	-1.257
.9165	.9001	-.0164	-1.791
.9159	.9017	-.0141	-1.545
.9210	.8821	-.0388	-4.221
.8583	.8475	-.0108	-1.266
.8534	.8351	-.0183	-2.147
.8271	.8349	.0078	.948
.7102	.6986	-.0115	-1.629
.7001	.7002	.0001	.027
.6751	.6956	.0204	3.032
.6944	.7180	.0235	3.388
.6720	.7196	.0475	7.078
.6944	.6999	.0055	.798
.9165	.9001	-.0164	-1.791
.9159	.9017	-.0141	-1.545
.9210	.8821	-.0388	-4.221
.9814	1.0052	.0237	2.415
.9818	1.0068	.0249	2.539
.9815	.9871	.0056	.578
.9948	1.0332	.0384	3.860
.9945	1.0348	.0403	4.054
.9946	1.0151	.0205	2.068
.9987	.9841	-.0145	-1.456
.9977	.9857	-.0119	-1.199

APPENDIX C-III Continued

P OBS	P CAL	DIFF	PERCENT
.9983	.9661	-.0321	-3.223
.9557	.9434	-.0122	-1.283
.9428	.9301	-.0126	-1.345
.9468	.9375	-.0092	-.975
.9301	.9466	.0164	1.770
.9380	.9453	.0072	.777
.9303	.9515	.0211	2.278
.9165	.9001	-.0164	-1.791
.9159	.9017	-.0141	-1.545
.9210	.8821	-.0388	-4.221
.6369	.6080	-.0288	-4.533
.6244	.6189	-.0054	-.874
.6183	.6154	-.0028	-.460
.0028	.0275	.0246	.85272019E 03
.0030	.0013	-.0016	-53.709
.0029	-.0084	-.0113	-.38765232E 03

APPENDIX C-IV

RAW DATA FOR TESTING PREDICTION EQUATION

9 3 5

```
5 2.9375 .080 .170 1186. .074 .132  45.0    .0  9    9
87.8 201.8 258.2 262.3 262.5   .0    .0    .0    .0    .0

6 2.9375 .080 .170 1189. .074 .116  45.0    .0  9    9
69.8 174.6 228.7 233.8 234.1 234.2   .0    .0    .0    .0

5 2.9375 .080 .170 1188. .074 .122  45.0    .0  9    9
74.3 181.5 232.1 235.9 236.2   .0    .0    .0    .0    .0

8 2.9375 .080 .170 1612. .054 .112  45.0    .0  9    9
87.2 203.8 272.5 291.2 294.9 295.7 295.8 296.0    .0    .0

8 2.9375 .080 .170 1606. .055 .112  45.0    .0  9    9
90.2 204.5 273.7 292.7 296.5 297.4 297.6 297.7    .0    .0

8 2.9375 .080 .170 1611. .054 .110  45.0    .0  9    9
87.0 200.7 266.5 284.5 287.7 288.4 288.8 288.9    .0    .0

9 2.9375 .080 .170 1806. .049 .106  45.0    .0  9    9
87.8 197.9 279.1 308.2 315.6 317.2 317.8 318.0 318.1    .0

9 2.9375 .080 .170 1810. .048 .111  45.0    .0  9    9
89.5 208.2 292.1 320.7 328.1 330.0 330.7 331.0 331.2    .0

9 2.9375 .080 .170 1810. .047 .109  45.0    .0  9    9
87.0 204.1 295.7 327.8 335.3 337.3 338.0 338.3 338.4    .0
```

APPENDIX C-V

COMPONENT EQUATION DATA FOR TESTING PREDICTION EQUATION

PI 2	45.0000		
PI 6	.4705		
PI 7	4.0252	STD DEV	.0483
PI 8	.8578	STD DEV	.0154
PI 10	21.2464		
PI 11	.5788		
PI 14	.0000		

PI 9	P	PI 7	PI 8
.0374	.9836	4.0426	.8656
.0376	.9765	4.0528	.8766
.0376	.9826	4.0494	.8413
.0505	.9206	4.0096	.8464
.0510	.9193	4.0687	.8544
.0504	.9224	4.0071	.8416
.0575	.8773	4.0762	.8578
.0566	.8819	4.0019	.8510
.0554	.8738	3.9185	.8855

APPENDIX D

CALIBRATION CURVE FOR VOLUME
MEASURING MANOMETER

CALIBRATION CURVE FOR VIBRATORY FEEDER

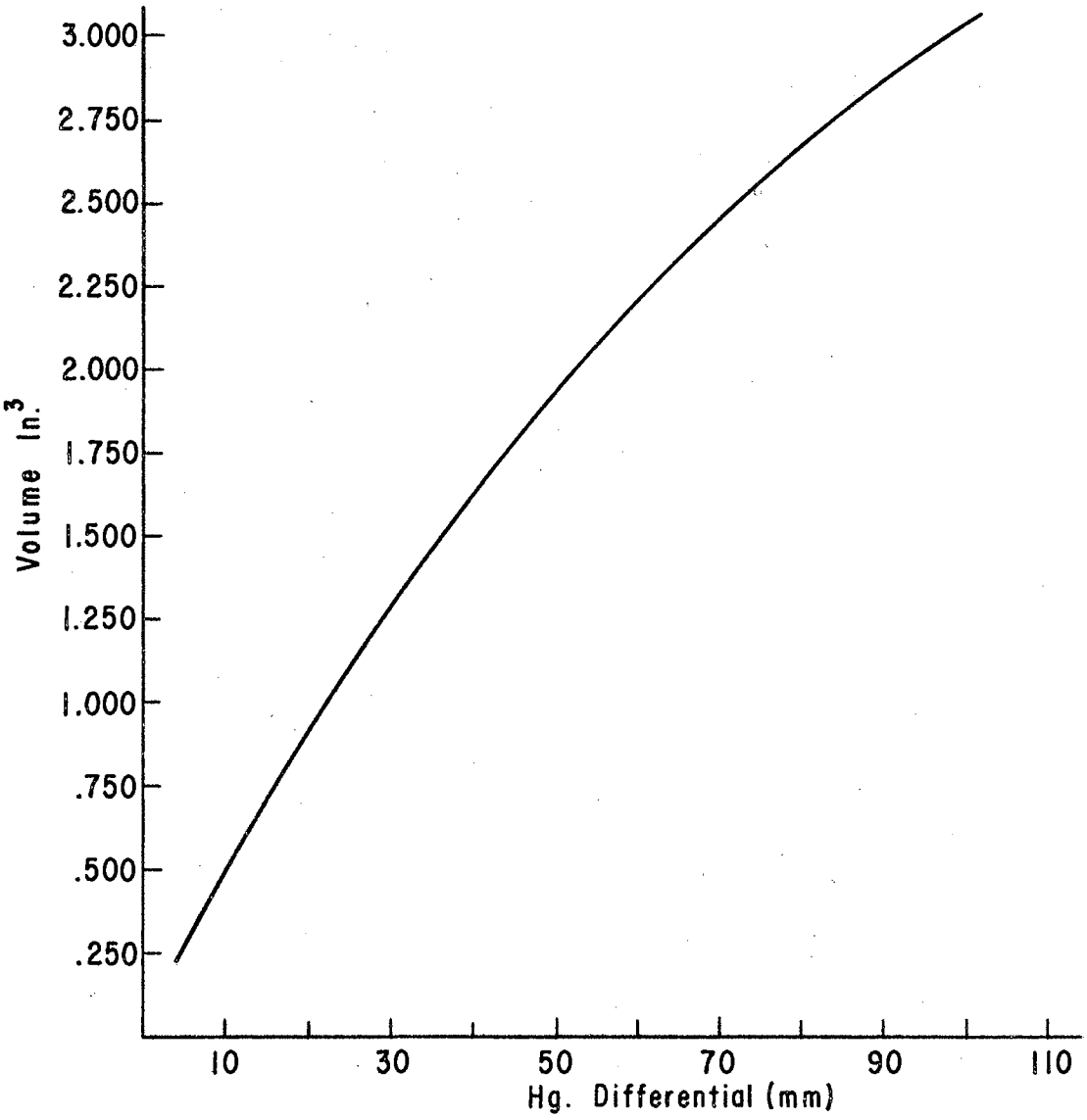

APPENDIX D-I

CALIBRATION CURVE FOR VOLUME
MEASURING MANOMETER

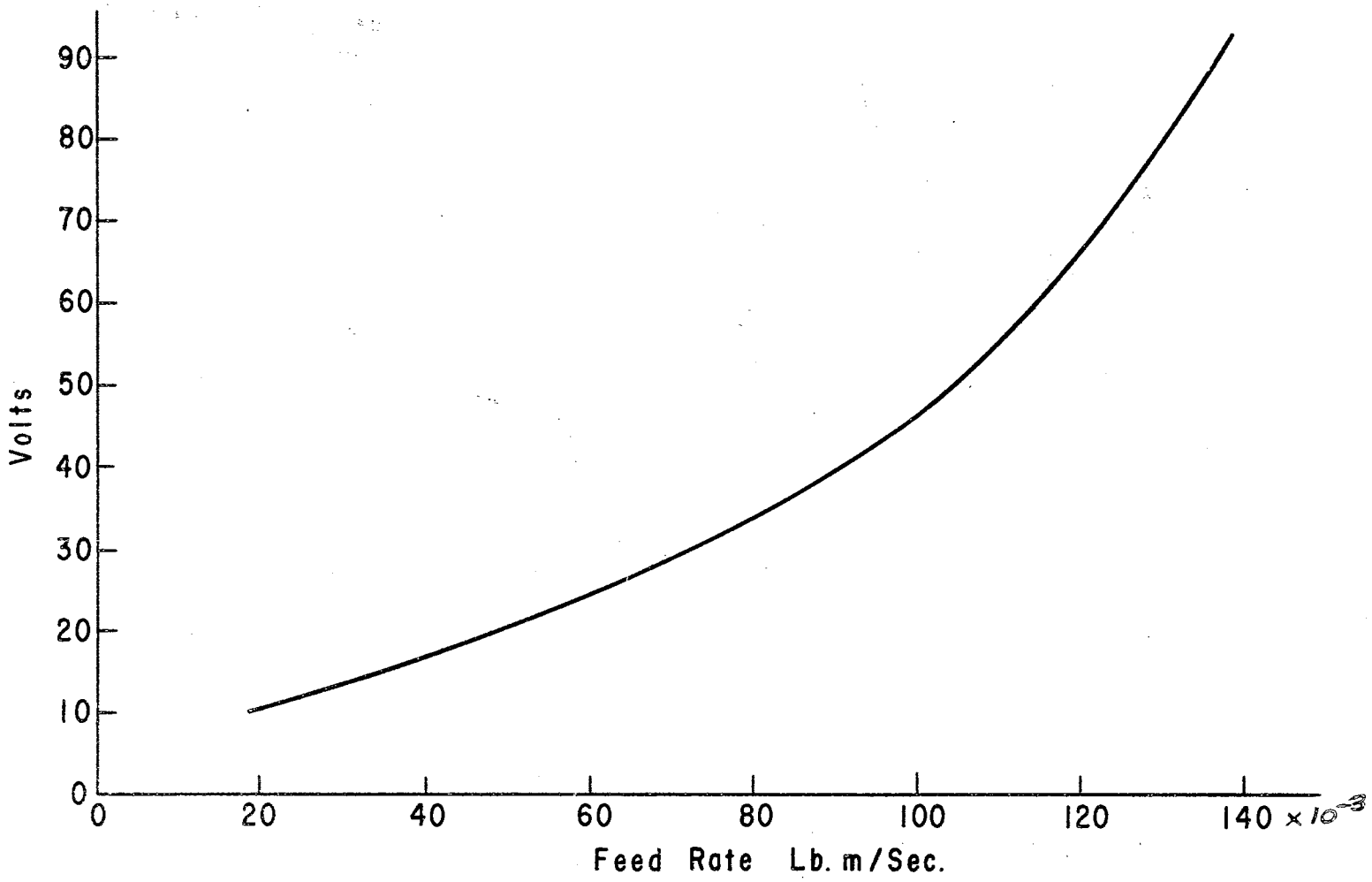

APPENDIX D-II

CALIBRATION CURVE FOR VIBRATORY FEEDER

APPENDIX E

FORTRAN PROGRAM

SELECTED SAMPLE CALCULATIONS FOR A MULTI-SCREEN SYSTEM

APPENDIX E-I

FORTRAN PROGRAM

```
C       PAUL TURNQUIST
C       SEPT 3,1964
C       APPLICATION OF PREDICTION EQUATION
C       TO 3 SCREENS IN SERIES
C       IBM 1620 FORTRAN WITH FORMAT
C       A1 = A(2,2)/A(1,2)
C       A2 = A(3,2)/A(2,2)
C       L2 = MAXIMUM LENGTH OF SCREEN 2,   INCHES
C       L3 = MAXIMUM LENGTH OF SCREEN 3,   INCHES
C       PI62 = VALUE OF PI 6 FOR SCREEN 2
C       PI63 = VALUE OF PI 6 FOR SCREEN 3
C       Q1 = FEED RATE TO SCREEN ONE, LBM PER SEC PER
C       INCH OF WIDTH
C       SENSE SWITCH 1  ON = PUNCH  OFF = TYPE
C       SENSE SWITCH 2   ON = TYPE K,PCAL
        DIMENSION A(3,5),B(3)
        READ 99,A1,A2
        TYPE 99,A1,A2
        READ 100,L2,L3,PI62,PI63
        TYPE 100,L2,L3,PI62,PI63
        PI8M = .59216929/(2.*.61024423)
        PI10M = (5.2918966E-02/(2.*7.6819983E-04))
5       READ 90,PI2,PI6,PI7,PI8,PI9
        READ 91,PI10,PI11
        K = 0
        CEY = ((PI9*4.11E-05)*.1412)/(PI7*2.73E-09)
        A(1,2) = .0984/PI11
        AMP = ((PI7*2.73E-09)*385.728)/((CEY*4.11E-05)*.1412)
        K = K + 1
        GO TO 14
11      TEST = AL/.1412
        IF(PI10M-TEST)12,12,13
12      PI10 = PI10M
        GO TO 14
13      PI10 = TEST
14      P1 = -.9115902 + (-6.3099464E-03*PI2)
        PA = P1 + (7.6858091E-05*(PI2**2))
        PB = PA + (-5.8851930E-02*PI6) + (-.23026625*(PI6**2))
        P2 = PB + (-8.3348270E-02*PI7)
        PC = P2 + (1.3077284E-02*(PI7**2))
```

APPENDIX E-I Continued

```
      PD = PC + (.59216929*PI8) + (-.61024423*(PI8**2))
      PE = PD + (3.0397990*PI9) + (-105.34173*(PI9**2))
      P3 = PE + (5.2918966E-02*PI10)
      PG = P3 + (-7.6819983E-04*(PI10**2))
      PCAL = PG + (6.1202131*PI11) + (-6.3257509*(PI11**2))
      IF(PCAL-0.0)60,60,61
60    TYPE 111,K
      GO TO 5
61    IF(1.0-PCAL)5,5,16
16    IF(SENSE SWITCH 2)20,21
20    TYPE 103,K,PCAL
21    GO TO(17,30,50),K
17    A(1,3) = A(1,2)*PI6
      A(1,4) = .1412 * PI10
      Q1 = (((.0503*CEY)*PI8)*(A(1,2)**2))
      B(1) = Q1
      Q2 = (1.0-PCAL)*B(1)
      B(2) = Q2
      A(1,1) = 1.0
      PI6 = PI62
      PI8 = PI8M
      A(2,1) = 2.0
      A(2,2) = A1*A(1,2)
      IF(A(2,2)-.0984)5,5,18
18    PI11 = .0984/A(2,2)
      IF(PI11-.43)5,19,19
19    IF(PI11-.88)29,29,5
29    AL = L2
      K = K + 1
      GO TO 11
30    A(2,3) = PI6*A(2,2)
      A(2,4) = PI10* .1412
      Q3 = (1.0-PCAL)*Q2
      B(3) = Q3
      K = K + 1
      A(3,1) = 3.0
      PI6 = PI63
      AL = L3
      PI8 = PI8M
      A(3,2) = A2*A(2,2)
```

APPENDIX E-I Continued

```
      IF(A(3,2)-.0984)5,5,31
31    PI11 = .0984/A(3,2)
      IF(PI11-.43)5,32,32
32    IF(PI11-.88)33,33,5
33    A(3,3) = PI6*A(3,2)
      GO TO 11
50    A(3,4) = PI10*.1412
      Q4 = (1.0-PCAL)*Q3
      PT = (Q1-Q4)/Q1
      IF(SENSE SWITCH 1)52,51
51    TYPE 105,Q1
      TYPE 106,PT
      TYPE 107,CEY
      TYPE 108,AMP
      TYPE 109
      DO 70 I = 1,3
      TYPE 110,A(I,1),A(I,2),A(I,3),A(I,4)
70    CONTINUE
      GO TO 5
52    PUNCH 105,Q1
      PUNCH 106,PT
      PUNCH 107,CEY
      PUNCH 108,AMP
      PUNCH 109
      DO 54 I = 1,3
      PUNCH 110,A(I,1),A(I,2),A(I,3),A(I,4)
54    CONTINUE
      GO TO 5
90    FORMAT(F13.9,F13.9,F13.9,F13.9,F13.9)
91    FORMAT(F13.9,F13.9)
99    FORMAT(F6.2,F6.2)
100   FORMAT(I3,I3,F6.3,F6.3)
103   FORMAT(I2,F7.4)
105   FORMAT(16X,10H FEED RATE,2X,F6.3/)
106   FORMAT(16X,13H P FOR SYSTEM,2X,F6.4/)
107   FORMAT(16X,10H FREQUENCY,2X,F7.2,2X,4H CPS/)
108   FORMAT(16X,10H AMPLITUDE,2X,F7.4,2X,7H INCHES/)
109   FORMAT(8X,7H SCREEN,7X,5H APER,7X,4H DIA,7X,7H LENGTH/)
110   FORMAT(9X,F4.1,7X,F7.4,5X,F7.4,7X,F6.2/)
111   FORMAT(I2)
      END
```

APPENDIX E-II

SELECTED SAMPLE CALCULATIONS FOR A MULTI-SCREEN SYSTEM

FEED RATE .020

P FOR SYSTEM .9999

FREQUENCY 28.38 CPS

AMPLITUDE .0246 INCHES

SCREEN	APER	DIA	LENGTH
1.0	.1700	.0799	2.99
2.0	.1530	.0765	4.86
3.0	.1377	.0688	4.86

FEED RATE .051

P FOR SYSTEM .9999

FREQUENCY 28.43 CPS

AMPLITUDE .0251 INCHES

SCREEN	APER	DIA	LENGTH
1.0	.1700	.0799	2.99
2.0	.1530	.0765	4.86
3.0	.1530	.0765	4.86

APPENDIX E-II Continued

FEED RATE .042

P FOR SYSTEM .9996

FREQUENCY 32.95 CPS

AMPLITUDE .0201 INCHES

SCREEN	APER	DIA	LENGTH
1.0	.1700	.0799	2.99
2.0	.1530	.0765	4.86
3.0	.1530	.0765	4.86

FEED RATE .050

P FOR SYSTEM .9893

FREQUENCY 39.83 CPS

AMPLITUDE .0171 INCHES

SCREEN	APER	DIA	LENGTH
1.0	.1700	.0799	2.99
2.0	.1530	.0765	4.86
3.0	.1530	.0765	4.86

VITA

Paul Kenneth Turnquist

Candidate for the Degree of

Doctor of Philosophy

Thesis: SIZE CLASSIFYING OF GRANULAR PARTICLES IN A VIBRATORY SCREENING SYSTEM

Major Field: Agricultural Engineering

Biographical:

Personal Data: Born in McPherson County, Kansas, January 3, 1935, the son of Leonard and Myrtle Turnquist.

Education: Graduated from Kansas State University in 1957 with a Bachelor of Science degree, majoring in Agricultural Engineering; received the Master of Science degree from Oklahoma State University in 1961 with a major in Agricultural Engineering; completed the requirements for the Doctor of Philosophy degree from Oklahoma State University in May, 1965.

Professional Experience: During college--worked one summer for the Soil Conservation Service. After graduation--employed as a Research Engineer by the Caterpillar Tractor Company for eight months; Instructor in the Agricultural Engineering Department at Oklahoma State University, 1958-1961; Assistant Professor in the Agricultural Engineering Department at Oklahoma State University, 1961-1962.

Professional and Honorary Organizations: Member of the American Society of Agricultural Engineers; Associate member of Sigma Xi, honorary science society; Registered Professional Engineer in Oklahoma; member of Sigma Tau, honorary engineering fraternity.